Investigating the Catalytic and the Metabolic Role of the Thiol Dioxygenase and a Sulfurtransferase in the *mdo* Operon from *Pseudomonas aeruginosa*

by

Laura Katherine Tombrello

A dissertation submitted to the Graduate Faculty of
Auburn University
in partial fulfillment of the
requirements for the Degree of
Doctor of Philosophy in Chemistry

Auburn, Alabama
December 14, 2019

Approved By

Holly R. Ellis, Chair, Professor of Chemistry and Biochemistry
Douglas C. Goodwin, Associate Professor of Chemistry and Biochemistry
Steven Mansoorabadi, Assistant Professor of Chemistry and Biochemistry
Sang-jin Suh, Assistant Professor of Biological Sciences

Abstract

Mammalian cysteine dioxygenase (CDO) is a mononuclear iron containing enzyme that belongs to the cupin superfamily. CDO catalyzes the oxidation of cysteine to cysteine sulfinic acid. It contains an amino acid-derived cofactor formed between residues Cys93-Tyr157. Reported CDO homologs have been identified in several bacteria; however, all known bacterial thiol dioxygenase enzymes lack the Cys-Tyr post-translational modification because of a highly conserved Gly in place of Cys93.[1] Bacterial thiol dioxygenase enzymes are subdivided into the Arg-type and Gln-type, based on the identity of a conserved active site residue involved in substrate binding. The Arg-type has an alleged substrate specificity for L-cysteine and the Gln-type has a putative specificity for 3-mercaptopropionate (3-MPA).[2] The Gln-type CDO enzyme homologs convert 3-MPA to 3-sulfinopropionate (3-SPA). However, the metabolic role of either 3-MPA or 3-SPA is unclear in these bacteria systems. The Gln-type enzymes are currently referred to as 3-mercaptopropionate dioxygenase (MDO). Substitutions of Cys93, Gln62, and Arg60 were made to evaluate the functional role and substrate specificity among thiol dioxygenases. The C93G CDO variant was unable to form the crosslink, and only showed a slight reduction in the catalytic efficiency with L-cysteine. The results from the studies performed with R60Q and Q62R, suggest that Arg60 plays a more defined role in substrate specificity in mammalian CDO than the comparable glutamine residue does in bacterial MDO.

In bacteria that express "Gln-type" MDO, the gene is on the same operon as an annotated sulfurtransferase, but the existence of the sulfurtransferase has not been recognized by groups

working with MDO. As both genes are located on the same operon, they likely catalyze reactions in a common metabolic pathway. Both the MDO and sulfurtransferase genes are located in low-sulfur islands, suggesting these genes are turned on when sulfur is limiting. The annotated sulfurtransferase on the *mdo* operon has an amino acid sequence similarity to mercaptopyruvate sulfurtransferase enzymes, which suggest that mercaptopyruvate could be a potential substrate for MDO or the sulfurtransferase. Kinetic studies were repeated for R60Q CDO and Q62R MDO using 3-mercaptopyruvate as a substrate. The increase of activity with wild-type MDO suggest that 3-mercaptopyruvate is a viable substrate for bacterial thiol dioxygenase, which is further justified by the decrease in catalytic activity for Q62R MDO.

Natural fusions between thiol dioxygenases and sulfurtransferases have also been identified in certain bacteria. Existence of these fusions suggest that interactions among the dioxygenase and the sulfurtransferase could occur. Therefore, protein-protein interaction studies were performed with MDO and the sulfurtransferase. Our studies suggest that protein-protein interactions are occurring between MDO and the sulfurtransferase.

The *mdo* operon in *Pseudomonas aeruginosa* is located in the same gene cluster as sulfur starvation enzymes. In order to determine if the *mdo* operon was regulated under sulfur limitation, growth and expression assays were performed on transposon insertions of each gene and analyzed with various sulfur sources. However, based on the results of the studies, the *mdo* operon is not involved in sulfur starvation. Instead, the *mdo* operon may be involved in hydrogen sulfide or cyanide detoxification.

The studies described herein evaluated the functional role and substrate specificity of MDO and the sulfurtransferase in *P. aeruginosa*. Gln62 appears to play a role in substrate specificity but it does not seem to be as important as the role of Arg60 in mammalian CDO. Based on the evidence provided, MDO and the sulfurtransferase are able to interact. However, based on the results the *mdo* operon is more likely to be involved in hydrogen sulfide or cyanide detoxification rather than sulfur limitation. These studies also provided a foundation for future studies regarding the *mdo* operon in *P. aeruginosa*.

Acknowledgements

My time here at Auburn University has been an experience of a lifetime. I first would like to express my sincere appreciation to my advisor, Dr. Holly R. Ellis, for always believing in me and constantly motivating me to persevere through the good and the bad. I am beyond grateful for your encouragement and guidance through my time at Auburn. Thank you for providing me with my opportunities to grow and succeed as a scientist. I would also like to thank my committee members Dr. Douglas C. Goodwin, Dr. Steven Mansoorabadi, and Dr. Sang-jin Suh for agreeing to be a part of my committee. I appreciate the supply of support, constructive criticism, and meaningful discussions I have received from each of you. A special thanks to Dr. Suh for the use of his plate reader and lab space when I needed it and to Dr. Mansoorabdi for use of his fluorometer. I also would like to thank Dr. Patrick Frantom for allowing me to visit the University of Alabama to perform HDX-MS and Dr. Tonya N. Zeczycki for running our SPR experiments. I would also like to thank Dr. Jin Wang for your willingness to serving as my outside reader. Thank you Auburn University and the Department of Chemistry and Biochemistry for allowing me this opportunity.

I would like to the my current and former labmates Paritosh Dayal, Dr. Jonathan Musila, Dr. Dianna Forbes, Dr. Claire Graham, Richard Hagen, Shruti Somai, and Helen Aloh. I could have never survived this wild ride without you guys, and for that I thank each and every one of you. Thank you Dr. Rene Fuanta for your friendship and scientific discussions at our time

together at Auburn. Thank you to Dr. Claire Graham and Dr. Dianna Forbes for the laughs, memories, and forever friendship I made with you both.

Finally, I would like to dedicate this dissertation to my husband, Robby Tombrello and our daughter, Addison Tombrello. I will never be able to tell you enough how thankful I am for your constant love and support. Thank you, Robby, for taking on many long nights/early mornings in the lab and never once complaining. Also, a huge thank you to my parents Neal and Melinda Stanford for always believing in me and giving me the opportunity to follow my dreams. I love you all and none of this would have been possible without you.

Table of Contents

List of Tables

List of Figures

List of Abbreviations

CDO	cysteine dioxygenase
CSA	cysteine sulfinic acid
MDO	mercaptopropionate dioxygenase
SPA	sulfinopropionic acid
ADO	cysteamine dioxygenase
APS	adenosine 5'-phosphosulfate
PAPS	3'-phosphoadenosine 5'-phosphosulfate
tRNA	transfer ribonucleic acids
RSSH	persulfide
RSH	thiol
PLP	pyridoxal 5'-phosphate
GSH	glutathione
TST	thiosulfate sulfurtransferase
CBS	cystathionine β-synthase
CSE	cystathionine Δ-lyase
MST	3-mercaptopyruvate sulfurtransferase
SQR	sulfide:quinone oxidoreductase
EPR	electron paramagnetic resonance

LSI	low sulfur island
MSA	methanesulfonate
LC-MS	liquid chromatography-mass spectrometry
HPLC	high performance liquid chromatography
HDX-MS	hydrogen deuterium exchange-mass spectrometry
SPR	surface plasmon resonance spectroscopy

CHAPTER ONE

Literature Review

1.1 Sulfur Utilization Among Bacteria

Sulfur is one of the six most common essential elements found in life on Earth. It is typically found around hot springs and volcanic regions. Sulfur can exist as dissolved sulfate or dimethyl sulfide in the ocean, as well as a trace gas within the atmosphere.[3] Sulfur can also be produced from sulfates, which are commonly found in sulfur reducing bacteria.[3]

Sulfur is a major component of two essential amino acids, cysteine and methionine. Cysteine provides protein structure stabilization through the formation of disulfide bonds. Cysteine is also able to mediate electron transfers within oxidoreductases (such as cytochromes, thioredoxins, and Fe-S proteins).[4] Methionine is typically found in the interior hydrophobic core of globular proteins, while in membrane-spanning protein domains it interacts with the lipid bilayer.[5] In the synthesis of eukaryotic proteins, the initiating amino acid is methionine; however in prokaryotic proteins it is *N*-formyl methionine. After translation, the methionine residues may be removed and no longer contributes to protein structure.[5]

Sulfur participates in unique chemistry and comprises diverse metabolites. Sulfur can act as a source of energy (sulfate reduction or sulfide oxidation) and energy storage in the form of adenosine 5'-phosphosulfate (APS) and 3'-phosphoadenosine 5'-phosphosulfate (PAPS).[6] Sulfur also plays a role in the formation of iron sulfur clusters and thionucleosides of transfer ribonucleic acids (tRNA). The formation of these iron sulfur clusters involves the transfer of sulfur from L-cysteine, a reaction known to be catalyzed by cysteine desulfurases.[7,8]

The sulfur cycle is complex because sulfur can be transformed biologically and chemically, as well as having a broad range of oxidation states from -2 (completely reduced) to +6 (completely oxidized).[9] Moreover, the sulfur cycle is very closely related to other elemental cycles, such as nitrogen and carbon cycles.[9] In bacteria, sulfur is assimilated from organic and inorganic sources. The sulfur cycle consists of a group of sequential reactions in which sulfur goes through different oxidation states. The main oxidation states of sulfur are 0 for elemental sulfur, -2 for thiolate and thiols such as hydrogen sulfide and cysteine, and +6 for sulfate. Microorganisms are responsible for a number of transformations of sulfur, such as mineralization, immobilization, oxidation of inorganic compounds, and volatilization of inorganic and organic sulfur compounds.[10]

1.2 Incorporation of Sulfur into Cofactors

The functional role of sulfur in cofactors and biomolecules and their involvement in diverse metabolic processes have been evaluated in numerous studies. It is not fully understood how sulfur is delivered for the synthesis of these cofactors and nucleosides but it is proposed to be mediated through a persulfide intermediate. The limited studies on the delivery and incorporation of sulfur into macromolecules is due to several factors. First, the biological role of persulfides is a fairly new discovery; second, persulfides are extremely unstable, making them difficult to investigate.[11] The persulfide group (R-S-SH) primarily serves as the sulfur donor for sulfur incorporation in macromolecules.[9] There are several possible products from the decomposition of persulfides, some of which include thiol, disulfides, polysulfides, H_2S, and elemental sulfur (S_8).[11]

The reactivity of persulfides with various nucleophiles have been studied over several years. There are four possible pathways when RSSH is reacted with a nucleophile: (1) the sulfhydryl group becomes deprotonated; (2) the outer sulfur atom is attacked by a nucleophile; (3) the inner

sulfur atom is attacked by a nucleophile; (4) the alpha-carbon becomes deprotonated.[11] Reaction of different nucleophiles (hydroxide, sulfite, cyanide, and thiolate) with benzyl persulfide (BnSSH) generates various products such as H_2S, benzyl disulfide, benzyl polysulfide, and S_8 (Figure **1.1**).[11,12] Cyanide and thiolate (stronger nucleophilic reagents) attack both sulfur atoms, while hydroxide and sulfite (less nucleophilic reagents) prefer the inner sulfur atom.[9] The reactivity of persulfide substrates are often affected by steric hindrance. For example, a more sterically hindered persulfide-Ph_3CSSH could not undergo nucleophilic attacks with CN^-, I^-, Br^-, AcO^-.[13] However, these nucleophiles were able to deprotonate the persulfide to generate Ph_3CS^-, which breaks down to Ph_3SH and elemental sulfur (Figure **1.1**).

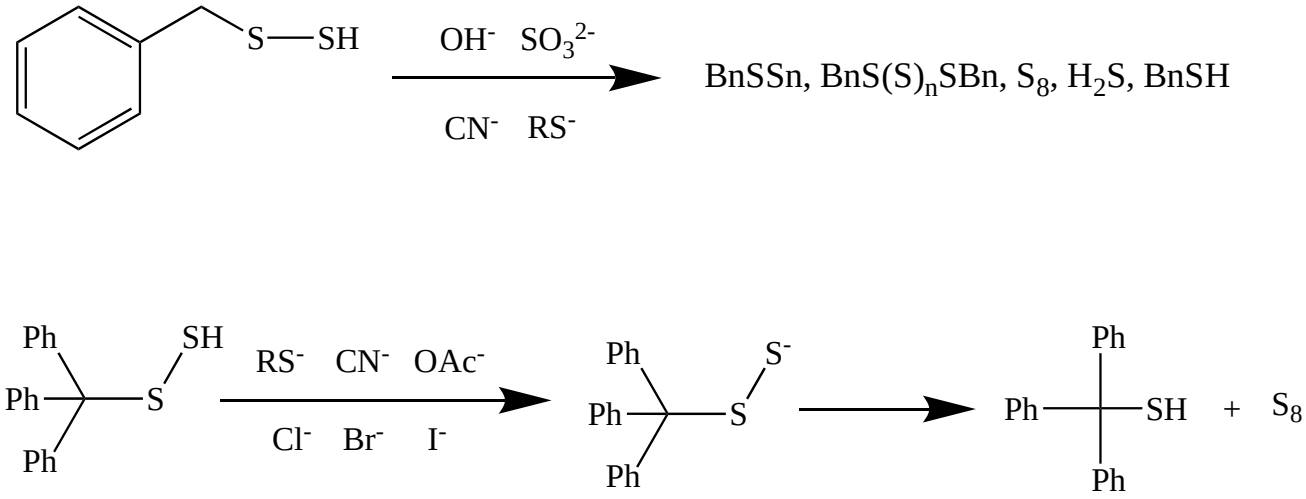

Figure 1.1. Reactions of persulfides with various nucleophiles (Adapted from[9]).

Persulfides (RSSH) tend to be more nucleophilic than thiols (RSH), however, there have been limited studies evaluating the nucleophilicity of persulfides. Even though there is a large number of known thiol blocking reagents that should be able to react with RSSH, very few reactions have been reported.[11] Thus far, only N-ethylmaleimide (NEM), 2,4-dinitrochlorobenzene (DNCB), and iodoacetate have shown to derivatize RSSH (Figure **1.2**)[9] The reaction between these

electrophiles and RSSH were relatively slow. The addition of an ethyl group to the nitrogen of NEM increases the reaction rate, but could lead to the breakdown of RSSH, decreasing product yield.[9]

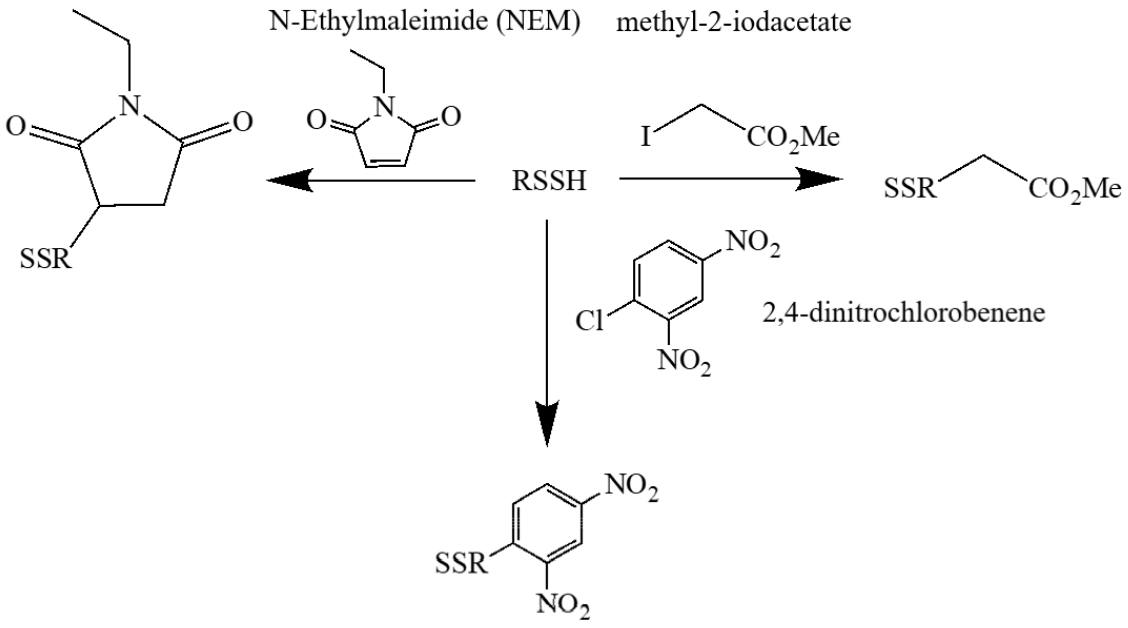

Figure 1.2. Reactions of persulfides with selected electrophiles (adapted from[9]).

In prokaryotes and eukaryotes, cysteine participates in the biosynthesis of most sulfur containing cofactors. Enzymes referred to as cysteine desulfurases play a critical role in thiol incorporation and transfer. Cysteine desulfurase is a pyridoxal 5'-phosphate (PLP) dependent homodimeric enzyme that converts L-cysteine to L-alanine utilizing PLP to cleave the carbon sulfur bond of cysteine after the formation of a persulfide enzyme intermediate (Figure **1.3**).[14]

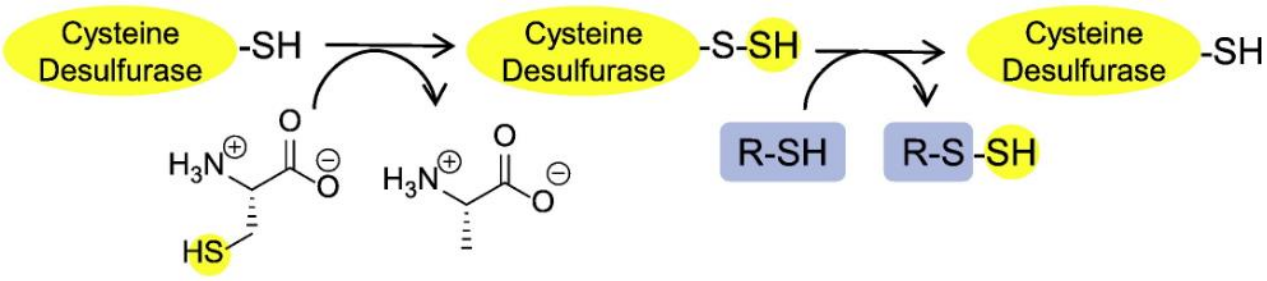

Figure 1.3. The transfer of sulfur from free L-cysteine catalyzed by cysteine desulfurase. (Adapted from [15]). Copyright 2014 Elsevier B.V. All rights reserved.

In *E.coli* there are four distinct cysteine desulfurases: CsdB, IscS, CsdA (CSD), and SufS.[16–18] CsdB is a NifS homologue that is involved in the biosynthesis of nitrogenase Fe-S clusters.[16] IscS is also involved in the mobilization of sulfur for Fe-S cluster biosynthesis. However, it also transports sulfur for the biosynthesis of thionucleosides and thiamin, and is involved in the incorporation of selenium into selenoproteins and selenouridine residues in tRNA.[19–21] SufS generates and repairs iron-sulfur clusters when ion deprivation or oxidative stress cannot use the IscS-dependent system[19,21,22] In most organisms one cysteine desulfurase is denoted as the central hub of sulfur mobilization for various pathways such as thionucleosides, thiamin, biosynthesis of iron-sulfur clusters, molybdenum cofactor, biotin, and lipoic acid (Figure **1.4**).[15] However, under certain physiological or environmental conditions additional cysteine desulfurases may be needed.[15]

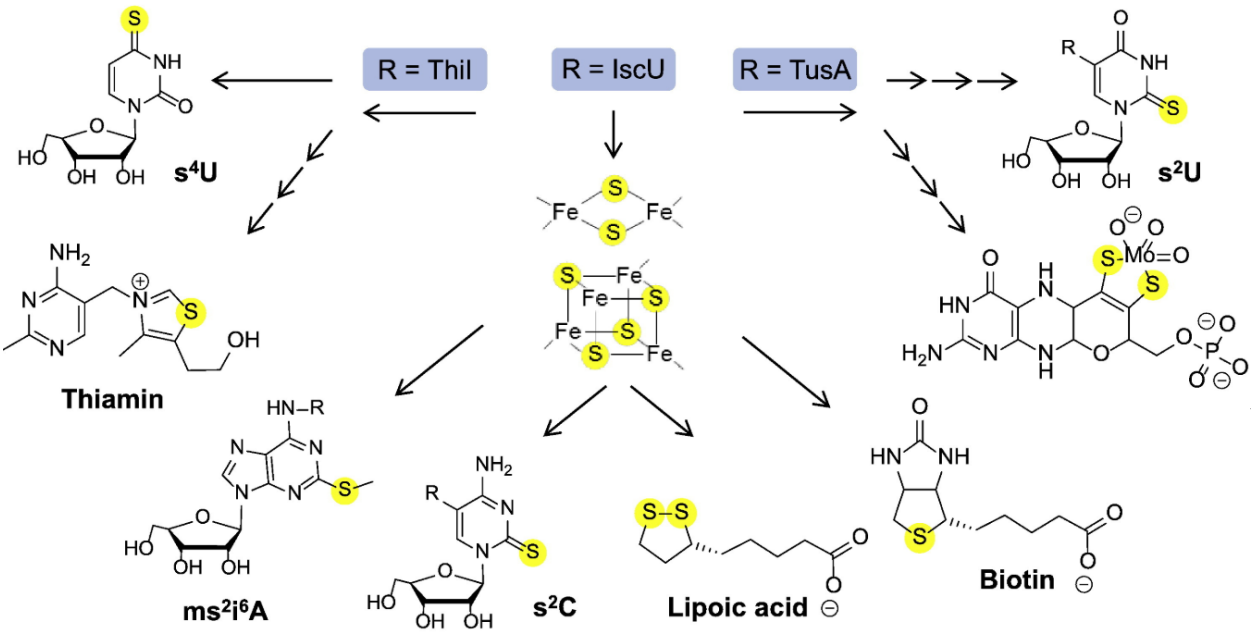

Figure 1.4. Biosynthetic pathways in *E. coli* that recruit IscS for sulfur mobilization. (Adapted from [15]). Copyright 2014 Elsevier B.V. All rights reserved.

1.3 Sulfur Limitation in Bacteria

Sulfur-containing biomolecules are involved in various chemical and structural functions.[19] In general, most bacteria prefer inorganic sulfate as the main sulfur source. However, inorganic sulfur only makes up roughly 3-6% of total soil sulfur reserves.[23] The remainder is primarily made up of carbon-bound sulfur and ester sulfates.[24,25 26] Therefore, bacteria within these environments must have other mechanisms for obtaining this element to meet their sulfur requirements.[27] When sulfate is limiting, sulfate starvation induced (Ssi) proteins are expressed to provide bacteria with an alternative means of obtaining sulfur.[28,29] In *E.* coli, eight Ssi proteins were identified using two dimensional gel electrophoresis and comparing cells grown in the absence and presence of sulfate or cysteine. It was determined that these genes are upregulated when *E.coli* is grown in media

containing sulfur sources other than cysteine or sulfate.[30,31] The proteins expressed during sulfur limitation play a role in sulfur acquisition from organic compounds, organosulfur uptake, and protection against reactive oxygen species.[32,33]

The regulation of specific operons in *E. coli* in response to sulfur limitation has primarily focused on two operons (*ssuEADCB* and *tauABCD*) involved in the utilization of alkanesulfonate and taurine as a sulfur source, respectively (Figure **1.5**). The *ssuABC* genes encode for an ABC-type transporter system responsible for the uptake of alkanesulfonates into the cell.[34–36] *ssuD* and *ssuE* encode for an FMN reductase and monooxygenase involved in the desulfonation of diverse alkanesulfonates. The *tauABC* gene cluster also encodes an ABC-type transporter system, and a taurine oxygenase enzyme, TauD, which is an α-ketoglutarate dependent, non-heme Fe (II) protein that catalyzes the release of sulfite from taurine.[37] The mechanism in which the substrates are transported across the external membrane through the periplasm and cytoplasm is not well understood; however, the substrate transport order of enzymes has been identified (Figure **1.6**). TauA and SsuA are suggested to be the periplasmic sulfonate binding proteins, while TauC and SsuC are involved in substrate transportation across the membrane permease. TauB and SsuB are enzymes that directly hydrolyze ATP. Alkanesulfonates have the ability to be transported by both operons, while taurine is only exclusively transported by *tauABC*.[33]

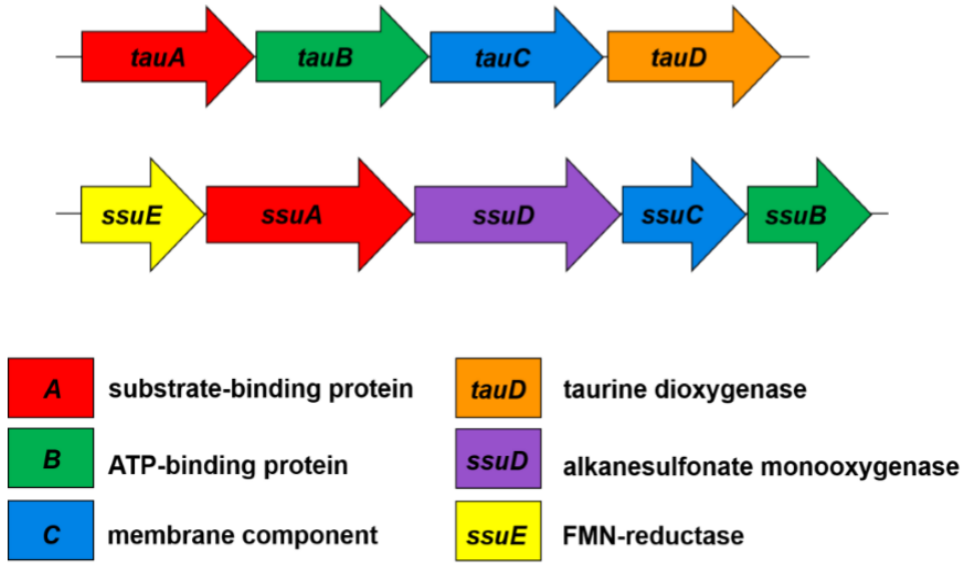

Figure 1.5. *tau* and *ssu* gene clusters responsible for synthesis of proteins involved in the uptake and utilization of taurine and alkanesulfonates in *E. coli* (Adapted from [38]).

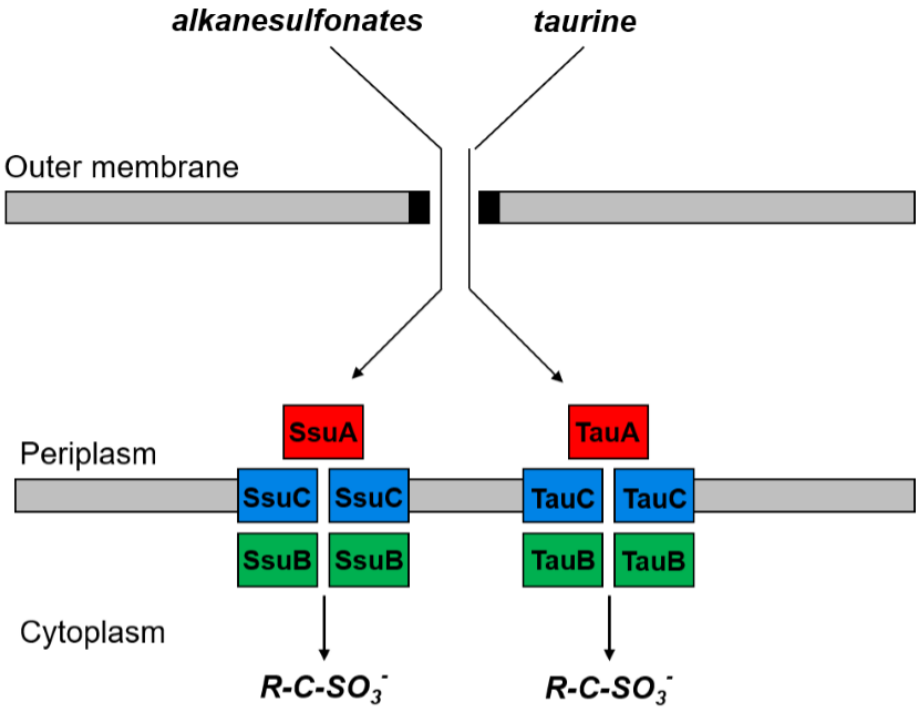

Figure 1.6. Sulfonate uptake and desulfonation in *E.coli* (Adapted from [38]).

The expression of the genes that encode proteins in the sulfate reduction pathway are under the control of the CysB protein, a LysR-type transcriptional regulator.[39] CysB is conserved among gram-negative bacteria and plays a key role in the expression of the *cys* genes *(cysKJIHPTWAM)* and *ssi* genes (*ssuEADCB* and *tauABCD*) responsible for sulfate assimilation.[13] Transcription of the *cbl* gene is activated once CysB interacts with the co-inducer *N*-acetylserine. (Figure **1.7 A**).[29,36] The expression of the *ssu* and *tau* genes is repressed when *E.coli* is grown in the presence of sulfate. During sulfate starvation, the Cbl protein binds upstream of the *ssuEADCB* and *tauABCD* operons to activate their transcription (Figure **1.7 C**).[39,40] CysB is also required for *tau* activation, however *ssu* does not require it for transcription (Figure **1.7 D**). CysB interaction with *N*-acetylserine activates the transcription of the *cys* genes, however sulfide and thiosulfate act as an anti-inducer (Figure **1.7 B**).[29] *Cys*genes are involved in sulfur assimilation, while the *ssi* and *tau* genes are involved in sulfur acquisition. The proteins induced by sulfate starvation in *E. coli* appear to be "sulfur scavenging enzymes" involved in the utilization of non-preferred sulfur sources.[41] Ssi proteins have been identified in both Gram-positive and Gram-negative species, including soil bacteria as well as human pathogens.[29]

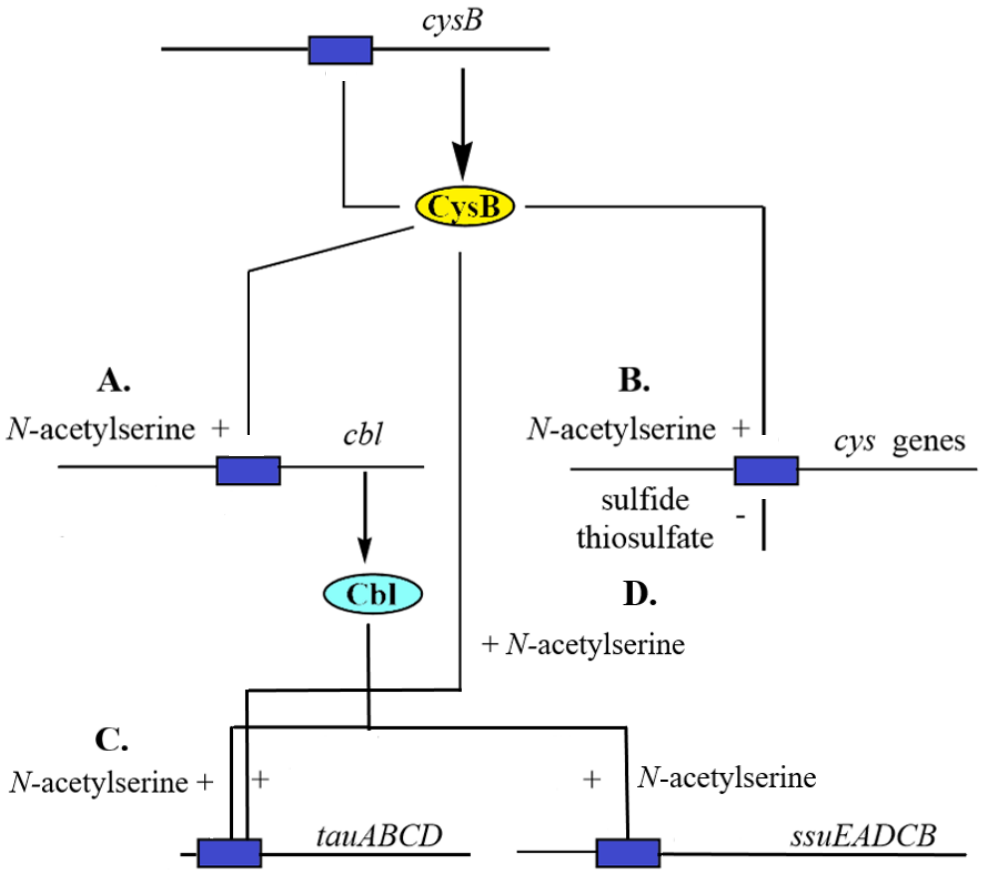

Figure 1.7. Regulation of sulfur assimilation pathways in *E.coli* (Adapted from [29]).

Pseudomonas spp. are able to utilize a variety of organosulfur compounds such as alkanesulfonates, taurine, and/or alkanesulfate esters as sulfur sources.[29,36,41,42] Similar to *E.coli*, Ssi proteins are found among *Pseudomonas* spp. and enable proteins to adapt to sulfur limiting conditions because there are more diverse mechanisms for sulfur acquisition.[27,43] However, the regulation of *ssi* gene expression in the *Pseudomonas* spp. is understood to be different from that of *E.coli*, because the pseudomonad genome lacks the *cbl* gene.[28] Although, there has been specific regulators reported to be involved in the regulation of the particular organosulfur assimilatory genes, it is unclear how pseudomonads globally regulate genes under sulfur starvation conditions and control the expression of organosulfur-assimilating pathways.[28,44–46] In *P. putida*, sulfur

utilization studies have proposed that CysB regulates the sulfate starvation response of the *sfn* operons, which is similar to the role of CysB in the regulation of the *E. coli* sulfonate utilization gene important in dimethylsulfone metabolism (Figure **1.8**). It contains the transcriptional activator SfnR, a σ^{54}-dependent transcriptional activator.[13] In the absence of downstream metabolites in the sulfate assimilatory pathways, such as cysteine and sulfide, CysB binds to the upstream region of *sfnECR* to directly activate expression. When sulfate is not present, SfnR activates the expression of *sfnFG*, but also represses *sfnECR* transcription.[28] This negative autoregulation is proposed to maintain appropriate levels of *sfnR* expression.[28] The regulation of SfnR would ensure quick switching of utilized sulfur sources from $DMSO_2$ to sulfate, when sulfate is supplied.[28] SfnF is a hypothetical NAD(P)H-dependent FMN-reductase, but activity assays have determined SfnF is unable to reduce or transfer flavin.[47] SfnG is considered to be an $FMNH_2$-dependent monooxygenase, that catalyzes conversion of $DMSO_2$ to methanesulfonate (MSA) (Figure **1.9**).[47] SfnE is NADH-dependent FMN-reductase, and SfnC is a hypothetical monooxygenase, however the role of SfnC is undetermined. Similar to *P. putida*, *P. aeruginosa* contains SfnR homologs and CysB, however, the functional role has not been evaluated.[13]

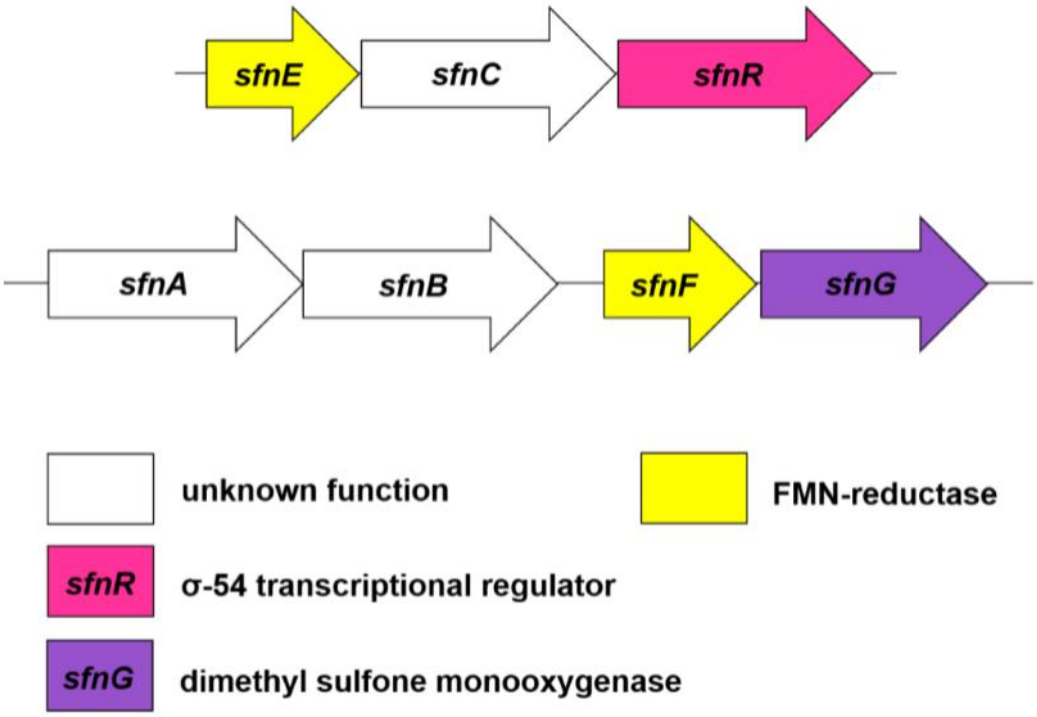

Figure 1.8. *sfn* genes expressed during sulfur limiting conditions in *Pseudomonas putida*.

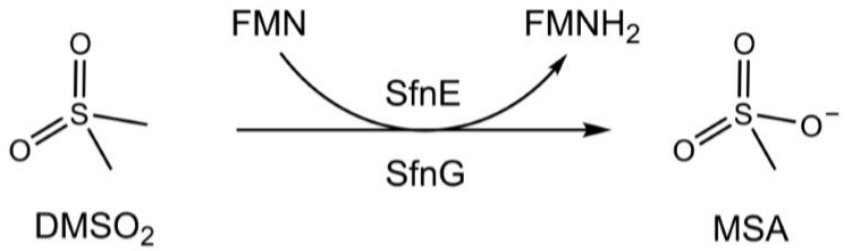

Figure 1.9. Conversion of $DMSO_2$ to MSA by SfnG, with reduced flavin supplied by SfnE as proposed by Toshio Omori [47].

1.4 The Cupin Superfamily

Some enzymes expressed during sulfur limitation are members of the cupin superfamily. The cupin superfamily is very diverse and the enzymes found within this superfamily are found in both prokaryotes and eukaryotes.[48] The cupin superfamily was first identified in the wheat protein, germin. These germin proteins were characterized by a conserved nine amino acid sequence (HI/THPRATEI), and are involved in protecting plants under different environmental stress conditions.[49] Overall, members of the cupin superfamily are able to catalyze an assorted range of reactions and have a relatively low sequence similarity. However, the common trait among members of the cupin superfamily is the β-barrel fold. This cupin domain consists of two conserved motifs, each containing two β-strands that are separated by a less conserved region that contains two more β-strands.[49] Originally, $G(X)_5HXH(X)_{3,4}E(X)_6G$ was defined as the conserved sequence for Motif 1 and $G(X)_5PXG(X)_2H(X)_3N$ for Motif 2, however, not all enzymes within this superfamily contain these two motifs.[48,49] The two motifs together represent a 3-His/1 Glu motif responsible for the coordination of the active site metal.

Most cupin superfamily proteins are metalloproteins and their active sites are located at the center of the β-barrel (Figure **1.10**). The most common type of metal found within the active site of cupins is iron; however, copper, nickel, manganese, cobalt, and zinc have also been identified.[48,49] Initial studies were focused on cupin enzymes with a 3 His/1 Glu motif, but enzymatic cupins are now known to contain diverse motifs (Figure **1.11**).[48]

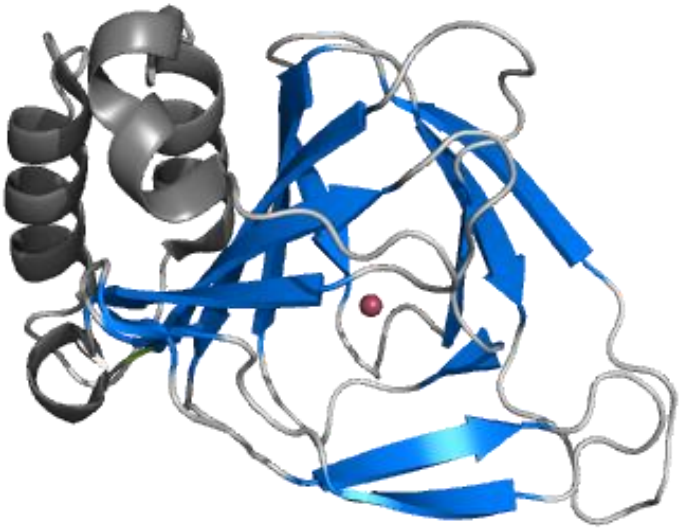

Figure 1.10. CDO crystal structure depicting the cupin superfamily fold: beta sheets (blue), alpha helices (dark grey), loops (light grey), iron metal center (brown). PDB: 4KWJ.[50]

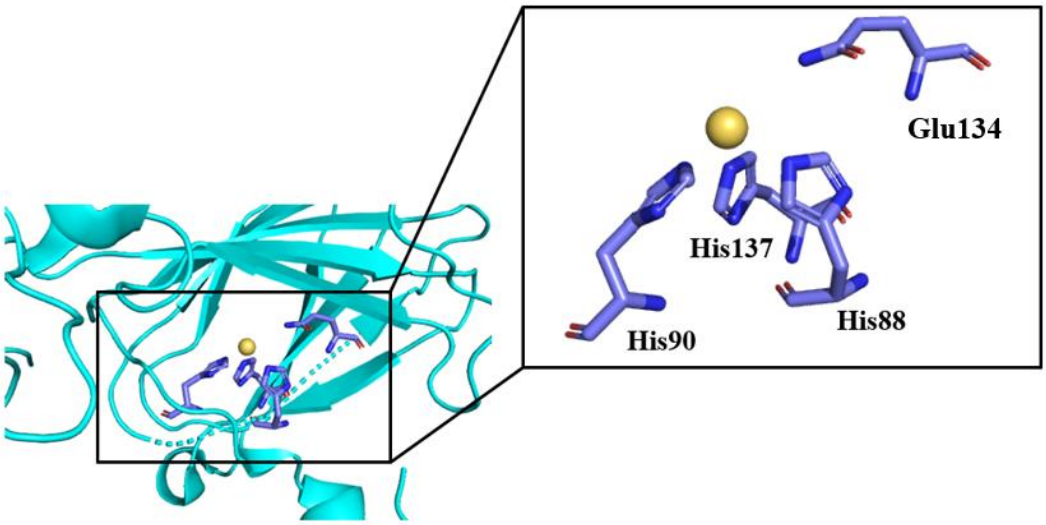

Figure 1.11. Crystal structure of cupin oxalate oxidase depicting the traditional 3-His/1-Glu coordination of the metal. Mn cation (yellow). PDB: 2ET1[51].

1.4.1 Thiol Dioxygenases within the Cupin Superfamily

Thiol dioxygenase enzymes utilize a mononuclear ferrous iron active site to catalyze the O_2-dependent oxidation of sulfur containing thiol compounds to corresponding sulfinic acid derivatives. Cysteine dioxygenase (CDO) and cysteamine dioxygenase (ADO) are the only known mammalian thiol dioxygenase enzymes that belong to the cupin superfamily. Both enzymes contain a 3-His coordinated iron center. ADO catalyzes the oxidation of cysteamine to hypotaurine, which is then further oxidized to taurine. CDO catalyzes the oxidation of L-cysteine to L-cysteine sulfinic acid (CSA), and CSA is further metabolized to either taurine or pyruvate and sulfite (Figure **1.12**).[52] It has been proposed that if cysteine regulation is disturbed, it will create reactive oxygen species in the cell. This dysregulation creates an imbalance in cysteine metabolism which is often associated with numerous neurodegenerative diseases. Therefore, CDO is a potential drug target for diseases such as Parkinson's, Alzheimer's, and other motor neuron diseases.[53]

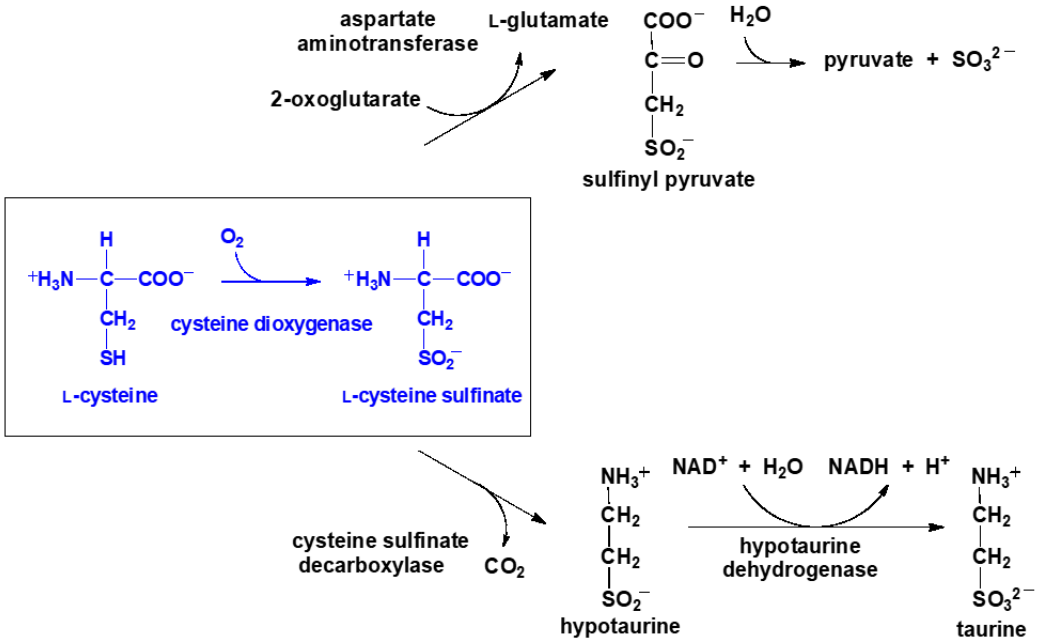

Figure 1.12. CDO metabolic pathway: L-cysteine is oxidized to L-cysteine sulfinic acid, to further go on to form pyruvate and sulfite, or taurine.

In CDO, the 3-His-1 carboxylate ligand binding motif found in many cupin enzymes is replaced by a 3-His facial triad and the carboxylate residue is replaced by the amino acid cysteine (Cys93). The Cys93 residue participates in a thioether crosslink with a tyrosine (Tyr157) close to the iron active site (Figure **1.13**).[54] There are several proposed roles for the crosslink in mammalian CDO. The post translational modification has been proposed to aid in positioning the substrate to coordinate the iron center by the amine and thiolate groups resulting in a five-fold increase in catalytic activity compared to non-crosslinked CDO.[54] Some studies suggest the crosslink indirectly enhances activity by removing all potential side reactions that could occur with the free thiol of Cys93.[55] Other studies have proposed the crosslink positions the hydroxyl group of Tyr157 for acid/base catalysis in order to stabilize the iron superoxo species that is generated during catalysis.[56–59] The crosslink has been reported to be involved in substrate specificity, given that the

Tyr157 is within hydrogen-bonding distance from the carboxylate of the L-cysteine substrate.[60,61] Crosslink formation occurs at elevated cysteine concentrations to enhance activity, and may act as a *in vivo* regulatory mechanism to decrease elevated cysteine concentrations that could be potentially toxic.

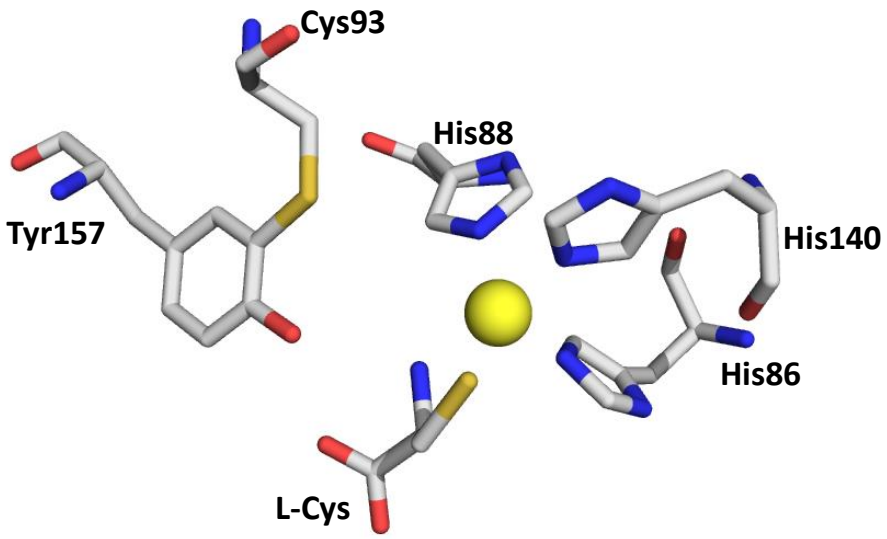

Figure 1.13. 3-His facial triad found in the active site of mammalian cysteine dioxygenase. PDB: 4IEV.[62]

Mammalian CDO is specific for the L-cysteine. Substrate specificity studies have been performed by utilizing cysteine analogs and measuring dioxygen consumption coupled with product formation. Various L-cysteine analogs were tested, but the rates of oxygen utilization and product formation were decreased by several orders of magnitude compared to the L-cysteine substrate.[60] Due to diminished activity and low product formation with the L-cysteine analogs, it was determined that L-cysteine was the preferred substrate for CDO.[60] Three-dimensional

structures of wild-type CDO show that L-cysteine binds bidentate by the amino and thiol groups leaving the carboxylic group to be coordinated by a nearby arginine residue.[54,57] The bidentate coordination of L-cysteine decreases the reduction potential of the mononuclear iron active site, resulting in a higher reactivity of the substrate-bound CDO toward O_2.[54]

In mammalian CDO, there are several conserved residues that contribute to substrate stabilization. In three-dimensional structural studies, the guanidinium group of a conserved Arg (Arg60) is extended towards the iron center in the absence of L-cysteine substrate. When the L-cysteine substrate is bound, the guanidinium group of Arg60 moves away from the iron center and is within 3 Å away from the carboxylate group of the L-cysteine substrate (Figure **1.14**).[62] When Arg60 was substituted with glutamine and alanine, both variants displayed a ~50% decrease in bound iron and a ~70% decrease in catalytic activity compared to that of wild-type CDO.[57] The decrease in iron content did not fully account for the decrease in activity.[57] The diminished activity observed by the substitution of the Arg60 residue combined with the close proximity of the guanidinium group to the carboxylate group of L-cysteine substrate, suggested that Arg60 contributes to the substrate specificity of mammalian CDO through electrostatic interactions.[56,57,62]

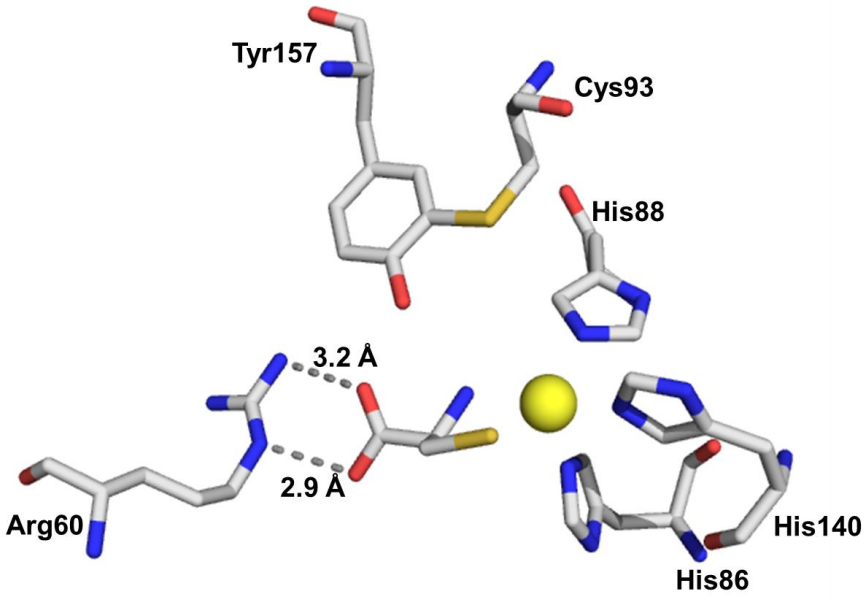

Figure 1.14. The guanidium of Arg60 is within 3 Å away from the carboxylate group of the Cys substrate. PDB: 4IEV.[62]

1.4.2 3-Mercaptopropionic acid Dioxygenase (MDO)

Putative thiol dioxygenases have also been identified in several bacteria. These bacterial thiol dioxygenase homologs have ~30-80% amino acid sequence identity to mammalian CDO.[63] Bacterial thiol dioxygenase homologs also share a common cupin fold with mammalian CDO (Figure **1.15**). Similar to mammalian CDO, bacterial thiol dioxygenase homologs have an octahedrally coordinated metal center coordinated by three histidine residues and share a common cupid fold with mammalian CDO (Figure **1.16**). These enzymes lack the Cys-Tyr post-translational modification because of a highly conserved Gly in the place of Cys93.[58]

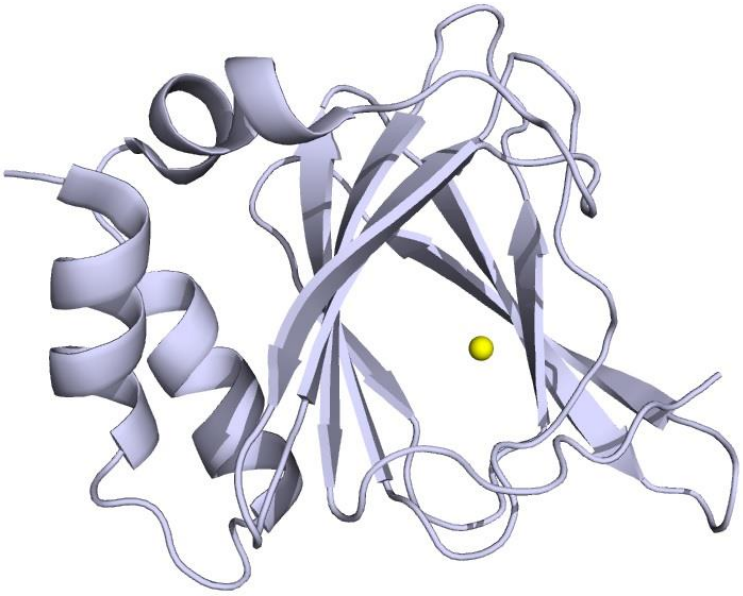

Figure 1.15. Crystal structure of bacterial CDO PDB: 4QM8.[64]

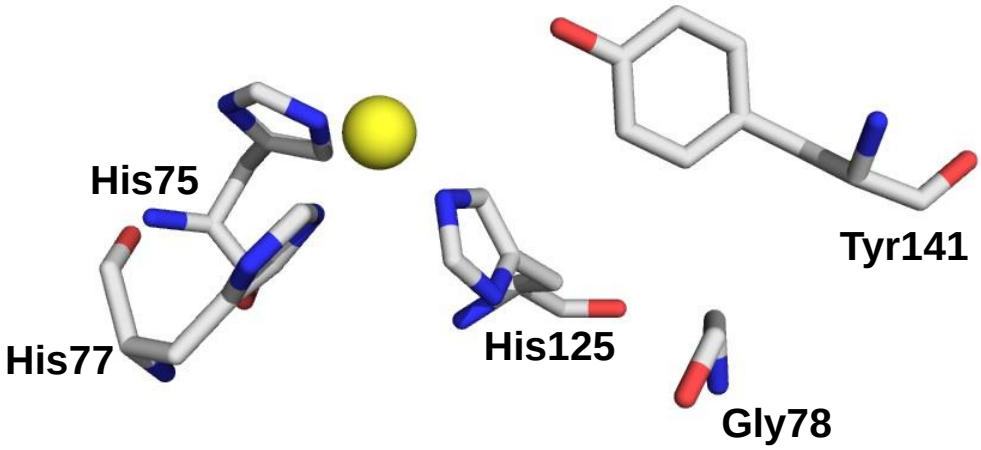

Figure 1.16. Active site of Bacterial CDO PDB: 4QM8.[64]

Bacterial thiol dioxygenases are divided into two subgroups based on which amino acid residue is located in a similar conformation as the Arg residue involved in substrate binding in mammalian CDO. However, all bacterial thiol dioxygenases are unable to form the cross-link,

because the Cys93 equivalent is a glycine residue.[65] One enzyme subgroup contains the conserved arginine residue and has alleged substrate specificity for L-cysteine (Figure **1.17**). Another subgroup replaces the arginine with a glutamine residue and has been proposed to utilize 3-mercaptopropionic acid (3-MPA) as a substrate.[2,58,63] The Gln subgroup of thiol dioxygenase enzymes are currently referred to as 3-mercaptopropionate dioxygenases (MDO).[66]

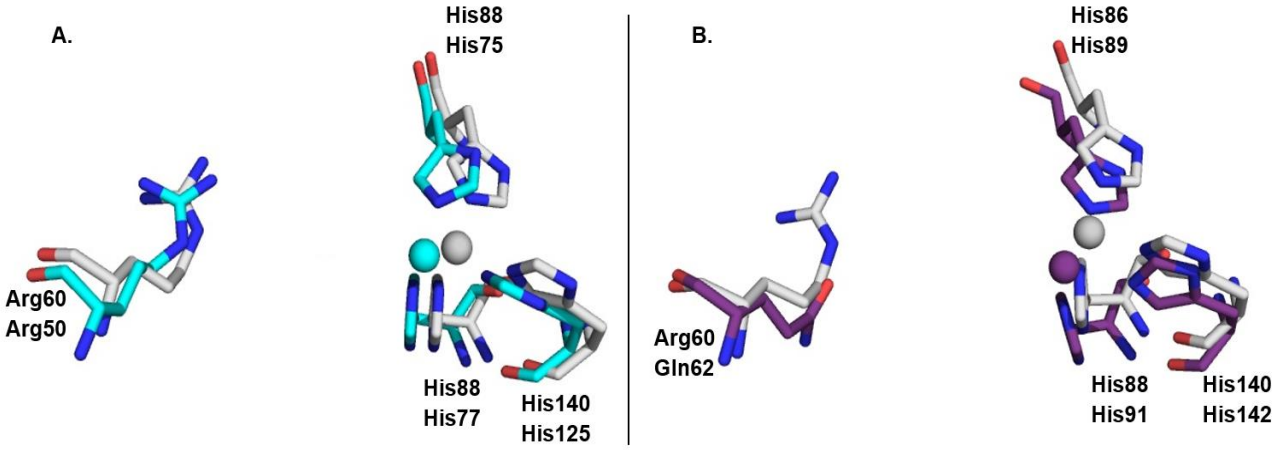

Figure 1.17. Three-dimensional structure comparing conserved residues in mammalian and bacterial CDO. **A.** Similar to CDO found in *R. norvegicus* (grey), CDO in *B. subtilis* (teal) contains a 3-His coordinated iron and an Arg in a similar position as Arg60. PDB: 2B5H and 4QM9. **B.** A 3-His coordinated iron is found in both *R. norvegicus* (grey) and *P. aeruginosa* (purple). However, in *P. aeruginosa* the Arg60 is replaced with a Gln residue. PDB: 2B5H and 4QM9.[2,63,67]

As previously mentioned, the proposed substrate for the Arg subgroup of bacterial thiol dioxygenases is L-cysteine, which is oxidized to cysteine sulfinic acid similar to mammalian CDO (Figure **1.18 A**). Conversely, several substrates including 3-mercaptopropionate, have been

proposed for the Gln subgroup of bacterial thiol dioxygenases. These Gln subgroup enzymes convert 3-MPA to 3-sulfinopropionate (3-SPA); however, the metabolic role of either 3-MPA or 3-SPA is unclear (Figure **1.18 B**). 3-MPA is an organic sulfur compound that has been identified in coastal marine sediments and is a breakdown product of dimethylsulfoniopropionate (DMSP).[68,69] DMSP is an organic sulfur compound produced by marine phytoplankton and macroalgae, and functions as an organic osmolyte.[68,70] In bacteria and algae, DMSP is broken down to DMS, a volatile compound that is one of the most abundant natural sources of sulfur in the atmosphere (Figure **1.19**).[68] DMS can further be oxidized to dimethyl sulfoxide (DMSO) and dimethyl sulfone ($DMSO_2$) via the cleavage pathway (Figure **1.20**). Initially, 3-MPA was proposed to be a major breakdown product of DMSP; however, more recent studies suggest it is a minor product of the DMSP demethylation pathway.[68] The demethylation pathway sequentially removes methyl groups from DMSP, resulting in the formation of acetaldehyde, which can be further oxidized to acetate and methanthiol.[71,72]

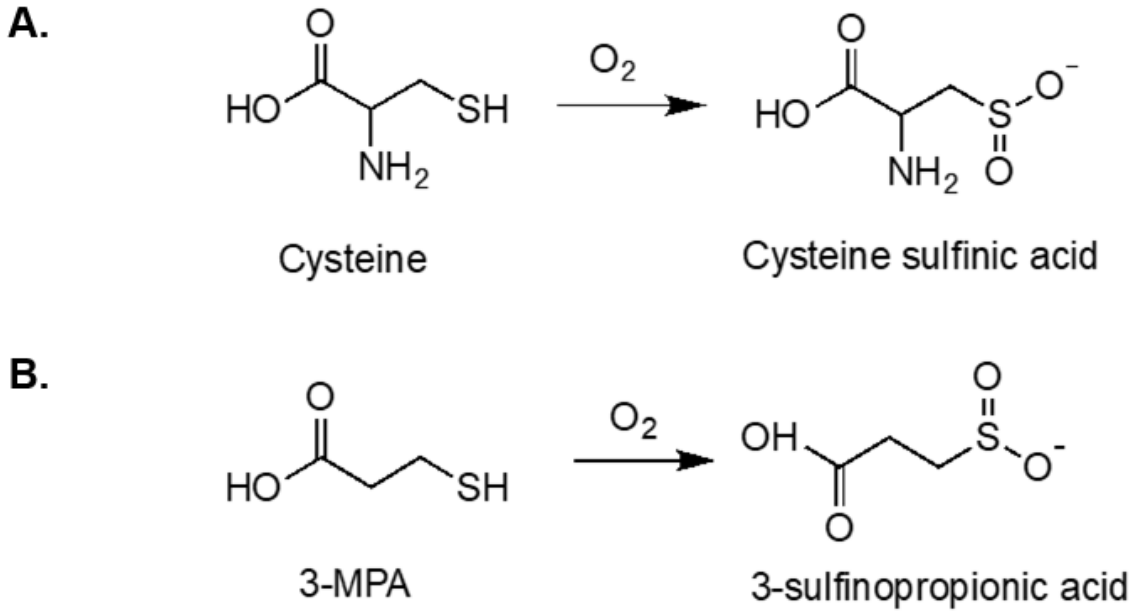

Figure 1.18. A. Arg subgroup oxidation reaction with cysteine to yield cysteine sulfinic acid. **B.** Gln subgroup oxidation reaction with 3-mercaptopropionic acid to yield 3-sulfinopropionic acid.

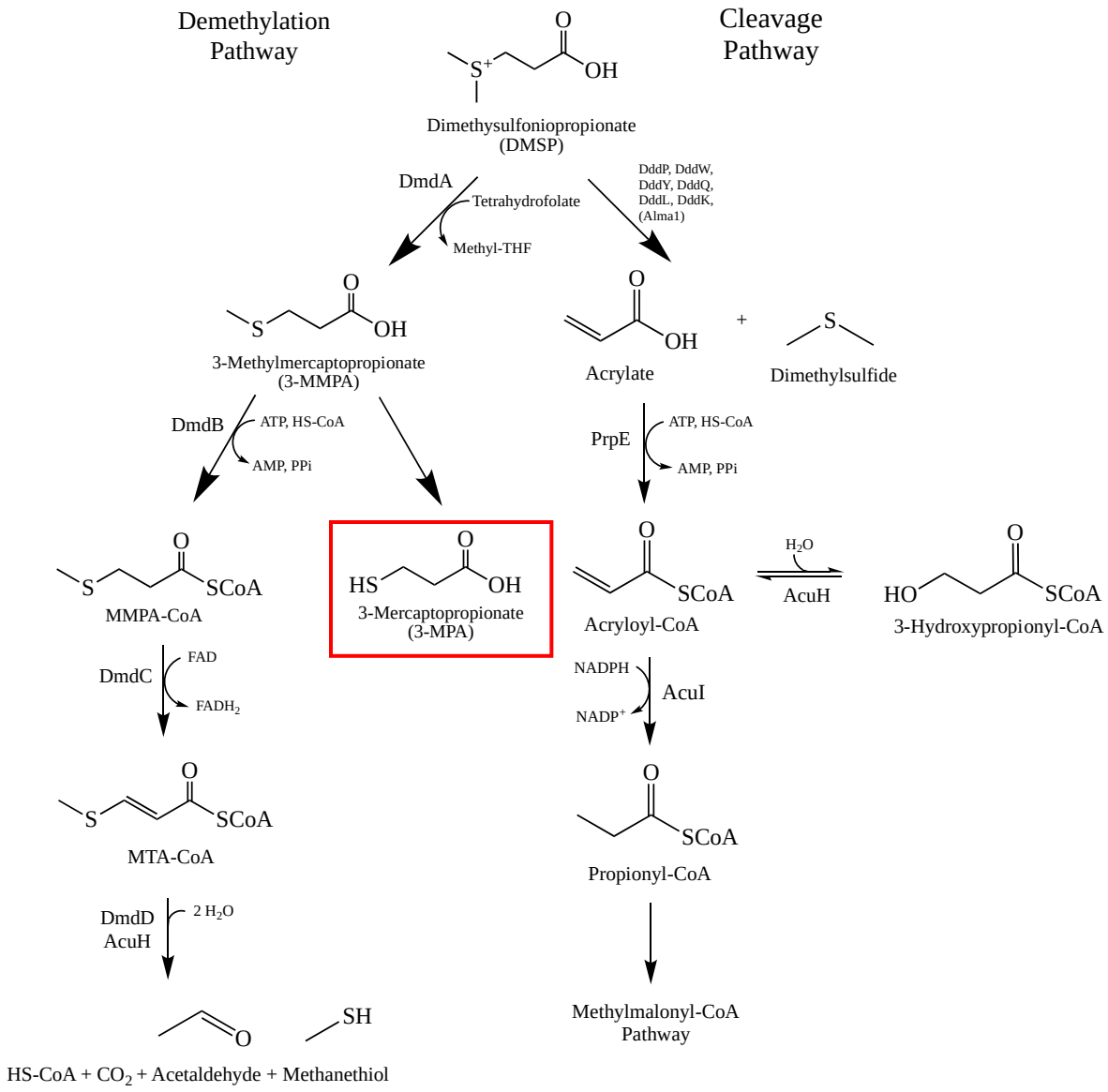

Figure 1.19. Organic sulfur compound degradation. The DMSP demethylation pathway is catalyzed by DmdA (DMSP demethylase), DmdB (MMPA-CoA ligase), DmdC (MMPA-CoA dehydrogenase, and either DmdD (MTA-CoA hydratase) or AcuH (acrylate utilization hydrotase). The cleavage pathway is catalyzed by DMSP lyase (DddP, DddW, DddY, DddQ, DddL, DddK, or the algaI AlmaI), PrpE (acrylate-CoA ligase), and AcuI(acryloyl-CoA reductase). AcuH catalyzes a side reaction that forms 3-hydroxypropionyl-CoA in the cleavage pathway. (Adapted from [71,73,74]).

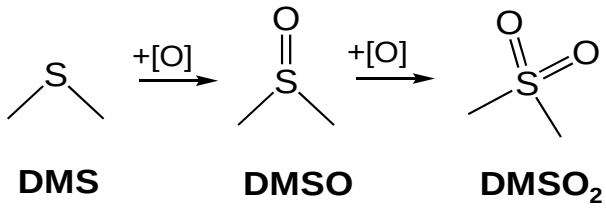

Figure 1.20. Non-enzymatic oxidation of DMS to $DMSO_2$. (Adapted from [29]).

1.5 Sulfurtransferases and Proposed Physiological Roles

Sulfurtransferases are made up of a group of enzymes widely dispersed in nature. They are found in plants, animals, bacteria, and archaea. Sulfurtransferases catalyze the transfer of a sulfane sulfur atom from a donor molecule to a thiophilic acceptor substrate, such as thiols, cyanide, sulfite and sulfinates.[75] Structural modules within sulfurtransferases are well-defined. They exist as tandem repeats, with the C-terminal domain containing the active site cysteine residue.[76] They also can be found as single-domain proteins or as members of multi-domain proteins.[76,77] Results from *in vitro* assays have shown sulfurtransferase activity to be associated with rhodanese-like domains, however the specific role of these domains have yet to be identified. There are distinct members within the sulfurtransferase family (rhodanese, thiosulfate sulfurtransferase, and 3-mercaptopyruvate sulfurtransferase) that are closely related by their primary amino acid sequence as well as the type of reaction they are able to catalyze.[75] The major differences between these sulfurtransferases are conserved amino acids within the active site. The conserved motif found within thiosulfate sulfurtransferase is CRXGX[R/T], while 3-mercaptopyruvate sulfutransferase has a CG[S/T]GVT motif, respectively.[78] There have been no conserved motifs identified for rhodanese. The properties of these amino acids within the active site loop of the sulfurtransferases correlates with the ionic charge of their *in vitro* substrates.[77,78] The thiosulfate sulfurtransferase catalyzed reaction is similar to the rhodanese reaction in which the cleavage of the sulfur-sulfur

bond of the sulfur-donor substrate with transfer or the sulfane sulfur to a sulfhydryl nucleophile. However, the enzymes differ in both acceptor substrate specificity and mechanism. Unlike MST and rhodanese, thiosulfate sulfurtransferase will use GSH or cysteine as an acceptor substrate, but is not able to use cyanide There are many proposed physiological reactions for these enzymes, including control over the cytotoxicity of reactive oxygen species in aerobic tissues, cyanide detoxification, sulfur metabolism, Fe-S cluster biosynthesis and repair, and H_2S.[75,79–84]

1.5.1 Rhodanese Enzymes (Thiosulfate:Cyanide Sulfurtransferase)

Rhodanese is the most well-characterized type of sulfurtransferase and is properly named thiosulfate:cyanide sulfurtransferase based on the reaction it catalyzes. In the overall reaction, a persulfide intermediate is formed by transferring the sulfur atom of the thiosulfate to an active site cysteine. The persulfide intermediate is then attacked by the cyanide ion to produce thiocyanate (Figure **1.21**). Cyanide is produced by bacteria for defense purposes and is highly toxic in most living organisms because of its ability to form stable complexes with transition metals. Rhodanese enzymes are very promiscuous with respect to sulfur donors and acceptors.[80,85] For example, both thiosulfonates and persulfides are able to function as sulfur donors. For the sulfur acceptors, cyanide may be substituted by various dithiol compounds, sulfinates, or sulfite.[80,85]

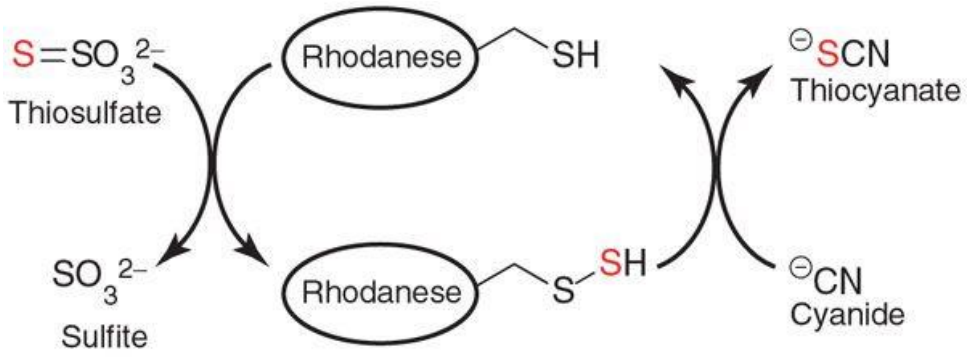

Figure 1.21. The active site cysteine receives sulfane sulfur from thiosulfate and releases it to cyanide. (Adapted from [19]).

Rhodanese is a ubiquitous enzyme that has been purified and characterized from several prokaryotes and eukaryotes. In mammals, rhodanese is found in the mitochondrial membrane and matrix of liver and kidney tissues[86] Recombinant rhodaneses from different animal tissues have been expressed in *E. coli*. The first three-dimensional structure of a rhodanese was determined for bovine liver rhodanese.[87,88] The enzyme is approximately 32 kDa and is comprised of two comparable structural domains. These two structural domains have been considered to be generated by gene duplication from a common ancestral protein. The conformational similarity was maintained under selective pressure, but the sequence conservation was lost. Even though these two domains are similar in conformation, only the C-terminal domain contains the catalytic cysteine in its active site. This cysteine is replaced by Asp in the N-terminal domain. The C-terminal domain is referred to as the catalytic domain, while the N-terminal domain is considered a pseudorhodanese domain. The Cys247 thiolate anion is the essential nucleophile, while the positive charges of a nearby Arg and Lys may play a role in binding the thiosulfate in the correct orientation (Figure **1.22**).[39,79,89–91] Single catalytic rhodanese domains have also been identified in some sulfurtransferases. These single domain rhodanese have been connected with proteins involved in stress responses. [92]

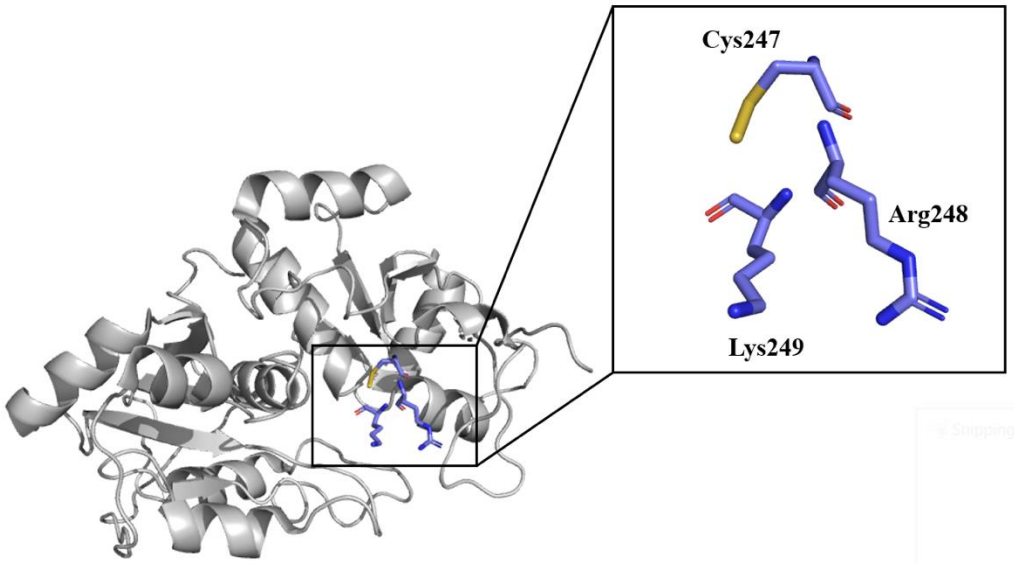

Figure 1.22. Structure of bovine rhodanese domain with thiosulfate forming a persulfide at Cys247. Active site containing the cysteine responsible for activity and Arg and Lys residues responsible for substrate binding. PDB: 1RHD.[90]

1.5.2 3-Mercaptopyruvate Sulfurtransferase (MST)

3-Mercaptopyruvate sulfurtransferase is evolutionarily related to rhodanese and functions in the detoxification of cyanide and mediates the transfer of a sulfur ion to cyanide or other thiol compounds, as shown in the reactions below (Figure **1.23**).

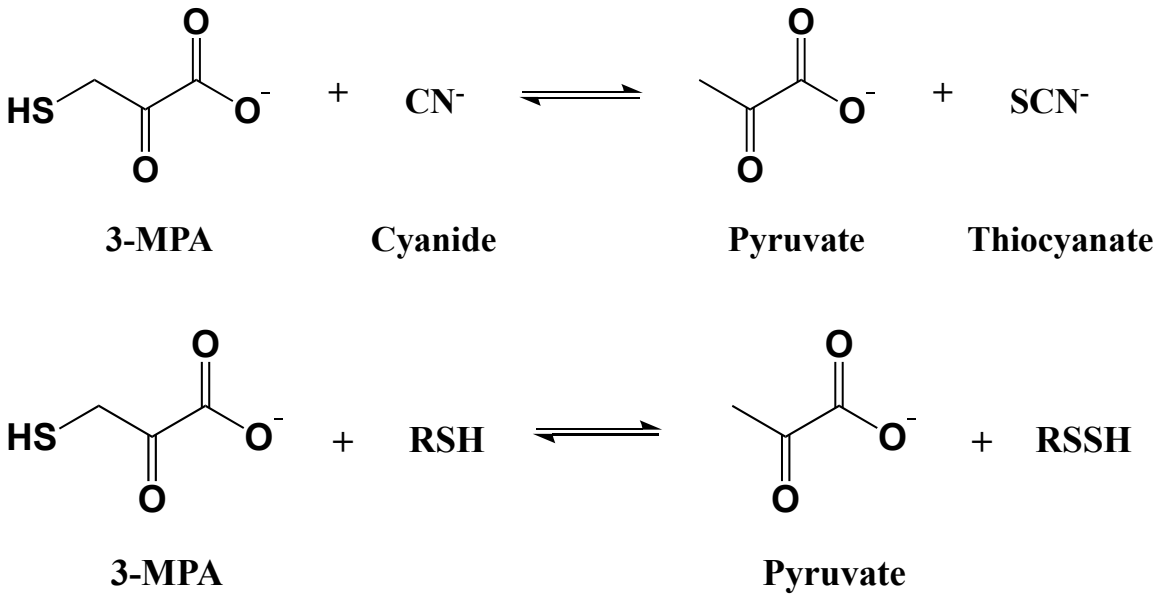

Figure 1.23. Two types of MSTs reactions, in which 3-mercaptopyruvate is used as the sulfur donor and catalyzes the transfer of sulfur from various thiophiles such as sulfite, cyanide, and low molecular weight thiols.

MST is found among prokaryotes and eukaryotes. MST and cysteine aminotransferase contributes to the catabolism of cysteine, and the generation of hydrogen sulfide in the brain, retina, and vascular endothelial cells.[93] This enzyme is also involved in the maintenance of cellular redox homeostasis and defense against oxidative stress.[94] Similarly to rhodanese, MST contains a catalytic cysteine which contributes to redox-dependent regulation as well as the conserved arginine residue. However, the active site residues Arg and Lys found among rhodaneses, are replaced by Gly and Ser in MST (Figure **1.24**). A decrease in rhodanese activity was observed with a concurrent increase in MST activity after substituting the Arg and Lys residues of rhodaneses with Gly and Ser.[94] The same group was also able to successfully convert MST from

Leishmania major, to a rhodanese by replacing the Gly and Ser with the Arg and Lys found within the active site of rhodanese.[95]

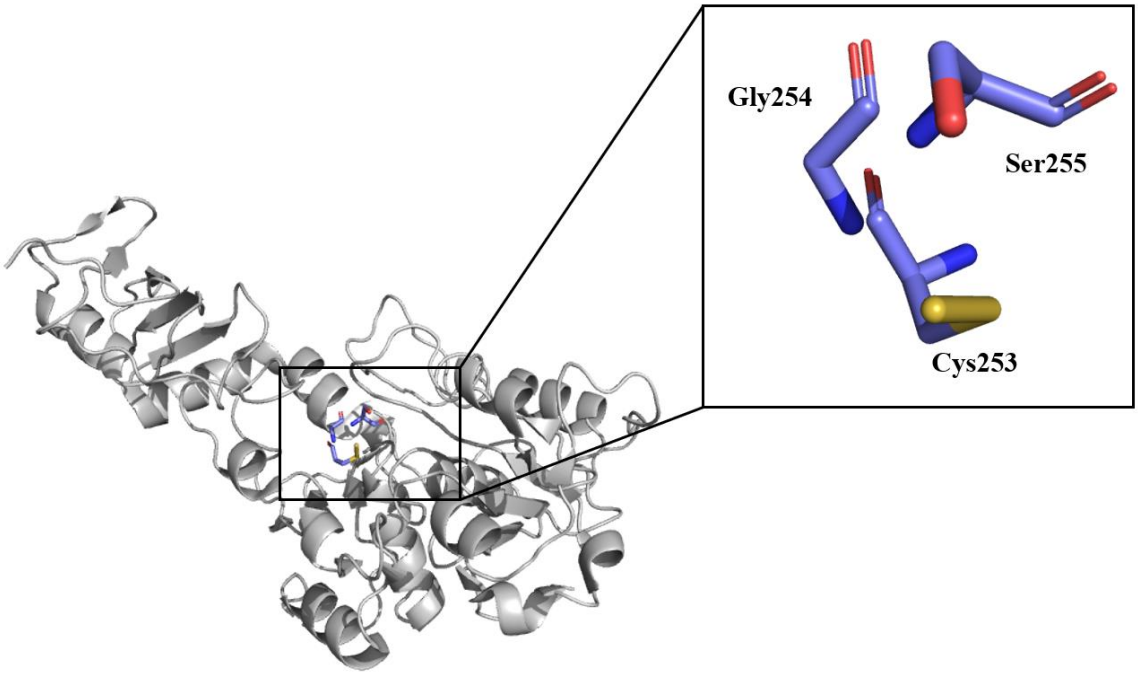

Figure 1.24. Crystal structure of 3-mercaptopyruvate sulfurtransferase from *Leishmania major* soaked with 3-mercaptopyruvate forming a persulfide at Cys253. Active site containing the cysteine responsible for activity and Ser and Gly residues responsible for substrate binding. PDB: 1OKG.[96]

MSTs have also been identified in plants. Two complementary DNA clones were successfully isolated and characterized from *Arabidopsis thaliana*. Both proteins showed a substrate preference for 3-mercaptopyruvate instead of thiosulfate as the sulfur donor, but were differentially expressed in the mitochondria or cytosol.[97,98]

Recently, a gene (*sseA*) from *E. coli* was identified and shown to have MST activity.[99] This is the first prokaryotic gene to be identified and characterized among the MST enzymes. The active site motif in SseA is similar to eukaryotic MSTs, which further suggests these enzymes prefer 3-mercaptopyruvate as a substrate over thiosulfate.[99] Moreover, several studies have shown that SseA is unable to form an active site cysteine persulfide with thiosulfate as a substrate as is commonly observed for sulfurtransferases.

1.5.3 Thiosulfate:Thiol Sulfurtransferase (TST)

Thiosulfate:thiol sulfurtransferases (thiosulfate reductase) are widespread in nature.[80] These enzymes use electrons from glutathione (GSH) *in vivo* in order to reduce the sulfane sulfur atoms of inorganic thiosulfate and organic thiosulfonate anions to sulfide (Figure **1.25**).[100] Several studies suggest that TSTs are used in the formation of iron sulfur cluster proteins.[101–103]

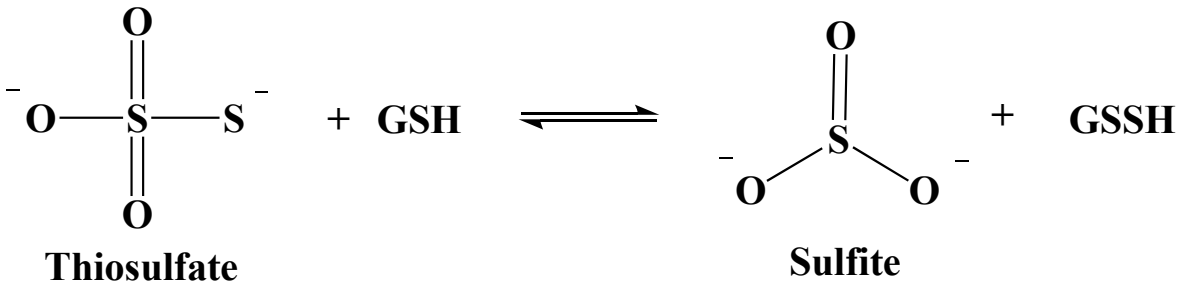

Figure 1.25. Thiosulfate sulfurtransferase reaction.

Thiosulfate sulfurtransferase (TST) is found in the heart, liver, brain, and kidney of eukaryotes, similar to that of MSTs. The yeast enzyme has been purified and characterized, and is a monomer with an apparent molecular weight of 17,000 Da. The donor substrates of yeast were determined to be $S_2O_3^{2-}$ and $RS(O_2)S^-$, and the acceptor substrates were GSH, homocysteine and

cysteine.[100] The sulfhydryl group of thiosulfate sulfurtransferase contains only one cysteine residue, but it does not form a persulfide intermediate. The enzyme uses the sulfhydryl group of the acceptor substrate to cleave the sulfur-sulfur bond of the donor substrate. Moreover, this enzyme requires a thiol substrate for persulfide production.[100] However, when cyanide is available, the sulfur from the persulfide can transfer to cyanide and produce thiocyanate nonenzymatically.[100]

1.5.4 Uncharacterized Sulfurtransferase Proposed Functions

Although there are several different organisms that have characterized sulfurtransferases, their detailed physiological functions often remain unknown. Sulfurtransferases have many functions such as the biosynthesis of sulfur containing cofactors, cyanide detoxification, biosynthesis of thionucleosides, utilization of sulfur for biosynthetic repair of iron sulfur clusters, selenium metabolism, and several aspects of sulfur metabolism in general. Sulfurtransferases are a diverse group of enzymes and play a critical role in the transfer of sulfur in diverse metabolic processes.

1.6 Dioxygenase and Sulfurtransferase Coupled Reactions

In various bacteria, the MDO gene is on the same operon as an annotated sulfurtransferase, but the presence of the sulfurtransferase gene has not been recognized. The sulfurtransferase contains multi-rhodanese domains with the C-terminal domain containing the CGSSLL motif, which is similar to the 3-mercaptopyruvate sulfurtransferase motif CG(T/S)GV(T/S). Recently, natural fusions between a non-heme iron containing dioxygenase and rhodanese have been identified in some bacterial systems. However, the metabolic role of these dioxygenase-rhodanese fusions has yet to be identified.[104]

In several bacteria, cystathionine β-synthase (CBS), cystathionine Δ-lyase (CSE), and 3-mercaptopyruvate sulfurtransferase (MST), are three major H_2S generating enzymes that enhance resistance to oxidative stress.[101] *Staphylococcus aureus* relies on CBS and CSE for the synthesis of endogenous H_2S. [101] Endogenous production of H_2S by pathogenic bacteria enhances their pathogenicity and survival, however a high cellular bisulfide level is toxic.[105] Therefore, regulation of intracellular H_2S concentrations is required. In *S. aereus,* the *cst* (copper-sensing operon repressor-like sulfur transferase) operon has been suggested to play a crucial role in sulfide detoxification.[101] The *cst* operon encodes *cstA, cstB,* and *sqr* to alleviate the effects of cellular hydrogen sulfide toxicity.[101,106] SQR encodes a sulfide:quinone oxidoreductase and is responsible for mitigating the effects of cellular sulfide toxicity.[101,106] CstA is characterized as a multidomain sulfurtransferase that reacts with a persulfide formed on SufS.[101,107] CstB consists of three domains containing an N-terminal metallo-β-lactamase-like (MBL), non-heme Fe(II)-containing PDO (persulfide dioxygenase) domain, a pseudo-rhodanese homology (RHD) domain, and a C-terminal rhodanese (Rhod) domain (Figure **1.26**).[101] In *S. aureus,* H_2S is converted to bisulfide (HS^-) in the cytoplasm, in which the bisulfide is bound to sulfide:quinone oxidoreductase (SQR) to form SQR-bound persulfide (Figure **1.27**).[101] The bisulfide is transferred to the reduced cellular low molecular weight thiol (LMW-SH) by a reaction that eventually forms a LMW persulfide (LMW-SSH). However, a LMW-SSH can also be formed directly by HS^- when molecular oxygen (O_2) is available.[101] $CstB^{PDO}$ is able to oxidize LMW persulfides to LMW-S-sulfonate or CstB-S-sulfonate ($R\text{-}S\text{-}SO_3^-$). The thiosulfate (TS) is produced by $CstB^{Rhod}$ (or other cellular rhodanese proteins) through persulfide transferase activity, or directly by the LMW persulfide reacting with CstB-S-sulfonate or LWW-S-sulfonate (Figure **1.27**).[101] The thiosulfate is catalyzed by $CstB^{Rhod}$, $CstA^{Rhod}$, or similar thiosulfate sulfurtransferases, to SO_3^{2-} and sulfane sulfur (S^0). Finally, the sulfite is

exported from the cell by TauE and sulfane sulfur is proposed to be transferred to a cellular sulfur acceptor for further assimilation.[101] Similar rhodanese systems have been identified in human pathogenic bacteria and proposed to regulate intracellular bisulfide concentrations.[101]

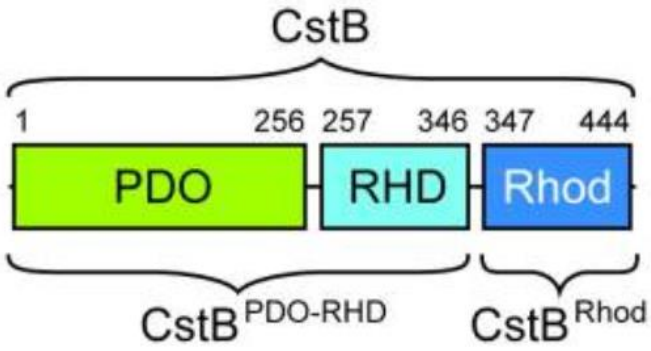

Figure 1.26. Domain organization of *S. aureus* CstB, with N-terminal persulfide dioxygenase (PDO) domain, middle rhodanese homology domain (RHD), and C-terminal rhodanese domain (Rhod). (Adapted with permission from [101]). Copyright (2015) American Chemical Society.

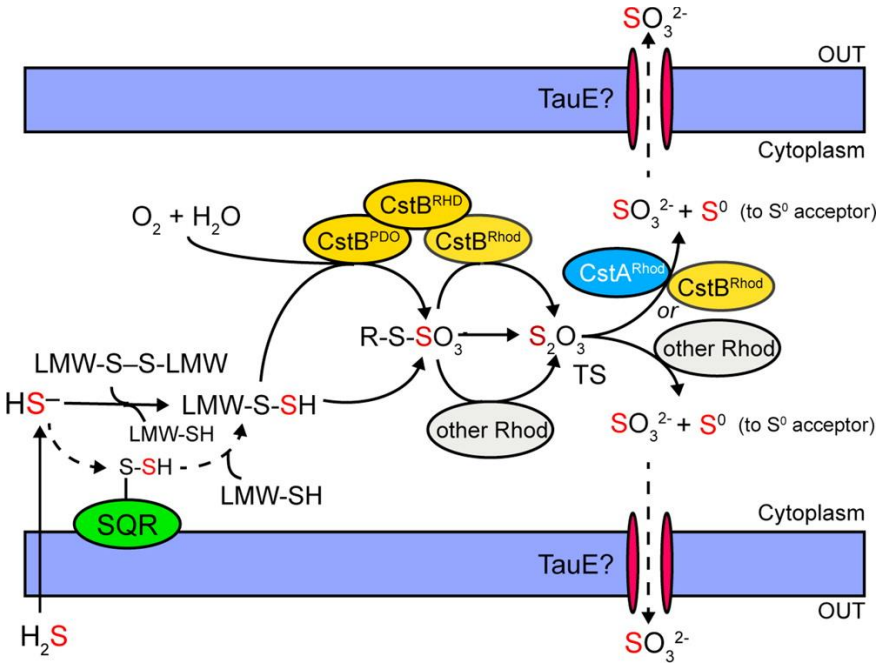

Figure 1.27. Proposed model for cellular H_2S detoxification by *cst* operon enzymes in *Staphylococcus aureus*. (Adapted with permission from [101]). Copyright (2015) American Chemical Society.

Biogenesis of H_2S in mammalian systems involves transulfuration pathway enzymes cystathionine β-synthase (CBS) and cystathionase (CSE). CBS and CSE are primarily responsible for production of H_2S, while the mitochondrial sulfide oxidation pathway is responsible for catabolism of H_2S. Catabolism of H_2S takes place in the mitochondria and connects sulfur metabolism to the electron transport chain, therefore providing a link to sulfide oxidation with ATP and reactive oxygen species production. Sulfite oxidase, rhodanese, sulfide quinone oxidoreductase and persulfide dioxygenase (ETHE1) control low levels of H_2S by oxygen-dependent catabolism.[108] Recombinant human ETHE1 was expressed in *E. coli* and exhibited sulfur-dependent oxygenase activity, in the presence of glutathione persulfide (GSSH).[108] ETHE1 is a proposed sulfur dioxygenase that catalyzes the second step in the mitochondrial sulfide

oxidation pathway downstream of a sulfide quinone oxidoreductase by converting persulfide to sulfite.[108] Sulfide quinone oxidoreductase uses a quinone to oxidize H_2S to a persulfide, which is bound to an active site cysteine (SQR-SSH) and transfers the electrons to the electron transport chain. (Figure **1.28**)[108]. Transfer of the persulfide from sulfide quinone oxidoreductase to glutathione or a similar acceptor provides ETHE1 with a persulfide substrate that is further oxidized to sulfite. [108] Finally, rhodanese catalyzes the conversion of sulfite to thiosulfate or sulfite is further oxidized to sulfate by sulfite oxidase to prevent toxicity.[108]

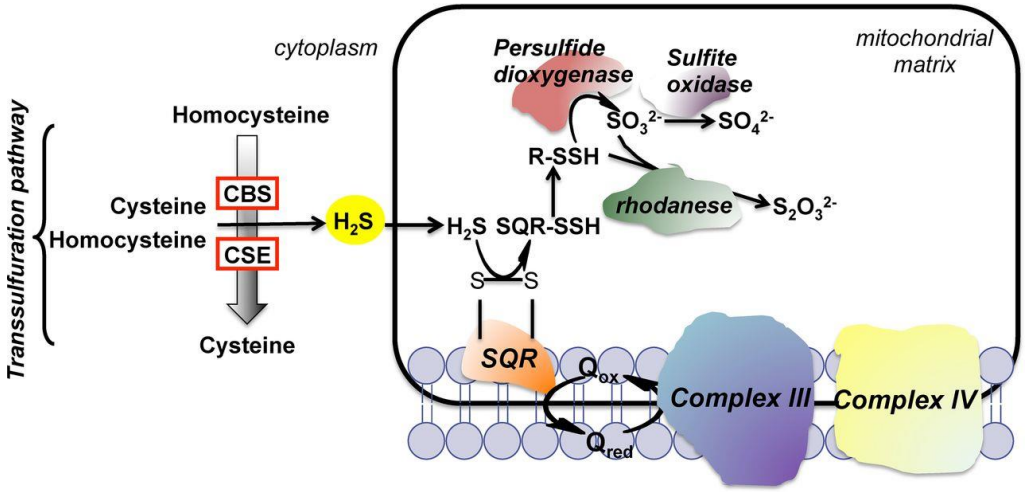

Figure 1.28. Pathway for H_2S biogenesis and degradation. (Adapted with permission from [108]). Copyright. (2012). The Journal of Biological Chemistry.

In bacteria, *ETHE1*-like sequences are on the same operon or are fused with orthologs of thiosulfate sulfurtransferases, which suggests they could interact. Natural fusions between other PDO and rhodanese have also been recently identified in bacterial proteins.[101,104] These fusion proteins are referred to as PRF (PDO rhodanese fusion). The existence of PRFs in nature suggest that their mitochondrial homologs, which exist as stand-alone proteins, might interact.[104] However, interaction studies over these PRFs have not been performed. CstB and *Alicyclobacillus*

acidocaldarius PRF are the only two available structures of PRFs, however, CstB is the only PRF that has been biochemically characterized. Therefore, the role of these bacterial PRFs in sulfur metabolism and how they may interact is still unknown. However, fusion of the PDO and rhodanese domain in bacteria could increase their effective local concentration and promote transfer of substrate between them.

1.7 Summary

Sulfur is essential for all organisms as a component of amino acids and enzyme cofactors. In many bacterial organisms, sulfur is acquired through sulfate assimilation pathways leading to the production of sulfide, which is then incorporated into sulfur-containing organic molecules.[29] Often, bacteria reside in environments with low sulfate availability and therefore, can utilize organosulfonates as an alternative source of sulfur through desulfonation. Desulfonation of organosulfonates requires cleavage of the carbon-sulfur bond by either alkanesulfonate monooxygenase or taurine dioxygenase thus releasing sulfite. In aerobic bacteria, organosulfonates serve as a sulfur source when desulfonation enzymes are induced by sulfate-starvation-induced (*ssi*) stimulon.[33] Ssi proteins play an important role in sulfur acquisition from organic compounds, organosulfur uptake, and protection against ROS.

In prokaryotes and eukaryotes, cysteine is utilized in many metabolic processes including redox signaling, biosynthesis of thiol containing cofactors, protein synthesis, and catabolic reactions. Cysteine is involved in diverse metabolic pathways, including the oxidation of L-cysteine to L-cysteine sulfinic acid which is catalyzed by cysteine dioxygenase. Cysteine sulfinic acid is an imperative branch point in sulfur metabolism because of its ability to form pyruvate and sulfite or taurine. These metabolites formed are essential for many metabolic processes, therefore,

the absence of cysteine dioxygenase can lead to an increase in cysteine concentrations, which in mammals often leads to many neurodegenerative diseases.

Mammalian CDO contains a ferrous iron center that is coordinated by 3-His residues and contains a Cys residue in place of the Glu residue, which is typically found in many members of the cupin superfamily. There is a key Tyr157 residue adjacent to the iron center that participates in a thioether crosslink with Cys93. A conserved active site Arg residue is located in mammalian CDO that is responsible for substrate specificity. Putative CDO enzymes have also been identified in several different bacterial organisms.

"Gln-type" bacterial enzymes typically have less than a 30% amino acid sequence identity with mammalian CDO and has a cupin fold comparable to mammalian CDO. However, all knowns bacterial thiol dioxygenase enzymes lack the Cys-Tyr crosslink. The bacterial CDO homologs are often divided into two subclasses based on the presence of a conserved Arg or Gln residue within the active site. These residues have been proposed to confer substrate specificity similar to the Arg residue in mammalian CDO. Several substrates including 3-mercaptopropionate, have been proposed for bacterial MDO.[109] Although, 3-mercaptopropionate is the most commonly proposed substrate, the physiological relevance of 3-MPA is unclear. In various bacteria, the *mdo* gene is on the same operon as an annotated sulfurtransferase, but the presence of the sulfurtransferase gene has not yet been recognized. Sulfurtransferases and dioxygenases have been found on the same operon in other systems, and there are three proposed mechanisms in which dioxygenases utilize the product of the reaction catalyzed by sulfurtransferases. Therefore, MDO and the sulfurtransferase could be metabolically linked.

The focus of this dissertation is to determine how substrate specificity is defined by CDO and MDO. Additional studies are focused on identifying the physiological substrate for MDO and how

MDO and the sulfurtransferase are metabolically linked. Studies presented in this dissertation will focus on structural, kinetic, and spectroscopy studies of MDO. Coupling of MDO with the sulfurtransferase to determine potential protein-protein interaction as well as understanding the function role of the two enzymes in bacteria. Lastly, these studies of the MDO/sulfurtransferase system represents an additional pathway for bacteria to adapt to sulfur limiting conditions that have not been previously identified.

CHAPTER TWO

Bacterial Thiol Dioxygenase Metabolic Pathway and Substrate Identification

2.1 Introduction

CDO is a mononuclear iron enzyme that catalyzes the oxidation of L-cysteine to L-cysteine sulfinic acid.[110,111] The CDO metal center is coordinated by 3-His residues and deviates from the typical 3-His/1-Glu metal coordination motif found in many members of the cupin superfamily. The Glu is replaced by Cys in CDO resulting in a thioether crosslink formed between residues Cys93-Tyr157.[55–57,112] A heterogeneous mixture of crosslinked and noncrosslinked isoforms are present in the purified recombinant mammalian CDO. Previous studies have shown that the crosslink stabilizes the iron center and increases activity.[60] Putative CDO enzymes have also been identified in several bacteria; however, all known bacterial CDO enzyme homologs lack the Cys-Tyr amino acid derived cofactor due to the Cys residue (Cys93) being replaced by Gly.[66]

Bacterial thiol dioxygenases also belong to the cupin superfamily in which they contain an active site mononuclear iron center for thiol oxidation. There are two thiol dioxygenases found among bacteria that have been suggested to catalyze two different reactions. Thiol dioxygenases containing the conserved Arg residue catalyze the oxidation of L-cysteine to cysteine sulfinic acid.[66] In some thiol dioxygenases the conserved Arg is replaced with a Gln. (Figure **2.1**)[64,113,114]. These enzymes, referred to as 3-mercaptopropionate dioxygenases (MDO), catalyze the oxidation of 3-mercaptopropionate (3-MPA) to sulfinopropionic acid.

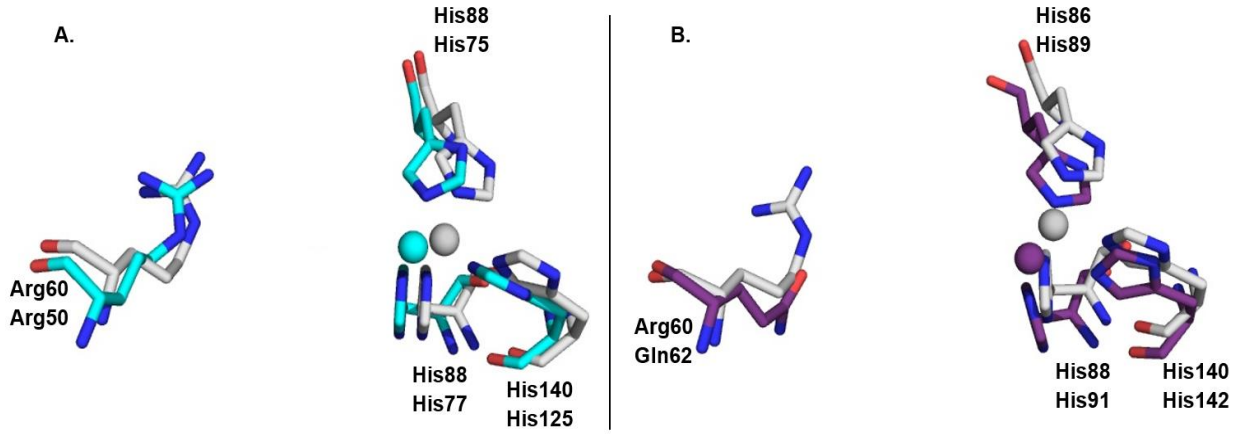

Figure 2.1. Three-dimensional structure comparing conserved residues in mammalian and bacterial CDO. **A.** Similar to CDO found in *R. norvegicus* (grey), CDO in *B. subtilis* (teal) contains a 3-His coordinated iron and an Arg in a similar position as Arg60. PDB: 2B5H and 4QM9. **B.** A 3-His coordinated iron is found in both *R. norvegicus* (grey) and *P. aeruginosa* (purple). However, in *P. aeruginosa* the Arg60 is replaced with a Gln residue. PDB: 2B5H and 4QM9.[2,63,67]

In order to determine the functional importance of the conserved active site arginine, single point mutations in CDO were made. Arg60 in CDO was substituted with an alanine and glutamine residue and the activity was evaluated with L-cysteine.[57] Both variants displayed a ~50% decrease in iron content and a ~70% decrease in catalytic activity compared to wild-type CDO.[57] It was suggested that the diminished activity was due to the lack of iron coordination; however, the decrease in iron content did not fully account for the decrease in activity.[57] Based on the three-dimensional structure, the guanidinium group of Arg60 is extended towards the iron center in the absence of the Cys substrate. When the Cys substrate is bound, the guanidinium group of Arg60 moves away from the iron center and is within 3 Å away from the carboxylate group of the Cys substrate (Figure **2.2**).[56] These combined studies suggest that Arg60 participates in the substrate specificity of mammalian CDO by coordinating the Cys substrate.[56,57,64]

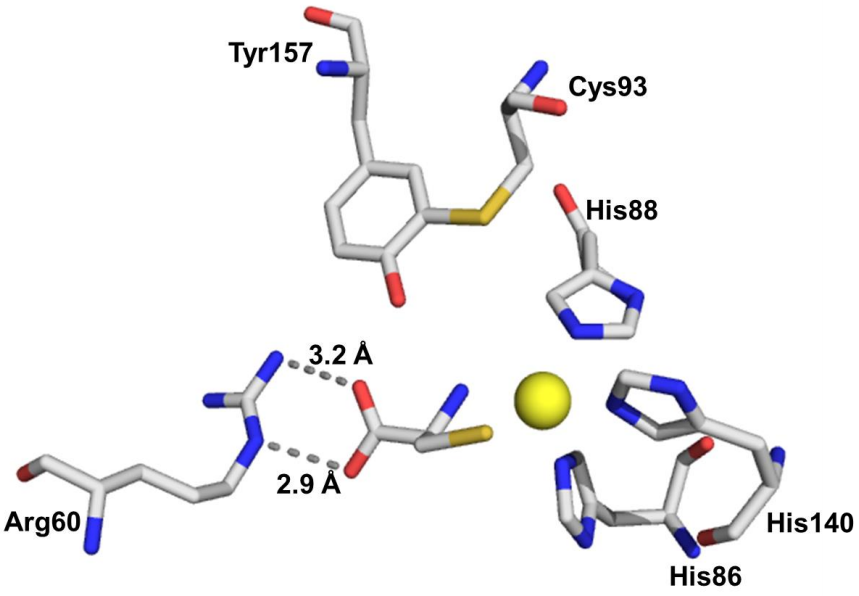

Figure 2.2. The guanidium of Arg60 is within 3 Å away from the carboxylate group of the Cys substrate. PDB: 4IEV.[62]

For the studies described herein, the Cys involved in thioether crosslink formation in mammalian CDO was substituted with Gly to mimic bacterial CDO. The role of Gln62 in MDO was also evaluated to determine if it is involved in substrate specificity similar to Arg60 in mammalian CDO. Previous studies have investigated the catalytic role of Arg60 in mammalian systems based on several mutations, however, there have been no studies performed on Gln62 MDO. By constructing these variants, the functional role of Cys93, Gln62, and Arg60 were probed by both kinetic and spectroscopic studies to examine the substrate specificity among thiol dioxygenases. These results from these studies further define how conserved amino acids in thiol dioxygenases contribute to catalytic function.

2.2 Materials and Methods

2.2.1 Materials

4-(2-Hydroxyethyl)piperazine-1-ethanesulfonic acid (HEPES), L-cysteine, 3-mercaptopropionate, sodium mercaptopyruvate, L-ascorbate, ampicillin, streptomycin sulfate, lysozyme, potassium chloride, ferrous ammonium sulfate, (3-(2-Pyridyl)-5,6-diphenyl-1,2,4-triazine-*p,p'*-disulfonic acid monosodium salt hydrate) ferrozine, and brilliant blue R were purchased from Sigma (St. Louis, MO). Isopropyl-β-d-thiogalactoside (IPTG) was purchased from Gold Biotechnology (St. Louis, MO). Glycerol and sodium chloride were purchased from Macron Fine Chemicals (Center Valley, PA). Difco-brand Luria-Bertani (LB) medium was purchased from Becton, Dickinson and Company (Sparks, MD). Oligonucleotide primers were purchased from Invitrogen (Carlsbad, CA). Pfu Turbo DNA polymerase was purchased from Agilent (La Jolla, CA). Herculase polymerase was purchased from Agilent (La Jolla, CA). Macro-prep® High Q Support was purchased from Bio-Rad Laboratories (Herculase, CA), SDS-PAGE resolving and stacking buffers, 30% acrylamide, and Blue Laemmli was purchased from Bio-Rad Laboratories (Herculase, CA). Amicon Ultra-4 Centrifugal Filter Devices (10 kDa MWCO) were purchased from Millipore (Billerica, MA).

2.2.2 Protein Expression and Purification of C93G and R60Q CDO

The cDNA gene for rat *cdo* was cloned into the pET21a expression vector as previously described.[113] The pET21a vector containing the rat *cdo* gene was used to construct the rat CDO variants (C93G and R60Q CDO) by site-directed mutagenesis. The primers for these variants were designed as 27 base oligonucleotides. In order to generate these variants, the Cys93 codon (TGC) in wild-type CDO was replaced with GGT (Gly), and the Arg60 codon (CGT) in wild-type CDO was replaced with CAG (Gln). These substitutions were confirmed by DNA sequence analysis (Eurofins MWG Operon). Both CDO variants were transformed into BL21(DE3) *E.coli* competent cells and stored as glycerol stocks at -80°C for further analysis.

To obtain purified CDO variants, the cells containing the CDO plasmid were isolated on LB-agar plates containing 0.1 mg/mL ampicillin (LB-amp). A single colony was selected from the plates and inoculated into 5 mL LB-amp medium and incubated at 37 °C for ~8 hours. A 1% inoculum from the overnight 5 mL culture was used to inoculate a 100 mL LB-amp and grown overnight at 37 °C. 20 mL of the overnight culture was used to inoculate 4 separate 1 L LB-amp flasks and grown at 37 °C until the cultures reached an A_{600} value of 0.4-0.6. The cells were induced with 0.4 mM IPTG and grown at 25 °C for an additional 6 hours. Cells were harvested by centrifugation at 5000 rpm for 20 minutes at 4 °C, and the pellets were resuspended in 25 mM HEPES (pH 7.5) and 10% glycerol supplemented with 2 mg/mL of lysozyme. Resuspended cells were lysed by sonication, followed by centrifugation at 10000 rpm for 15 minutes at 4 °C. Lysate was treated with 1.5% (w/v) streptomycin sulfate and stirred at 4 °C for 1 hour. The solution was centrifuged at 10000 rpm at 4°C for 20 minutes. Following centrifugation, the supernatant was then loaded on to a Macro-Prep® High Q support column. Protein was eluted from the column using a linear gradient from 0-150 mM sodium chloride in 25 mM HEPES (pH7.5) and 10% glycerol. Fractions were evaluated by SDS-PAGE, and fractions with the highest purity were pooled and iron loaded with a molar ratio of 1:1 ferrous ammonium sulfate:protein. Samples were dialyzed twice against one liter 25 mM HEPES (pH 7.5) containing 100 mM sodium chloride and 10% glycerol at 4 °C to remove excess iron. Aliquots of the protein were flash frozen and stored at -80°C.

Ferrozine was used to determine the amount of iron present in the purified protein as previously described with slight modifications.[114] CDO samples (10 µM) were incubated at 95 °C for 5 minutes with ferrozine (250 µM) and ascorbate (18 mM). After 5 mins, sodium acetate (1.5 M) was added and the samples were measured at 562 nm. A standard curve (0-15 µM) was created

using iron ICP standards and the standards were treated the same as the CDO samples. A standard curve is needed to determine the actual concentration on Fe^{2+} in the samples, and 25 mM HEPES (pH 7.5) was used as a negative control. The results were based on the average of three separate experiments.

2.2.3 Protein Expression and Purification of Wild-Type MDO and Q62R MDO

The DNA gene for *P. aeruginosa mdo* was cloned into the pET21a expression vector and synthesized by Eurofins Genomics. The *mdo* clone was confirmed by DNA sequence analysis (Eurofins MWG Operon). The MDO variant (Q62R MDO) was constructed by site-directed mutagenesis. Primers for Q62R MDO were designed as 27 base oligonucleotides and the Gln62 codon (CAG) in wild-type MDO was replaced with CGT (Gln). Successful mutations were confirmed by DNA sequence analysis (Eurofins MWG Operon). Both wild-type and Q62R MDO were transformed into BL21(DE3) *E. coli* competent cells and stored as glycerol stocks at -80°C.

Expression and purification of wild-type MDO and the variants were carried out as previously described with minor modifications.[113] Protein was eluted from the column using a linear gradient from 0 – 300 mM NaCl in 25 mM HEPES (pH 7.5) and 10% glycerol. Fraction purity was determined by SDS-PAGE (5% stacking with 12% resolving), and fractions with the highest purity were pooled and dialyzed twice against two liters of 25 mM HEPES (pH 7.5), 10% glycerol and 100 mM sodium chloride at 4 °C. Aliquots were flash frozen and stored at -80°C. The amount of iron present within the protein was determined by a ferrozine colorimetric assay as previously described.[114]

2.2.4 Circular Dichroism

Protein samples were buffer exchanged with 10 mM potassium phosphate (pH 7.5) using a 10 000 kDa MWCO Amicon Ultra Centrifugal Filters (Millipore) at 5000 RPM at 4°C. Far-UV circular dichroism spectra were obtained on a JASCO J-810 spectropolarimeter. Spectra of all enzymes (10 μM) were taken in 0.1 nm increments in continuous scanning mode from 300 to 185 nm in a 0.1 cm cuvette with a bandwidth of 1 nm and a scanning speed of 20 nm/min. Each spectrum is an average of eight scans. Background subtraction and smoothing of each data set were performed using the software provided. Final data were plotted using KaleidaGraph™ software (Synergy Software, Reading, PA).

2.2.5 Steady-State Kinetic Analyses of Wild-type MDO, Variants, and CDO Variants

Steady-state kinetic parameters were determined using a Clark-type oxygen electrode (Hansatech, Inc., Norfolk, United Kingdom) to monitor the rate of dioxygen utilization by each enzyme in the presence of substrate. Each reaction contained a final concentration of 2 μM protein and 1 mM ascorbate in 25 mM HEPES (pH 7.5) at 37 °C. The assays for wild-type CDO were initiated by the addition of L-cysteine (0.2 uM to 5 mM) or 3-MPA (1-50 mM), and the initial velocities were recorded from the linear portion of the trace. The assays for the CDO variants were initiated by the addition of L-cysteine (1-25 mM) or 3-MPA (1-25 mM), and the initial velocities were recorded from the linear portion of the trace. The assays for wild-type MDO were initiated by the addition of L-cysteine (1-25 mM) or 3-MPA (0.1-1 mM), and the initial velocities were recorded from the linear portion of the trace. The assays for the MDO variant was initiated by the addition of L-cysteine (1-25 mM) or 3-MPA (1-25 mM), and the initial velocities were recorded from the linear portion of the trace. The average initial velocities from three separate experiments were plotted against the substrate concentration and the data were fit to the Michaelis-Menten equation using KaleidaGraph™ software.

2.2.6 Crosslink Formation Studies of Wild-type and R60Q CDO

Crosslink formation was analyzed by varying L-cysteine concentrations. Each reaction contained 5 μM wild-type or R60Q CDO and incubated with 1mM ascorbate and 100 mM L-cysteine in 25 mM HEPES (pH 7.5) at 37 ℃ with gentle shaking over a 2-hour period. After incubation, each sample was quenched with 5 μL sample buffer (Blue Laemmli with 20% (v/v) 2-mercaptoethanol), heat denatured for 3 minutes, and analyzed by SDS (5% stacking, 12% resolving) following staining with Brilliant Blue.

2.2.7 EPR Analysis of Wild-type CDO, C93G CDO, and Wild-type MDO

The oxidation state of the iron center in wild-type CDO, C93G CDO, and wild-type MDO was analyzed by electron paramagnetic resonance spectroscopy (EPR). Samples were prepared by diluting the enzymes to 90 μM in 25 mM HEPES (pH 7.5), 100 mM NaCl, and 10% glycerol in a final volume of 300 μL. When L-cysteine was added to wild-type and C93G CDO, the samples were brought to a final concentration of 10 mM in a final volume of 300 μL. When 3-mercaptopropionate was added to wild-type MDO, the sample was brought to a final concentration of 10 mM in a final volume of 300 μL. EPR studies were performed on a Bruker EMX spectrometer at X-band frequency. Temperature was maintained at 4 K using an Oxford Instruments ESR 900 flow cryostat and an ITC4 temperature controller. All EPR spectra were obtained using the following settings: 9.39 GHz microwave frequency, 0.199 mW microwave power, 2×10^4 receiver gain, 100 kHz modulation frequency, 6 G modulation amplitude, with a time constant of 163.84 ms, and a sweep time of 167.77 seconds.

2.3 Results

2.3.1 Characterization and Steady-State Kinetic analysis of wild-type and C93G CDO

Mammalian CDO contains a conserved Cys (Cys93) residue that forms a thioether crosslink with a nearby Tyr residue (Tyr157). However, in bacteria there is a Gly residue in place of the conserved Cys residue. In this study, the conserved Cys residue in mammalian CDO was altered to Gly in efforts to resemble bacterial thiol dioxygenases. The C93G CDO variant was evaluated by steady-state kinetic analyses to determine the effect of the substitution on catalysis and substrate specificity. The purified C93G CDO variant was annotated as a homogeneously non crosslinked species (Figure **2.3**). Wild-type CDO exists as a heterogeneous mixture of both non crosslinked and crosslinked isoforms. Since C93G CDO is unable to form the thioether crosslink, the mutation existed solely as the noncrosslinked isoform. The % iron bound to each enzyme was determined to be 60% for wild-type CDO and 80% for the C93G CDO variant. Far-UV circular dichroism spectra of wild-type CDO and C93G CDO was obtained to ensure there were no changes to the overall gross secondary structure (Figure **2.4**) The C93G CDO variant had a similar CD spectrum as wild-type CDO.

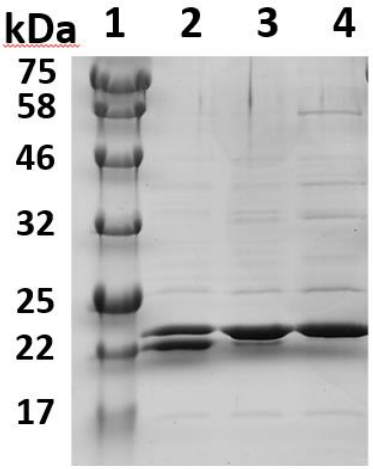

Figure 2.3. Analysis of wild-type, non-crosslinked and C93G CDO by SDS-PAGE. (1) Molecular weight marker, (2) purified wild-type CDO containing a heterogeneous mixture of non-crosslinked and crosslinked isoforms, (3) purified non-crosslinked CDO and (4) purified C93G CDO existing only as the non-crosslinked isoform.

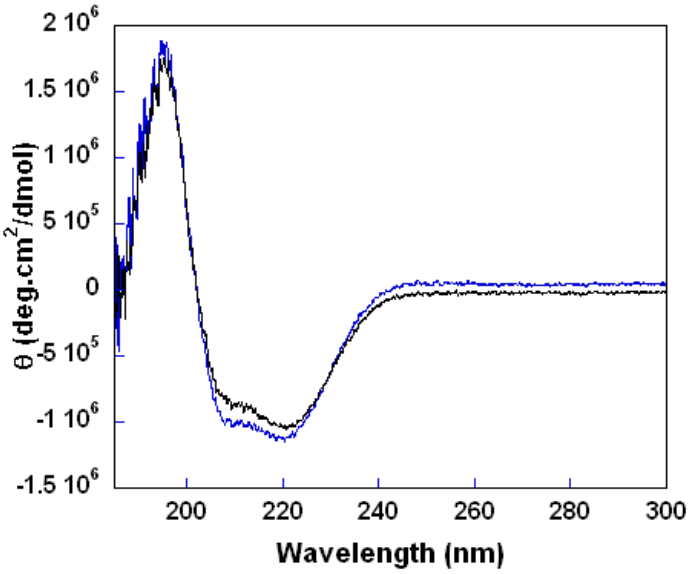

Figure 2.4. Circular dichroism spectra of wild-type and C93G CDO. Wild-type CDO (black line) and C93G CDO (blue line) spectra were taken with 10 μM protein in 10 mM potassium phosphate, pH 7.5.

Kinetic properties of wild-type and C93G CDO with L-cysteine were determined by measuring the rate of dioxygen consumption using a Clark-type oxygen electrode. The k_{cat}/K_m value for C93G CDO resulted in a ~3-fold decrease in catalytic efficiency compared to wild-type CDO (Table **2.1**). To evaluate the substitution with substrate coordination, three analogs of L-cysteine were used: D-cysteine, cysteamine, and 3-MPA (Figure **2.5**). None of the cysteine analogs displayed measurable activity with C93G CDO.

Table 2.1 Steady-state kinetic parameters of wild-type CDO and C93G CDO

	k_{cat} (min^{-1})	K_m (mM)	k_{cat}/K_m (mM^{-1} min^{-1})	% Fe
Wild-type CDO	128 ± 4	0.06 ± 0.01	2133 ± 362	60 ± 2
C93G CDO	56 ± 3	0.07 ± 0.01	756 ± 177	80 ± 3

The concentration of L-cysteine was varied from 0.2-5 mM for wild-type CDO and 10-200 mM for C93G.

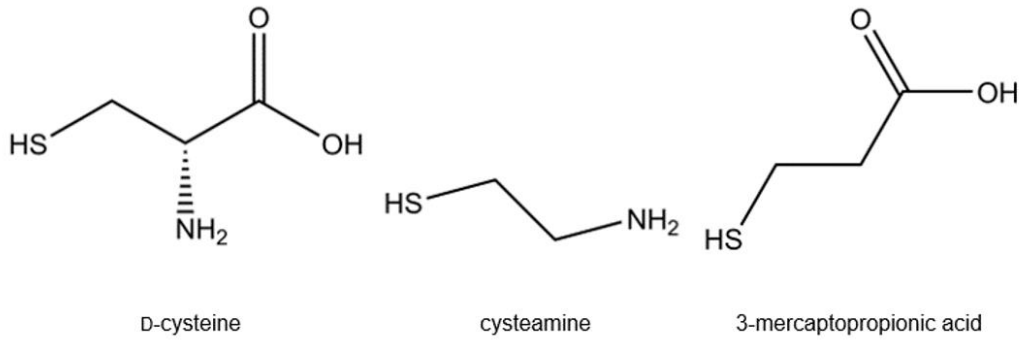

Figure 2.5. Structural analogs of L-cysteine: D-cysteine, cysteamine, and 3-mercaptopropionic acid (3-MPA).

2.3.2 EPR Analysis of C93G CDO

EPR analyses were performed to determine the oxidation state of the iron in the substrate bound and resting state of C93G CDO. Studies showed that C93G CDO existed in a high spin iron (III) oxidation state with an EPR signal of g= 4.3 (Figure **2.6**). In order to determine substrate binding in the active site, C93G was incubated with L-cysteine. The addition of L-cysteine resulted in an increase in the relative signal intensity compared to the resting state of C93G CDO (Figure **2.6**). The addition of L-cysteine substrate to wild-type CDO also resulted in a sharper Fe^{3+} signal compared to the ferric signal seen with wild-type CDO in the absence of L-cysteine. It was previously proposed that the sharper signal was attributed to the coordination of the L-cysteine substrate to the iron center or formation of the crosslink.[115,116]

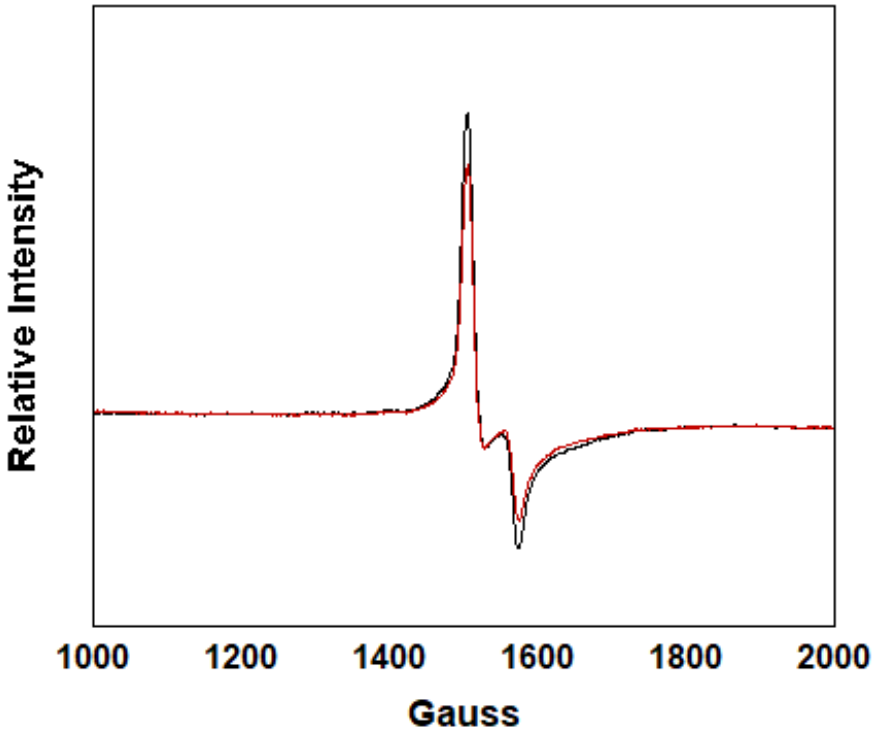

Figure 2.6. X-band EPR spectra of C93G CDO with L-cysteine (black trace) and without L-cysteine (red trace). All spectra were measured with 90 μM protein in 25 mM HEPES buffer (pH 7.5) 100 mM NaCl, and 10% glycerol. All spectra were recorded at 9.38 GHz, with a field modulation frequency of 100 kHz and modulation amplitude of 6 G. All spectra were recorded at 4 K.

2.3.3 Characterization and Steady-State Kinetic Analysis of Wild-type CDO and MDO

A conserved Arg (Arg60) plays a role in substrate specificity in mammalian CDO. However, in some bacterial CDO there is a Gln residue in place of the Arg residue that has a proposed role in substrate specificity among bacteria. The preferred substrate for mammalian CDO is L-cysteine, while the preferred substrate for the "Gln-type" bacterial thiol dioxygenase is 3-

MPA. In this study, wild-type MDO was cloned and purified and compared to wild-type CDO. The iron content for wild-type CDO was determined to be ~60%, while the iron content for wild-type MDO was ~55%. Kinetic properties of wild-type CDO and wild-type MDO were determined by measuring oxygen consumption using a Clark-type oxygen electrode. The k_{cat}/K_m value for wild-type CDO with L-cysteine was 35000 $M^{-1}s^{-1}$ (Table **2.2**). However, wild-type CDO displayed no activity with 3-MPA. The k_{cat}/K_m value for wild-type MDO was 72500 $M^{-1}s^{-1}$ with 3-MPA. However, the catalytic activity of wild-type MDO with L-cysteine resulted in a ~500-fold decrease in oxygen consumption with 3-MPA (Table **2.3**).

Gln62 in "Gln-type" bacterial thiol dioxygenase is proposed to play a role in substrate specificity similar to Arg60 in mammalian CDO. In this study, Gln62 MDO was replaced with an arginine and Arg60 CDO was replaced with a glutamine. Both the MDO and CDO variants were analyzed to determine if these residues had an effect on substrate specificity. The iron content was ~65% for Q62R MDO, and ~65% for R60Q CDO. Kinetic properties of R60Q CDO and Q62R MDO were determined by measuring oxygen consumption using a Clark-type oxygen electrode. The k_{cat}/K_m value for R60Q resulted in a ~400-fold decrease in oxygen consumption compared to wild-type CDO. (Table **2.2**) The cysteine substrate analog 3-MPA had no detectable activity with R60Q CDO. For Q62R MDO, the catalytic activity with 3-MPA was ~1000 fold lower compared to wild-type MDO. However, the catalytic activity increased ~4 fold with L-cysteine compared to wild-type MDO (Table **2.4**).

Table 2.2 Steady-state kinetic parameters of wild-type CDO and R60Q CDO

	k_{cat} (sec^{-1})	K_m ($M \times 10^4$)	k_{cat}/K_m (M^{-1} sec^{-1})	% Fe
Wild-type CDO	2.1 ± 0.2	0.6 ± 0.1	35000 ± 5800	60 ± 2
R60Q CDO	0.63 ± 0.05	80 ± 20	80 ± 20	65 ± 3

The concentration of L-cysteine was varied from 0.2-5 mM for wild-type CDO and 10-200 mM for R60Q.

Table 2.3 Steady-state kinetic analysis on wild-type MDO with 3-MPA and L-cysteine

Substrate	k_{cat} (sec^{-1})	K_m ($M \times 10^4$)	k_{cat}/K_m (M^{-1} sec^{-1})
3-MPA	2.9 ± 0.40	0.4 ± 0.1	72500 ± 6000
L-cysteine	0.25 ± 0.02	20 ± 5	125 ± 33

Table 2.4 Steady-state kinetic analysis on Q62R MDO with 3-MPA and L-cysteine

Substrate	k_{cat} (sec^{-1})	K_m ($M \times 10^4$)	k_{cat}/K_m (M^{-1} sec^{-1})
3-MPA	0.45 ± 0.02	70 ± 20	65 ± 20
L-cysteine	2.1 ± 0.10	40 ± 1	5250 ± 1350

2.3.4 Analysis of Crosslink Formation with Wild-type and R60Q CDO

Arg60 has been proposed to play a role in substrate specificity. Substrate specificity affects catalytic activity and crosslink formation. In order to evaluate crosslink formation, wild-type and R60Q CDO were incubated in the presence of L-cysteine at various time points over the course of

two hours. Purified wild-type CDO exists as a heterogenous mixture of non-crosslinked and crosslinked isoforms, however, the fully crosslinked species can be generated by incubating the enzyme with L-cysteine. The R60Q variant was unable to form the crosslink in the presence of 100 mM L-cysteine (Figure **2.7**).

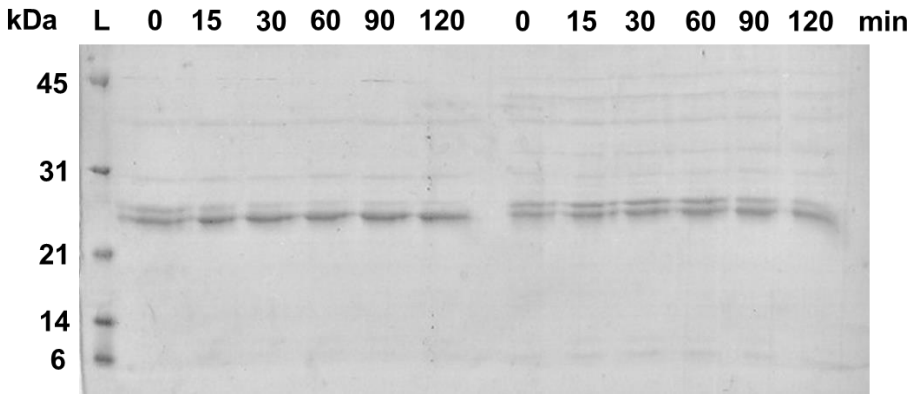

Figure 2.7. Crosslink formation analyses for the wild-type CDO and R60Q CDO. Wild-type CDO and R60Q CDO was incubated at 37 °C with 100 mM L-cysteine and 1 mM ascorbate in 25 mM HEPES (pH 7.5) with gentle shaking for 2 hours. Each sample was treated with 2% 2-mercaptoethanol and 5% SDS and analyzed on 12% SDS-PAGE.

2.3.5 Effects of 3-Mercaptopropionic Acid on The Iron Center in MDO

EPR measurements were performed to determine the oxidation state of the iron center in the resting and substrate bound state of wild-type MDO (Figure **2.8**). As previously mentioned, the addition of L-cysteine substrate to wild-type CDO resulted in a sharper ferric signal compared to wild-type CDO in the absence of L-cysteine. The sharp ferric signal observed upon the addition of L-cysteine with wild-type CDO was associated with L-cysteine coordination or crosslink

formation.[115,116] This study revealed that wild-type MDO and substrate (3-MPA) resulted in a sharper ferric signal compared to the ferric signal of wild-type MDO without 3-MPA (Figure **2.8**).

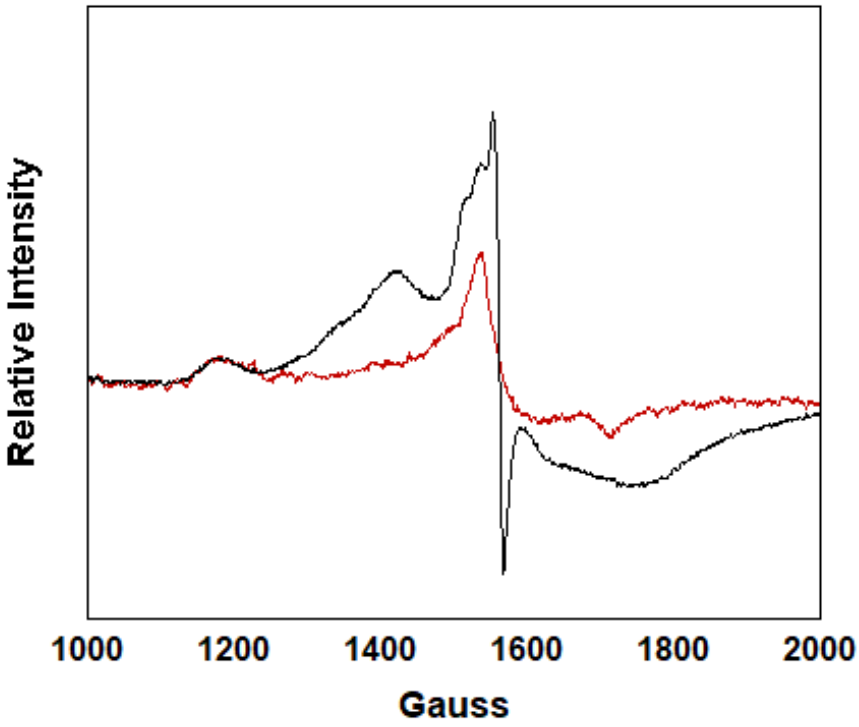

Figure 2.8. X-band EPR spectra of wild-type MDO with 3-MPA(black trace) and without 3-MPA (red trace). All spectra were measured with 90 μM protein in 25 mM HEPES buffer (pH 7.5) 100 mM NaCl, and 10% glycerol. All spectra were recorded at 9.38 GHz, with a field modulation frequency of 100 kHz and modulation amplitude of 6 G. All spectra were recorded at 4 K.

2.4 Discussion

Mammalian CDO is an iron dependent enzyme that oxidizes cysteine to cysteine sulfinic acid. CDO contains a thioether crosslink (between a Tyr residue (Tyr157) and a cysteine residue (Cys93) that is responsible for increasing catalytic activity ~5-fold. Following purification, wild-type CDO exists as a heterogeneous mixture of the non-crosslinked and crosslinked isoforms. Crosslink formation can be inhibited when recombinant wild-type CDO is expressed in the presence of the iron chelator 1, 10-phenanthroline, yielding only the non-crosslinked isoform.[115] However, the fully crosslinked isoform can be generated at increased L-cysteine concentrations.[61,61,65] Fully crosslinked CDO demonstrated enhanced catalytic activity compared to non-crosslinked CDO; therefore, it is proposed that the crosslink is formed in response to increase catalytic activity when cysteine levels are elevated.[65] Recent studies concluded that the crosslink isoform Tyr157 enables proper cysteine coordination and dioxygen stabilization, both essential for optimal active site chemistry.[115] Some thiol dioxygenases in bacteria are structurally similar to mammalian CDO; however, the bacterial systems do not contain the thioether crosslink. Instead, bacterial thiol dioxygenases contain a Gly residue in place of the C93 residue. In this study, a C93G variant was constructed to resemble bacterial CDO and determine if it contributed to substrate specificity. SDS-PAGE analysis confirmed that the crosslink was abolished and only a single homogenous species was observed (Figure **2.3**). C93G CDO had a ~3-fold decrease in catalytic activity compared to wild-type. It is suggested that the decrease in catalytic activity is because the crosslink can no longer be formed.

The percentage of iron bound to wild-type CDO varies among all groups studying mammalian CDO. (10-68%).[57,117] The iron content of C93G CDO was increased by ~20% compared to wild-type. The resting form of wild-type CDO has a high spin iron (III) oxidation state with a *g*-value of 4.3.[113,116] Moreover, the addition of L-cysteine results in an increase in the relative signal intensity.[54,118] The signal increase is due to L-cysteine coordination of the active site or increased iron coordination. The overall shape of the signal for C93G CDO was similar to wild-type. However, upon the addition of L-cysteine, the signal became sharper. The sharper ferric signal observed upon the addition of L-cysteine with wild-type and C93G CDO suggest that the increase in signal is due to L-cysteine coordination.

Previous studies have suggested that the substrate for the "Gln-type" bacterial thiol dioxygenase is 3-mercaptopropionic acid.[2,109,119,120] In order to further evaluate if these amino acids are involved in substrate specificity, constructed variants of R60Q CDO and Q62R MDO were generated and tested with various cysteine analogs to determine if these residues would confer altered substrate specificity. Results from kinetic studies showed that the catalytic activity of the R60Q CDO variant was ~400-fold lower with L-cysteine, compared to wild-type CDO. The R60Q CDO variant had no detectable activity with 3-MPA or 3-mercaptopyruvate. However, when compared to wild-type MDO the catalytic efficiency of the Q62R MDO variant diminished by ~1000-fold with 3-MPA but increased by ~4-fold with L-cysteine. These results suggest that the Arg residue and the Gln residue in mammalian and bacterial systems do play important roles in substrate specificity but are not interchangeable. However, based on the results, Arg60 seems to be more vital in mammalian CDO than Gln62 is in bacterial MDO, suggesting that other amino acids play a role in substrate specificity among bacterial MDO.

Moreover, previous studies have suggested that cysteine binds bidentate within the mammalian CDO active site as well as the "Arg-type" bacterial CDO active site; implying that all potential substrates must contain both thiol and amine functional groups.[54,60,121] These studies further suggest that substrate binding at the MDO iron site occurs exclusively by thiolate coordination rather than bidentate, because 3-MPA has no amine group to bind to the metal center. The 4-fold increase of the Q62R MDO variant with L-cysteine compared to wild-type MDO also suggests that the arginine residue in mammalian CDO plays a crucial role in the bidentate binding of the substrate further suggesting there are other amino acids that assist in substrate binding and reactivity among bacterial MDO.[122]

Wild-type CDO is able to fully form the crosslinked species over a time course of 2 hours with 100 mM L-cysteine. Conversely, the R60Q CDO variant was not able to form the crosslinked species with 100 mM of L-cysteine present. The replacement of the arginine with the glutamine may have disrupted binding of the L-cysteine resulting in a lack of crosslink formation as well as a reduction in enzyme activity. Consistent with previous studies, Arg60 in CDO appears to also play a role in substrate coordination.[57,122] The percent iron bound in wild-type MDO is similar to that of wild-type CDO, and varies among different research groups (20-65%).[66,120,123] Both Q62R MDO and R60Q CDO displayed a 10% increase in percent iron bound compared to wild-type. In EPR studies, wild-type MDO displayed a ferric signal at g=4.5. A sharper signal was observed once 3-mercaptopropionate was added, indicating substrate coordination or increased iron coordination. However, other studies have found that the ferric signal is not as sharp with other thiol substrates such as cysteine or cysteamine, demonstrating that 3-MPA is preferred over L-cysteine.[121]

Overall, these studies were able to effectively compare mammalian thiol dioxygenases with bacterial thiol dioxygenases. Results from sequence alignment studies revealed only Tyr157 is conserved among CDO in bacterial systems; however, C93 is replaced with a glycine. Indicating the crosslink is not essential for bacterial CDO.[61] The C93G variant successfully resembled bacterial CDO and the crosslink was no longer able to form. Not only do bacterial thiol dioxygenases not have a crosslink, but some also lack the conserved Arg residue reported to play a role in substrate specificity among mammalian CDO. These results from studies with R60Q CDO and Q62R MDO, support a more defined role for Arg60 in mammalian CDO in substrate specificity than the comparable glutamine residue in bacterial MDO. There are sequence alignments, mutagenesis, and sequence comparison of thiol dioxygenases based on an Arg or Gln at position 60. There are also key structural features that could define substrate specificity.[122] Among these are (1) the presence or absence of a *cis*-peptide bond between a serine and proline residue, (2) an Arg or Gln at position 60, and (3) a Cys or Arg at position 164.[122] However, further studies need to be performed on the other key active site residues in bacterial MDO to determine substrate specificity among these organisms.

CHAPTER THREE

Bacterial Thiol Dioxygenase Substrate Specificity and Protein-Protein Interactions

3.1 Introduction

Recently, it has been proposed that bacterial thiol dioxygenases that contain a Gln in the active site are mercaptopropionate dioxygenases (MDO). MDO oxidizes 3-MPA to 3-sulfinopropionate (3-SPA) (Figure **3.1**). Although, 3-MPA has been proposed to be a central metabolite in both catabolic and assimilatory sulfur metabolism, the metabolic role of 3-SPA is

unclear.[41,121] In many "Gln-type" bacteria, the MDO gene is on the same operon as an annotated sulfurtransferase, but the existence of the sulfurtransferase has not been recognized by groups working with MDO. Both the MDO and sulfurtransferase genes are located in low-sulfur islands (LSIs). LSIs are defined as runs of at least eight out of ten genes encoding proteins with low-sulfur content.[123] The predicted proteins encoded by LSIs strongly suggest that LSIs have a role in acquiring sulfur from organic sulfur sources during sulfur starvation.[124] The sulfurtransferase gene product is also thought to function in sulfur assimilation using organosulfate/sulfonates as substrates.[124]

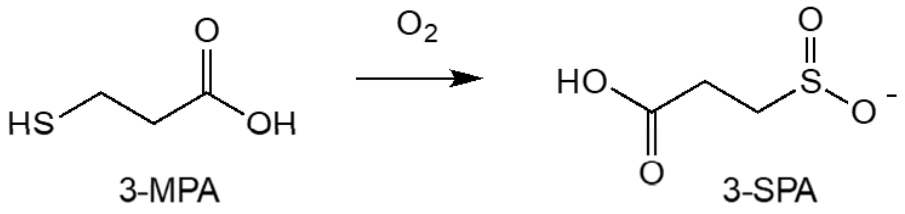

Figure 3.1. Oxidation of 3-MPA to 3-SPA by MDO.

There are two motifs found among sulfurtransferase. Thiosulfate sulfurtransferases have a CRKGX[R/T] motif, while mercaptopyruvate sulfurtransferases have a CGSGVT motif. In thiolsulfate sulfurtransferase, the positive charges on conserved lysine and arginine residues in the CRKGX[R/T] motif are predicted to form electrostatic interactions with the negative charges on the substrate.[125] The uncharged serine residue in the MST motif, CGSGVT, participates in a hydrogen-bonding network with two nearby arginines and the carboxyl groups of pyruvate.[94,125,126] MST catalyzes the trans-sulfuration reaction from mercaptopyruvate to thiol containing compounds (Figure **3.2**). The annotated sulfurtransferase on the MDO operon has an amino acid sequence similar to mercaptopyruvate sulfurtransferase enzymes. Therefore, mercaptopyruvate

could be a potential substrate for MDO or the sulfurtransferase. Natural fusions between the non-heme iron containing dioxygenase and rhodanese (sulfurtransferase) have recently been identified in some bacteria.[104] However, the role of this fusion is not yet known. Existence of a fusion suggest that the independently expressed dioxygenase and sulfurtransferase enzymes may interact to facilitate catalysis.[104] In this study, we wanted to evaluate a potential metabolic link between the sulfurtransferase and MDO by determining the substrate specificity of CDO and MDO variants with 3-mercaptopyruvate. In addition, protein-protein interaction studies were examined to determine the metabolic role of these enzymes.

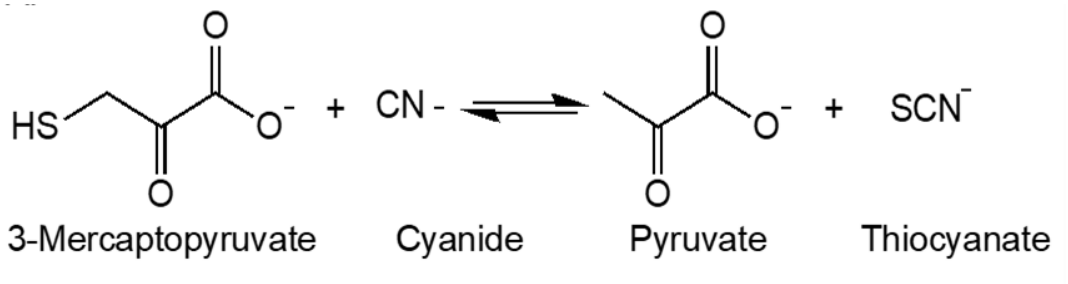

Figure 3.2. 3-Mercatopyruvate sulfurtransferase reaction.

3.2 Material and Methods

3.2.1 Materials

4-(2-Hydroxyethyl)piperazine-1-ethanesulfonic acid (HEPES), L-cysteine, 3-mercaptopropionate, sodium mercaptopyruvate, L-ascorbate, ampicillin, streptomycin sulfate, ammonium sulfate, lysoszyme, potassium chloride, 5,5'-dithiobis(2-nitrobenzoic acid) (DTNB), monopotassium phosphate, and brilliant blue R were purchased form Sigma (St. Louis, MO). Isopropyl-β-d-thiogalactopyranoside (IPTG) was purchased from Gold Biotechnology (St. Louis,

MO). Glycerol and sodium chloride were purchased from Macron Fine Chemicals (Center Valley, PA). Difco-brand Luria-Bertani (LB) medium was purchased from Becton, Dickinson and Company (Sparks, MD). Oligonucleotide primers were purchased from Invitrogen (Carlsbad, CA). Pfu Turbo DNA polymerase was purchased from Agilent (La Jolla, CA). Herculase polymerase was purchased from Agilent (La Jolla, CA). Phenyl Sepharose 6 Fast Flow was purchased from GE Healthcare Life Sciences (Pittsburg, PA). Macro-prep® High Q Support was purchased from Bio-Rad Laboratories (Herculase, CA). Ni-nitrilotriacetic acid (NTA) Superflow resin was purchased from QIAGEN (Valencia, CA). SDS-PAGE resolving and stacking buffers, 30% acrylamide, and Blue Laemmli was purchased from Bio-Rad Laboratories (Herculase, CA). Amicon Ultra-4 Centrifugal Filter Devices (10 kDa MWCO) were purchased from Millipore (Billerica, MA).

3.2.2 Steady-State Kinetic Analyses of Wild-type MDO, Variants, and CDO Variants

Steady-state kinetic parameters were determined using a Clark-type oxygen electrode (Hansatech, Inc., Norfolk, United Kingdom) to monitor the rate of dioxygen utilization by each enzyme in the presence of 3-mercaptopyruvate. The concentration range implemented for wild-type CDO and R60Q CDO with 3-mercaptopyruvate was 1-50 mM. The concentration range used for wild-type MDO with 3-mercaptopyruvate was 0.1-1 mM and 1-25 mM for Q62R MDO. Each reaction with wild-type and R60Q CDO contained a final concentration of 2 μM protein and 1 mM ascorbate in 25 mM HEPES (pH 7.5) at 37 °C. Each reaction with wild-type MDO and Q62R MDO contained a final concentration of 2 μM protein and 1 mM ascorbate in 25 mM HEPES (pH 7.5) at 37 °C. The assays were initiated by the addition of the specific substrate and the initial velocities were recorded from the linear portion of the trace. The average initial velocities from

three separate experiments were plotted against the substrate concentration and the data were fit to the Michaelis-Menten equation using KaleidaGraph™ software.

3.2.3 Cloning and expression of the Pseudomonas aeruginosa sulfurtransferase gene

The sulfurtransferase gene was obtained from genomic DNA prepared directly from *Pseudomonas aeruginosa*. The Zero Blunt® PCR Cloning Kit was used to clone the blunt PCR fragments into the PCR®-Blunt vector. The sulfurtransferase was PCR-amplified with Herculase II Fusion DNA polymerase using primers that included *Nde*I and *Xho*I restriction sites: 5´ GAT CAT ATG AGC CAG ATC GCC 3´ and 5´ GAT CTC GAG TCA GAT CAC GAA GAA 3´. Ligation into the PCR®-Blunt expression vector was performed with T4 DNA ligase at a 5:1 insert:vector molar ratio, and the ligation was incubated overnight at 16 °C. The vector was then transformed into *E. coli* One Shot® TOP10 expression cells. Representative clones were confirmed by DNA sequence analysis (Eurofins MWG Operon). Once confirmed, digestion using *Nde*I *and Xho*I restriction enzymes was performed on the blunt end clone as well as the pET21a vector. T4 DNA ligase was used to ligate a 3:1 insert:vector molar ratio into the pET21a expression vector. The vector was then transformed into *E. coli* XL-1 and BL21(DE3) expression cells. Representative clones were confirmed by DNA sequence analysis (Eurofins MWG Operon). Cell cultures were stored as glycerol stocks at -80 °C.

3.2.4 Protein synthesis and purification of ST

The cells containing the sulfurtransferase gene in the pET21a vector were isolated on LB-agar medium containing 0.1 mg/mL ampicillin (LB-amp). A single colony was selected from the plate and grown in 5 mL LB-amp medium at 37 °C for ~8 hours. A 1% inoculum was transferred

from the 5 mL culture to a 100 mL culture and grown overnight at 37 °C. A 2% inoculum from the overnight culture was transferred to four 1 L flasks and grown at 37 °C until the cultures reached an A_{600} value of 0.6-0.8. Cells were harvested by centrifugation at 5000 rpm for 15 minutes at 4 °C. Cell pellets were resuspended with 100 mL 25 mM HEPES (pH 7.5), 10% glycerol, and 0.2 mg/mL of lysozyme. Cells were lysed by sonication followed by centrifugation at 10,000 rpm, for 15 minutes at 4 °C. 1.5% streptomycin sulfate (w/v) was added to the supernatant and the solution was slowly stirred at 4 °C for 1 hour. Precipitated nucleic acids were pelleted via centrifugation at 10,000 rpm at 4 °C for 20 minutes. Ammonium sulfate precipitation was performed from 20-60%. The pelleted protein from the 60% salt cut was resuspended in 200 mL 25 mM HEPES (pH 7.5), 10% glycerol, and 20% ammonium sulfate and loaded on a phenyl sepharose column. After washing the column with 100 mL of 25 mM HEPES (pH 7.5), 10% glycerol, and 20% ammonium sulfate, the protein was eluted with a linear gradient from 20 – 0% ammonium sulfate in 25 mM HEPES (pH 7.5) and 10% glycerol. Fraction purity was determined by A_{280} values and SDS-PAGE (5% stacking and 12% resolving). Fractions determined to be of highest purity were pooled and loaded onto a Macro-Prep High Q Support anion exchange column. After washing the column with 25 mM HEPES (pH 7.5) and 10% glycerol, the protein was eluted from the column using a linear gradient from 0-300 mM NaCl in 25 mM HEPES (pH 7.5) and 10% glycerol. Fraction purity was determined as described above and pooled protein was dialyzed twice against 25 mM HEPES (pH 7.5), 10% glycerol, and 100 mM sodium chloride. After dialysis, the protein was centrifuged at 10,000 rpm at 4 °C for 15 minutes to remove any precipitated protein. Protein aliquots were flash frozen with liquid nitrogen and stored at -80 °C.

3.2.5 Construction of recombinant His-tagged mdo *gene*

The pET21a (Novagen, Madison, WI) vector containing the C-terminally His-tagged *mdo* gene was constructed by substitution of the native *mdo* stop codon with an Ala codon (GCG) as previously described.[127] The native construct was PCR amplified using the primers 5´ GAG AAC CCC GCA GCG CTC GAG CAC CAC 3´ and 5´ GTG GTG CTC GAG CGC TGC GGG GTT CTC 3´. The mutations were generated by site directed mutagenesis. The generated variant was verified by DNA sequence analysis (Eurofins MWG Operon).

3.2.6 Expression of His-tagged mdo *gene and affinity chromatography binding assays*

The native sulfurtransferase and His-tagged MDO protein were expressed as previously described with the following exceptions. The native sulfurtransferase and His-tagged MDO cell cultures were grown separately in LB medium containing 100 µg/mL ampicillin (LB-Amp). A single colony of *E. coli* BL21(DE3) containing the appropriate expression plasmid was used to inoculate 5 mL LB medium containing 100 mg/mL ampicillin (LB-Amp) with overnight incubation at 37 °C. A 1% inoculum of the 5 mL cell culture was transferred to 100 mL LB-Amp and incubated at 37 °C until the A_{600} reached 0.4. The cells were induced with 0.4 mM IPTG and grown for an additional 6 hours at 25 °C. Cells were harvested by centrifugation at 5000 rpm for 15 minutes at 4 °C and stored at -80 °C. Cells from the 100 mL growth were resuspended in 50 mL 25 mM HEPES (pH 7.5), 10% glycerol, and 0.2 mg/mL of lysozyme. Cell were lysed by sonication, followed by the addition of 1.5% streptomycin sulfate to precipitate nucleic acids. Each protein was purified according to the previously described protocols. The same protocol was performed for both His-tagged sulfurtransferase and native MDO.

The 50 mL cell lysate containing the expressed His-tagged MDO protein was loaded onto a column containing Ni-nitrolotriacetic acid (NTA) Superflow resin (QIAGEN, Valencia, CA).

The column was washed with 100 mL 25 mM HEPES (pH 7.5) and 10% glycerol to remove unbound protein prior to loading the cell lysate containing native sulfurtransferase. The column was washed again with 100 mL of 25 mM HEPES (pH 7.5), 10% glycerol, and 50 mM imidazole, followed by elution of the His-tagged MDO protein with 100 mL 25 mM HEPES (pH 7.5), 10% glycerol, and 75 mM imidazole. The eluted proteins from both buffer concentrations were collected and analyzed by SDS-PAGE. The same protocol was performed with His-tagged sulfurtransferase and native MDO.

3.2.7 Thiol quantification

5,5'dithiobis-(2-nitrobenzoic acid) (DTNB) was used to quantify free thiols in the native and denatured sulfurtransferase enzyme. In each reaction, 10 µM protein and 100 µM DTNB were incubated at 25 °C for 15 minutes in 25 mM HEPES (pH 7.5). In reactions where the samples were denatured, 6 M guanidinium chloride (GuHCl) was incubated with 10 µM protein at 25 °C for 1 hour prior to the addition of DTNB. Each reaction was monitored at 412 nm and quantified using the molar absorption coefficient value (ε_{412}=14,150 M^{-1} cm^{-1}). In the reactions using GuHCl, ε_{412}=13,700 M^{-1} cm^{-1} was used for thiol quantification. The results obtained were the average of three separate experiments.

3.2.8 Analysis of thiocyanate formation

The cyanide detoxification activity of sulfurtransferase was measured in a colorimetric assay as previously described.[87] The reaction contained a 1:1 ratio of thiosulfate or mercaptopyruvate to potassium cyanide (50 mM thiosulfate or mercaptopyruvate, 50 mM potassium cyanide) and 1 µM protein in 100 mM HEPES (pH 7.5) (300 µL total volume). The

reaction was initiated by the addition of enzyme. Following a 30-minute incubation at 25 °C the reaction was quenched with 100 µL of 15% (w/v) formaldehyde. Thiocyanate formation was measured by the addition of 500 µL ferric nitrate (165 mM ferric nitrate nonahydrate and 13.3% (v/v) nitric acid). The absorbance of the ferric thiocyanate complex was measured at 460 nm. A standard curve was used to determine the concentration of thiocyanate formed. The concentrations of thiosulfate or mercaptopyruvate and cyanide were varied from 0.5-50 mM in order to determine the dependence of enzyme activity on substrate concentration.

3.2.9 Persulfide Trapping

In order to trap the catalytic cysteine of IscS or the sulfurtransferase in its persulfide form, a persulfide trapping assay was performed. IscS (10 µM) was added to a solution (150 µL) of L-cysteine (400 µM) and pyridoxal phosphate (PLP) (160 µM) in 50 mM TrisHCl buffer, pH 8.5. After a one-hour incubation at 37 °C, an aliquot (100 µL) was removed and washed three times using a desalting column of Sephadex G-25 to remove any freed cysteine. Five equivalents (50 µM) of iodoacetamide was added to the eluate. After a 30 min incubation at 25 °C, reactions were washed once and analyzed by mass spectrometry. Mass analysis was performed on an Ultra Performance LC System (ACQUITY, Waters Corp., Milford, MA, USA) in conjunction with a quadrupole time of-flight mass spectrometer (Q-Tof Premier, Waters) with electrospray ionization (ESI-MS) in positive mode. The persulfide trapping procedure was also performed with the sulfurtransferase with minor modifications. Sulfurtransferase (10 µM) was added to a solution (150 µL) of L-cysteine (400 µM), pyridoxal phosphate (PLP) (160 µM) in 50 mM TrisHCl buffer, pH 8.5. After a one hour incubation at 37 °C, an aliquot (100 µL) was removed and washed three times using a desalting column of Sephadex G-25 to remove any free cysteine. Five equivalents

(50 µM) of iodoacetamide was added to the eluate. After a 30 min incubation at 25 °C, reactions were washed once and analyzed by mass spectrometry. The same technique was also used with both sulfurtransferase (10 µM) and IscS (10 µM) combined and added to a solution (150 µL) of L-cysteine (400 µM), pyridoxal phosphate (PLP) (160 µM) in 50 mM TrisHCl, pH 8.5. The same technique was also used with ST (10 µM) alone and added to a solution (150 µL) of L-cysteine, 3-MPA, mercaptopyruvate, or thiosulfate (400 µM), in 50 mM HEPES buffer, pH 7.5. IscS was used as a control to determine if the sulfurtransferase needed a sulfur-donating enzyme to help transfer the sulfur to form a persulfide. Various cysteine analogs were used to verify which one was the preferred sulfur source.

3.2.10 Verification of persulfide formation

In order to determine the concentration and identify the formation of a persulfide, a cold cyanolysis assay was performed. 400 µL of 1 M ammonium hydroxide, 3.6 mL of water and 500 µL of 0.5 M potassium cyanide were added to a 500 µL persulfide sample. After a 45 minute incubation at 25 °C, 100 µL of 38% formaldehyde and 1 mL of Goldstein's reagent (50 grams of ferric nitrate nonahydrate dissolved in 50 mL of water, 525 mL of nitric acid, diluted to 2 L) were added to the sample. The absorbance was determined at 335 nm and quantified using the persulfide molar extinction coefficient of 310 M^{-1} cm^{-1}. A blank was prepared excluding the persulfide sample.

3.2.11 Size exclusion chromatography binding assay

The oligomeric states of wild-type MDO and sulfurtransferase were determined using a protocol previously described with minor modifications.[128] Analytical size-exclusion

chromatography of the MDO and sulfurtransferase enzymes were evaluated on an Agilent 1260 Infinity GPC/SEC chromatograph. The molecular weights of each enzyme (50 µM) were determined using a Waters Biosuite HR SEC, 7.8 mm × 300 mm, 250 Å column. The enzymes were eluted from the column with 150 mM sodium phosphate (pH 7.0) and 100 mM NaCl with a flow rate of 0.2 mL/min monitored at 280 nm. A Bio-Rad gel filtration standard with a molecular weight range from 1.35 to 670 kDa was used to generate a curve to fit the molecular weights based on retention times. The standard curve (log of the molecular weight versus retention time) was generated on the basis of the elution time monitored at 280 nm. In experiments where MDO and sulfurtranferase were coupled, a 1:1, 4:1, and 8:1 molar ratio of Sulfurtransferase:MDO were run with and without the addition of 100 µM substrate (3-MPA, 3-mercaptopyruvate, or L-cysteine).

3.2.12 Hydrogen-Deuterium Exchange Mass Spectrometry (HDX-MS)

HDX-MS was performed to determine protein-protein interaction sites. An online pepsin column was applied to produce sulfurtransferase and MDO peptides, which were then analyzed by tandem mass spectrometry. 1 µL of each MDO and sulfurtransferase sample (15 µM) were mixed with 49 µL of assay buffer (25mM HEPES (pH 7.5)) and 50 µL of quench buffer (0.2 M KH_2PO_4 (pH 2.5) at 0 °C). The solution was injected into the HDX Manager Acquity UPLC, equipped with an online pepsin column. Digested proteins were trapped and desalted on a trapping column at a flow rate of 200 µL/min and desalted for 1 minute. After desalting, the flow path was changed to elution mode with the trapping column in line with the C-18 reversed phase analytical column. Peptides were eluted with a gradient of 5-85% acetonitrile (ACN) with a 5-minute flow rate of 30 µL/min and monitored by mass spectrometry. Mass spectrometry data were acquired in positive ion mode with a mass to charge (m/z) range of 100-1500. The peaks in the raw data files were

collected using the software ProteinLynx Global SERVER (PLGS) with 30 low energy and 150 high energy cutoffs. The files generated by PLGS were then imported into DynamX to obtain a sequence map of each enzyme.

Once protein maps were determined, HDX-MS was utilized to determine specific sites of interaction. 1 µL of sulfurtransferase (15 uM) was incubated in 49 µL of 95% D_2O in 25 mM HEPES (pH 7.5) at 25 ℃ for 15 seconds to 1 hour. The HDX reaction was quenched by the addition of 50 µL quench buffer on ice. The quenched sample was injected into the UPLC, where the protein was first digested into peptides by the pepsin column. The peptides were then loaded onto the C-18 reversed phase UPLC column and eluted with a gradient concentration of ACN from 5% to 85% over 5 minutes. The HDX-MS data was analyzed using DynamX (Waters Corporator). This same process was repeated for MDO. In order to determine the specific sites of interaction a similar process was performed, but with minor alterations. 1 µL of ST (15 µM) and 1 µL of MDO (15µM) were incubated together in 48 µL of 95% D_2O 25 mM HEPES (pH 7.5) at 25 ℃ for 15 seconds to 1 hour. The HDX reaction was quenched by the addition of 50 µL quench buffer on ice. The quenched sample was injected into the UPLC, where the protein was first digested into peptides by the pepsin column. The peptides were then loaded onto the C-18 reversed phase UPLC column and eluted with a gradient concentration of ACN from 5% to 85% over 5 minutes. The HDX-MS data was analyzed using DynamX (Waters Corporator). Prior to incubation with 95% D_2O 25 mM HEPES (pH 7.5), proteins were incubated together in 25 mM HEPES (pH 7.5) at 25 ℃ for 30 minutes at a 1:1 molar ratio as well as a 4:1 molar ratio sulfurtransferase:MDO. After incubation with 25 mM HEPES (pH 7.5), 1 µL of the protein mix was incubated with 49 µL of D_2O 25 mM HEPES (pH 7.5) at 25 ℃ for 15 minutes. The HDX reaction was quenched by the

addition of 50 µL quench buffer on ice. The quenched sample was injected into the UPLC, following the same procedure as previously stated.

3.2.13 Analysis of the sulfurtransferase:MDO complex by Native PAGE gels.

Protein complex formation was analyzed by native PAGE gels. Both MDO and sulfurtransferase were mixed in various molar ratios (1:1, 4:1, and 8:1). Each reaction contained a final volume of 15 µL and the enzymes were incubated at 25 ℃ for 20 minutes. After incubation, each sample was quenched with 2 µL of sample buffer (Blue Laemmli). Protein samples were loaded onto a 4% stacking/12% resolving gel and the proteins separated at 70 V for 16 hours at 4 ℃. Gels were stained with Brilliant Blue and analyzed by mass spectrometry. Individual protein samples (2.5 µg) were treated the same as the complex sample and separated on native PAGE.

Preparation of protein for mass spectrometry analysis was performed using an in-gel protein digestion protocol from Promega: Protease Max™ Surfactant. Proteins were resolved by gel electrophoresis and then stained in Coomassie Blue. The gel was destained for 1 hour at room temperature with gentle agitation. A clean razor blade was used to cut the protein bands of interest from the gel and gel slices were placed in a 0.5 mL microcentrifuge tube. The gel slices were destained with 0.2 mL of 100 mM NH_4HCO_3, 50% ACN for 45 minutes at 37 ℃. The gel slices were dehydrated for 5 minutes at 25 ℃ in 100 µL of 100% ACN. Gel slices were dried in a Speed Vac® concentrator for 15 minutes at 25 ℃ and were rehydrated in 100 µL of freshly prepared 25 mM DTT in 50 mM NH_4HCO_3 and incubated for 20 minutes at 56 ℃. The supernatant was discarded, 100 µL of 55 mM iodoacetamide in 50 mM NH_4HCO_3 was added to the gel slices and incubated in the dark for 20 minutes at 25 ℃. Supernatant was discarded and each sample was washed twice with 400 µL of H_2O. The sample was dehydrated with 200 µL ACN:NH_4HCO_3 (1:1)

for 5 minutes, with intermittent vortex mixing (10 seconds on, 10 seconds off). The supernatant was discarded and 200 µL of 100% ACN was added to the sample and incubated for 30 seconds. Following incubation, the supernatant was discarded and dried in a Speed Vac® concentrator for 15 minutes at 25℃. The sample was rehydrated in 20 µL of 12 ng/µL trypsin in 0.01% Protease Max™ Surfactant: 50 mM NH_4HCO_3 for 10 mins at 25 ℃. The sample was then overlaid with 30 µL of 0.01% Protease Max™ Surfactant: 50 mM NH_4HCO_3 and gently mixed for 10 seconds. The sample was incubated for 3 hours at 37 ℃. The condensate was collected by centrifugation at 12,000 rpm for 10 seconds. The sample was extracted into a new tube and 0.5% TFA was added to inactivate trypsin. The solution was frozen and then lyophilized with a Labconco 4.5 liter freeze dry system. Mass analysis was performed on an Ultra Performance LC System (ACQUITY, Waters Corp., Milford, MA, USA) in conjunction with a quadrupole time-of-flight mass spectrometer (Q-Tof Premier, Waters) with electrospray ionization (ESI-MS) in positive mode.

3.2.14 Surface Plasmon Resonance Spectroscopy

Surface Plasmon Resonance (SPR) data were obtained on an Open SPR system (Nicoya Life-sciences). For all experiments, 25 mM HEPES (pH 7.51), and 0.005% Tween-20 was used as the running buffer. MDO was diluted to 31 µg/mL in activation buffer and immobilized on a gold-plated carboxyl-functionalized nanosensor chip according to the manufacturer's instructions using carbodiimide cross-link chemistry (Nicoya Life-sciences). After immobilization and blocking (10 min), sulfurtransferase at varying concentrations (600 nM – 9 µM) was injected and allowed to interact with the protein-modified sensor for 10 minutes at a pump speed of 40 uL/min. Interactions were determined in triplicate using three different chips to eliminate the possibility of chip-to-chip variability.

3.3 Results

3.3.1 Steady-State Kinetic Analyses of Wild-type and Q62R MDO with Mercaptopyruvate and L-cysteine

Once the sulfurtransferase was identified on the MDO operon, the functional role of MDO was evaluated by determining the steady-state kinetic activity of wild-type and Q62R MDO with 3-mercaptopyruvate. Kinetic parameters of wild-type and Q62R MDO were determined by measuring oxygen consumption using a Clark-type oxygen electrode. The k_{cat}/K_m value for wild-type MDO was $(9.3 \pm 3.2) \times 10^4$ M^{-1} s^{-1} with 3-mercaptopyruvate similar to the k_{cat}/K_m value obtained with 3-MPA $(7.3 \pm 0.6) \times 10^4$ M^{-1} $s^{-}1$, Table **3.1**). Moreover, the catalytic efficiency of Q62R MDO with 3-mercaptopyruvate was 300 ± 40 M^{-1} s^{-1} and 65 ± 25 M^{-1} s^{-1} with 3-MPA (Table **3.2**). The k_{cat}/K_m value for wild-type MDO with L-cysteine was 125 ± 33 M^{-1} s^{-1}, while the catalytic efficiency of Q62R MDO with L- cysteine resulted in a ~40 fold increase compared to wild-type MDO (Table **3.2**).

Table 3.1 Steady-state kinetic parameters on wild-type MDO with 3-MPA, 3-mercaptopyruvate, and L-cysteine

Substrate	k_{cat} (sec^{-1})	K_m (M)	k_{cat}/K_m (M^{-1} sec^{-1})
3-MPA	2.9 ± 0.4	4.0 ± 1.0 ($\times 10^{-5}$)	7.3 ± 0.6 ($\times 10^4$)
3-mercaptopyruvate	2.8 ± 0.3	3.0 ± 1.0 ($\times 10^{-5}$)	9.3 ± 3.2 ($\times 10^4$)
L-cysteine	0.25 ± 0.02	2.0 ± 0.5 ($\times 10^{-3}$)	125 ± 33

Table 3.2 Steady-state kinetic parameters on Q62R MDO with 3-MPA, 3-mercaptopyruvate, and L-cysteine

Substrate	k_{cat} (sec^{-1})	K_m (M)	k_{cat}/K_m (M^{-1} sec^{-1})
3-MPA	0.45 ± 0.02	$7.0 \times 10^{-3} \pm 2.0 \times 10^{-3}$	65 ± 20
3-mercaptopyruvate	0.30 ± 0.02	$1.0 \times 10^{-3} \pm 0.1 \times 10^{-4}$	300 ± 40
L-cysteine	2.1 ± 0.10	$4.0 \times 10^{-3} \pm 1.0 \times 10^{-4}$	5250 ± 1350

3.3.2 Thiol Quantification and Sulfurtransferase Activity Analysis

The active site cysteine of a sulfurtransferase is generally redox active and essential for forming a persulfide intermediate, which is an important mechanistic step. The putative sulfurtransferase expressed on the same operon as MDO contains two cysteine residues. One of which has been identified as a putative active site cysteine (Cys485) based on sequence alignments with other sulfurtransferases. Cys485 is solvent accessible in the three-dimensional structure of the sulfurtransferase (Figure **3.3**). We propose Cys241 does not play a role in catalysis because it is not conserved among the sulfurtransferase motifs and it is not solvent accessible. To evaluate the ability of the Cys residues to form a persulfide intermediate, the accessibility of each cysteine free thiols was quantified.

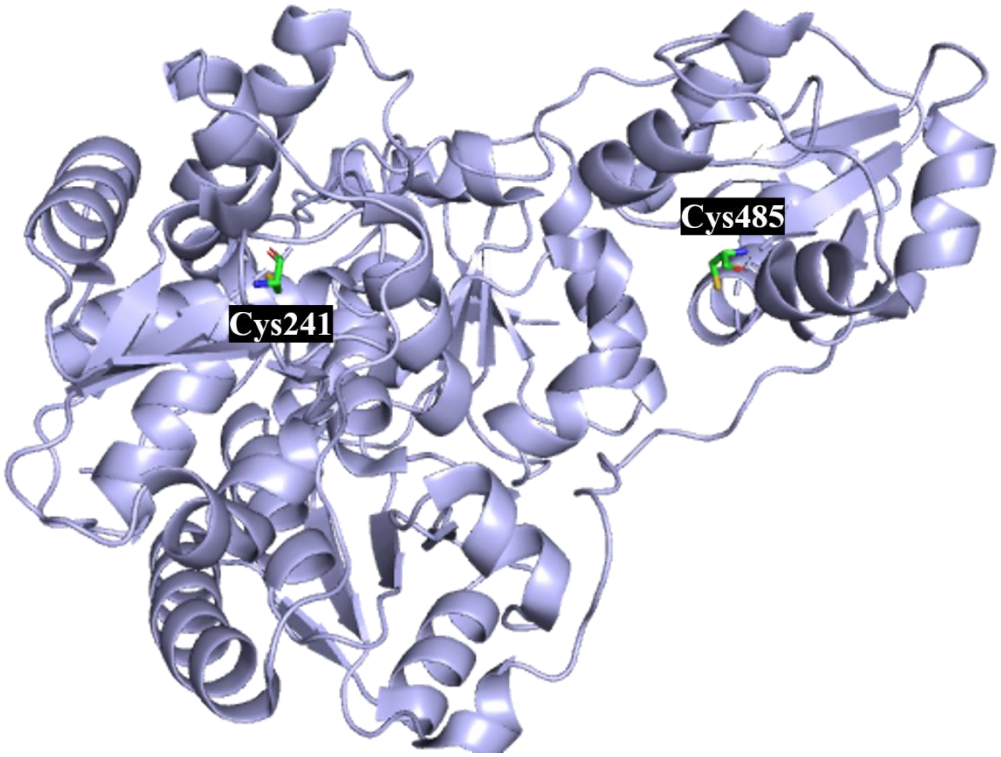

Figure 3.3 Three-dimensional structure depicting the cysteine residues in sulfurtransferase where Cys485 is at the surface of the active site and Cys241 is buried.

Results obtained from the DTNB assays revealed one free thiol. Given the accessibility of Cys485, it is likely the solvent accessible cysteine in the native state (Table **3.3**). The thiol of Cys241would likely be unreactive in the native state because it is not solvent accessible. In the denatured state, two free thiols were quantified indicating that both free thiols are accessible when the protein is completely unfolded (Table **3.3**).

Table 3.3 Free thiols present in the folded and denatured states of the sulfurtransferase

Free Thiols		
Enzyme	Folded	Denatured
Sulfurtransferase	1.00 ± 0.03	2.00 ± 0.05

3.3.3 Sulfurtransferase Activity Assays

Once results were obtained from the DTNB assay, conversion of cyanide to thiocyanate in the presence of thiosulfate or mercaptopyruvate was used to monitor the sulfurtransferase activity. However, there was no thiocyanate detected with either thiosulfate or mercaptopyruvate as the sulfur donor.

The predicted sulfurtransferase reaction involves the formation of a persulfide intermediate on the active site Cys. Assays were performed to trap the persulfide intermediate, where IscS was used as a control to determine if the sulfurtransferase needed a sulfur-donating enzyme to aid in the transfer of sulfur to form a persulfide. IscS is a PLP-dependent desulfurase, that uses L-cysteine as a substrate to generate a persulfide on its active site cysteine.[20,129] The activated sulfane sulfur is transferred to the second central component of the Isc system, IscU, where Fe-S clusters are formed. Mass spectrometry was performed to identify the persulfide formed by IscS, resulting in a mass to charge ratio of 47,298. There was no persulfide intermediate detected on the sulfurtransferase with IscS, PLP, and cysteine. Additional studies without IscS were performed with the sulfurtransferase and 3-MPA, sulfurtransferase with thiosulfate, or sulfurtransferase with cysteine. However, no persulfide was identified under any of the conditions described. Next, we attempted to monitor persulfide formation via a cold cyanolysis assay at 335 nm using the same reactions described in the persulfide trap. However, the persulfide intermediate was not detected in the cyanolysis assay.

Coupled assays monitoring oxygen utilization were performed with MDO and sulfurtransferase to determine if the addition of the sulfurtransferase enhanced the activity of MDO (Figure **3.7**). Assays were performed using a Clark-type oxygen electrode to monitor activity of MDO by adding sulfurtransferase (4 µM), thiosulfate or mercaptopyruvate (10 mM), MDO (2 µM), and ascorbate (1 mM) into the reaction chamber. However, no change in MDO activity was observed with the addition of sulfurtransferase and/or substrate.

3.3.4 Affinity Chromatography Binding Assay and Size Exclusion Chromatography, and HDX

Affinity chromatography experiments with individually expressed His-tagged MDO and native sulfurtransferase were performed to identify static protein-protein interactions. Initial studies tested the elution of His-tagged MDO to determine the concentration of imidazole. His-tagged MDO eluted from the column at 60 mM. His-tagged MDO in a cell lysate was loaded onto a Ni-NT A column. Following a HEPES buffer wash to remove unbound protein, native MDO in a cell lysate was loaded onto the Ni-NT A column containing bound His-tagged MDO. The column was first washed with 50 mM imidazole buffer to remove any unbound protein, followed by a second wash with 75 mM imidazole buffer to remove bound His-tagged MDO. Fractions from both the 50 mM and 75 mM imidazole buffer wash were collected from the column and analyzed by SDS PAGE (Figure **3.4 A** and Figure **3.4 B**). Native sulfurtransferase and MDO were also separated on the gel (Figure **3.4 A** lane 1 and 2), and a protein marker with the corresponding molecular masses was also included for molecular weight estimates (Figure **3.4 A** lane 1). The native sulfurtransferase was eluted off the column with 50 mM imidazole buffer (Figure **3.4 A,** lanes 3-10). However, most of the His-tagged MDO eluted off at 75 mM (Figure **3.4 B** lanes 4-10). The results showed that His-tagged MDO and native sulfurtransferase did not coelute from

the column with 50 mM imidazole buffer (Figure **3.4 A** and Figure **3.4 B**). His-tagged sulfurtransferase and native MDO were also evaluated to ensure that the His-tag was not blocking the potential interaction sites on MDO. However, His-tagged sulfurtransferase and MDO did not elute off together with elution buffer.

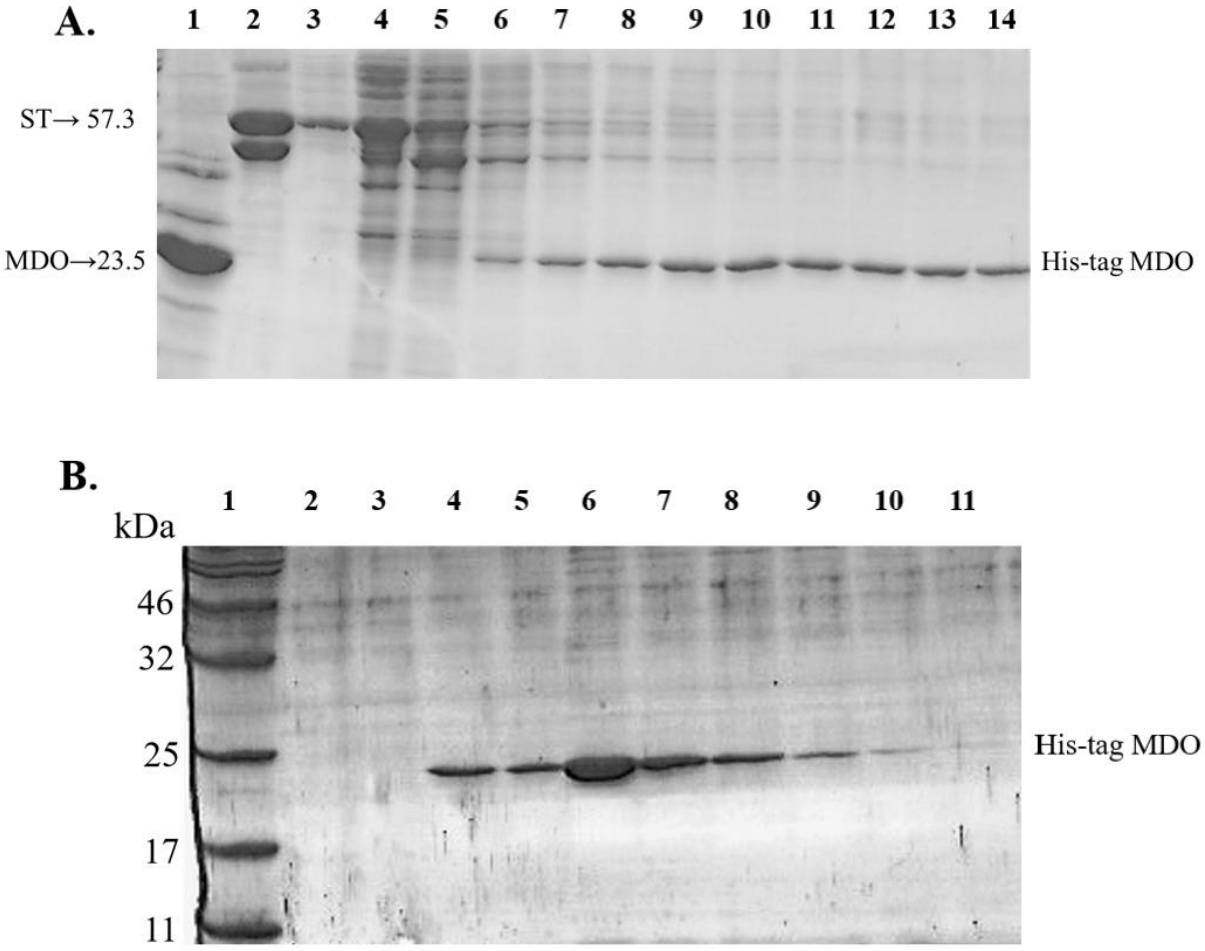

Figure 3.4 A. SDS-PAGE of fractions from the 50 mM imidazole elution of sulfurtransferase and His-tagged MDO from the Ni-NTA column. **B.** SDS-PAGE of fractions from the 75 mM imidazole elution from the Ni-NTA column.

High performance liquid chromatography coupled with size exclusion chromatography (HPLC-SEC) was also performed to evaluate oligomeric states and identify static protein-protein interactions. The molecular weight for MDO was determined by gel filtration to be 22.5 kDa, which is the monomeric molecular weight. Sulfurtransferase was also determined to exist as a monomer with a calculated molecular weight of 57.3 kDa. Various molar ratios of sulfurtransferase:MDO (1:1, 4:1, 8:1) were incubated for 20 minutes prior to injection to determine if there was potential static protein-protein interactions; however, MDO and sulfurtransferase eluted at similar retention times as the individual proteins.

3.3.5 Hydrogen-deuterium Isotope Exchange Mass Spectrometry

Hydrogen deuterium exchange mass spectrometry was performed to identify potential protein-protein interaction sites. Independent pepsin digestion of MDO and sulfurtransferase was initially performed to identify peptide fragments through collision-induced dissociation (Figure **3.5 A & B**). MDO displayed 95% coverage while sulfurtransferase displayed 98% coverage. The amount of deuterium exchanged for each individual protein was compared to that of the corresponding sulfurtransferase:MDO complex. For MDO, regions 79-90 (VWGPGQITPVHD), 112-132 (DAGGRPHOSGARRRLEPGEVE), 163-171 (IGAVRRAVF), and 184-194 (YSNSRLPNIWD) showed decreases in deuterium incorporation following incubation of MDO and sulfurtransferase. (Figure **3.6**). Sulfurtransferase regions 222-245 (GWTLAGQQLEHGQTRRFGAISQDT), 358-378 (FSERGAWSAPLPRQPRADTID), 432-439 (VLTCGSSL), and 469-497 (AGLPTEDGESLLASPRIDRYRRPYEGTDN) demonstrated comparable decreases in deuterium incorporation as MDO (Figure **3.7**). Although there was some change in deuteration, the change was not large enough to suggest protein-protein interactions

between MDO and sulfurtransferase. The observed decrease in deuterium incorporation does support conformational changes when both MDO and sulfurtransferase are incubated together prior to analysis.

A.

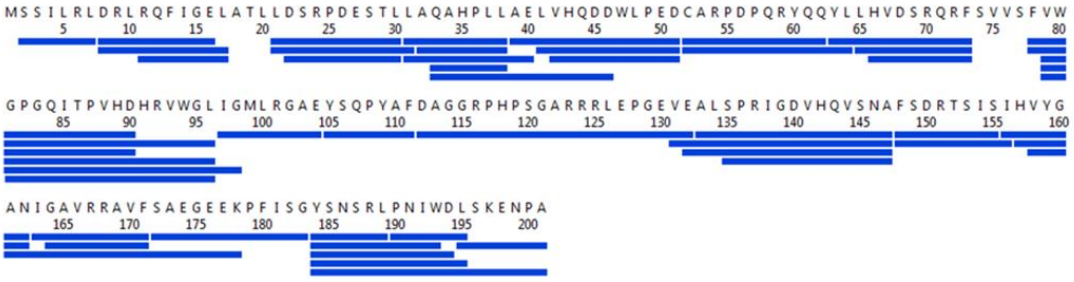

B.

Figure 3.5. The peptide map sequences of **(A.)** MDO and **(B.)** Sulfurtransferase. Peptides were sequenced and generated with PLGS and imported into DynamX to establish a sequence map.

Figure 3.6. Solvent protected regions in the sulfurtransferase:MDO complex identified by HDX-MS. MDO monomer highlighting regions 79-90 (VWGPGQITPVHD) (turquoise), 112-132 (DAGGRPHOSGARRRLEPGEVE) (magenta), 163-171 (IGAVRRAVF) (yellow), and 184-194 (YSNSRLPNIWD) (red). MDO changes in deuteration (red line) and sulfurtransferase:MDO complex changes in deuteration (blue line).

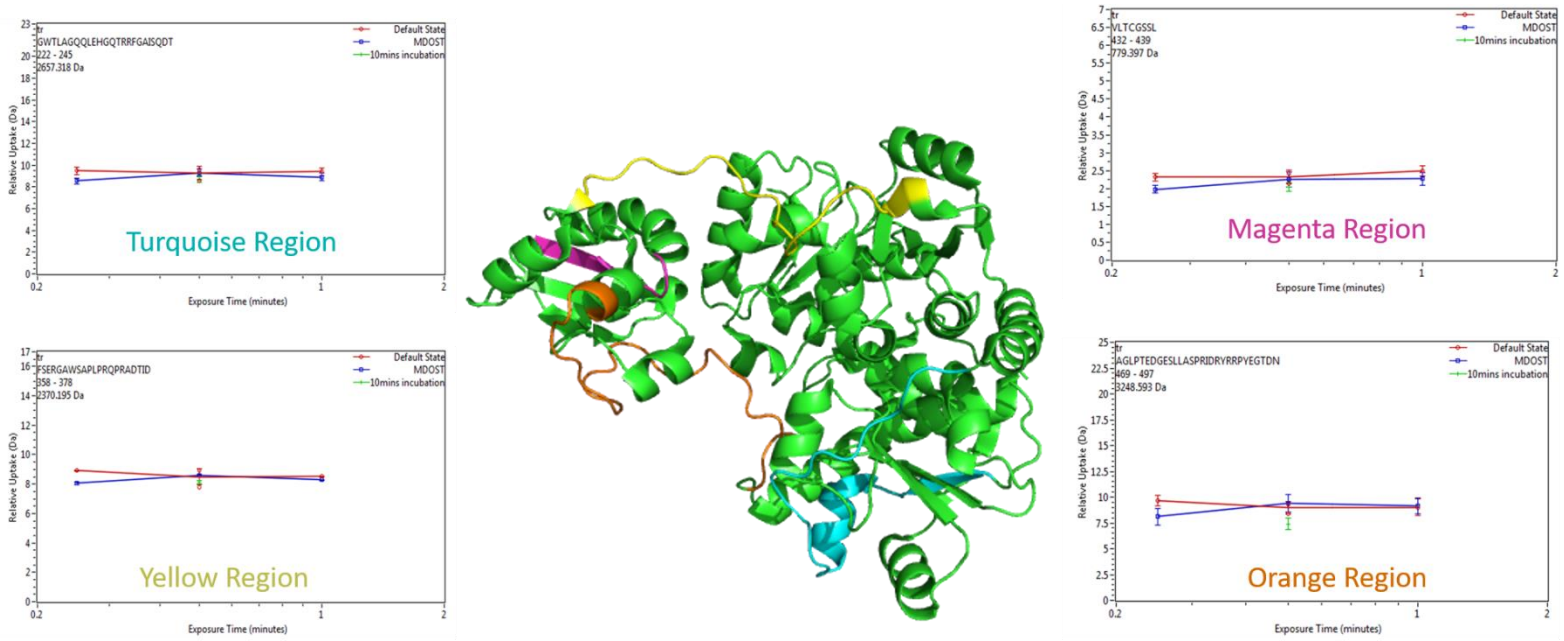

Figure 3.7. Solvent protected regions in the sulfurtransferase:MDO complex identified by HDX-MS. Sulfurtransferase monomer highlighting regions 222-245 (GWTLAGQQLEHGQTRRFGAISQDT) (turquoise), 358-378 (FSERGAWSAPLPRQPRADTID) (yellow), 432-439 (VLTCGSSL) (magenta), and 469-497 (AGLPTEDGESLLASPRIDRYRRPYEGTDN) (orange). Sulfurtransferase changes in deuteration (red line) and sulfurtransferase:MDO complex changes in deuteration (blue line).

3.3.6 Analysis of Sulfurtransferase:MDO Complex Formation by Native PAGE gels

Native gel electrophoresis enables separation of cellular proteins in their non-denatured state. This technique was used to identify potential protein-protein complexes between the sulfurtransferase and MDO. A 4:1 and 8:1 sulfurtransferase:MDO molar ratio without substrate was incubated for 15 minutes at 25 ℃ (Figure **3.8**). In order to determine if interactions were time dependent, a two hour time course (15 min, 30 min, 1 hour, 2 hour) was performed without

substrate at 25 ℃ with a sulfurtransferase:MDO molar ratio of 8:1. Both experiments displayed a band at ~100 kDa that was not present in controls with the individual protein (Figure **3.8**). 3-MPA was also added in ten-fold excess to the 8:1 mixture; however, no change was detected with the addition of substrate (Figure **3.8**). These results suggest that substrate does not affect the relative size or intensity of the band. An in-gel digestion coupled with mass spectrometry was performed to determine if the sulfurtransferase:MDO complex were components of the higher molecular weight band. The identities of the proteins were not confirmed, because the concentration of the sample was below the lower limit of detection of the mass spectrometer.

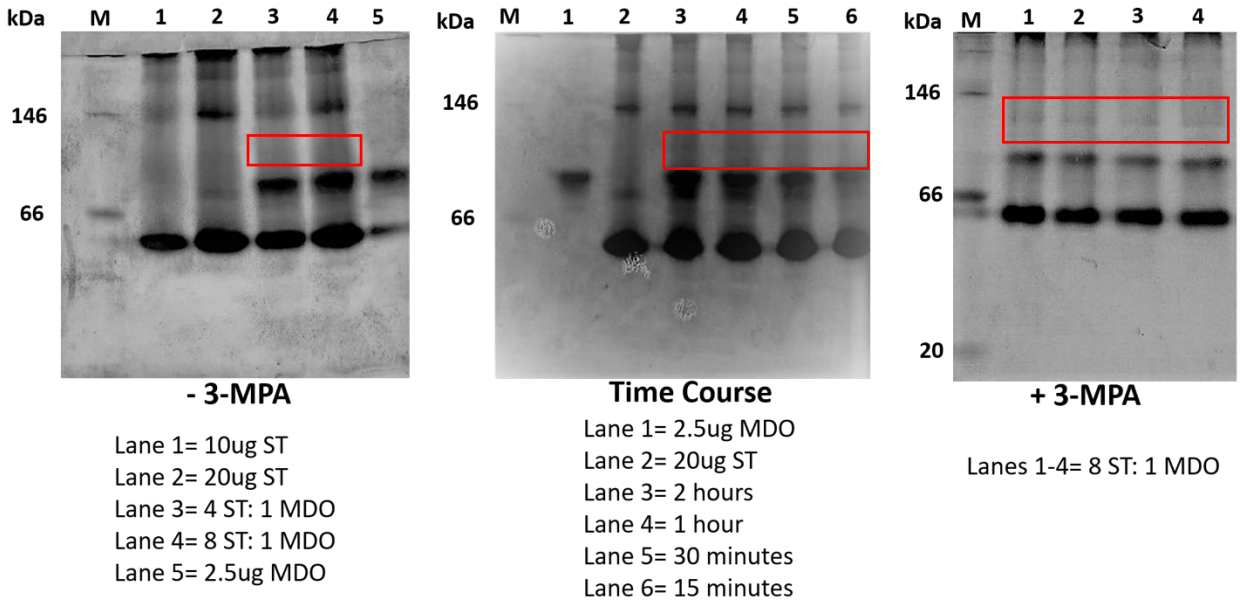

Figure 3.8. Native PAGE gel analysis of protein-protein interactions.

3.3.7 Analysis of Protein-Protein interactions via SPR

SPR is used to evaluate the equilibrium and kinetic parameters of protein-protein interactions and can provide quantitative real-time investigations of protein-protein interactions. Formation of the sulfurtransferase:MDO complex was observed at 3 minutes, while complete dissociation of the sulfurtransferase from the immobilized MDO was observed after 6 minutes (Figure **3.9**). The sensor-grams obtained were globally fit to a 1:2 site binding model using TraceDrawer (Nicoya Lifesciences). The first association constant was determined to be 530 M^{-1} sec^{-1} and the dissociation constant was 0.0028 sec^{-1}. The second association constant was determined to be 2200 ± 51 M^{-1} sec^{-1} and the dissociation constant was 0.049 sec^{-1}. The first equilibrium binding constant was 5.3 µM, while the second equilibrium binding constant was 0.23 µM (Table **3.4**). These results suggest that MDO and sulfurtransferase do interact, however, there are two conformations of MDO identified on the chip that bind to the sulfurtransferase. Each of these conformations have different affinities and different dissociation constants which further suggests conformational changes are occurring that affect binding. Electrostatic interactions also do not play a significant role in the binding process because increasing sodium chloride concentrations in the running buffer did not alter the sensorgram (data not shown).

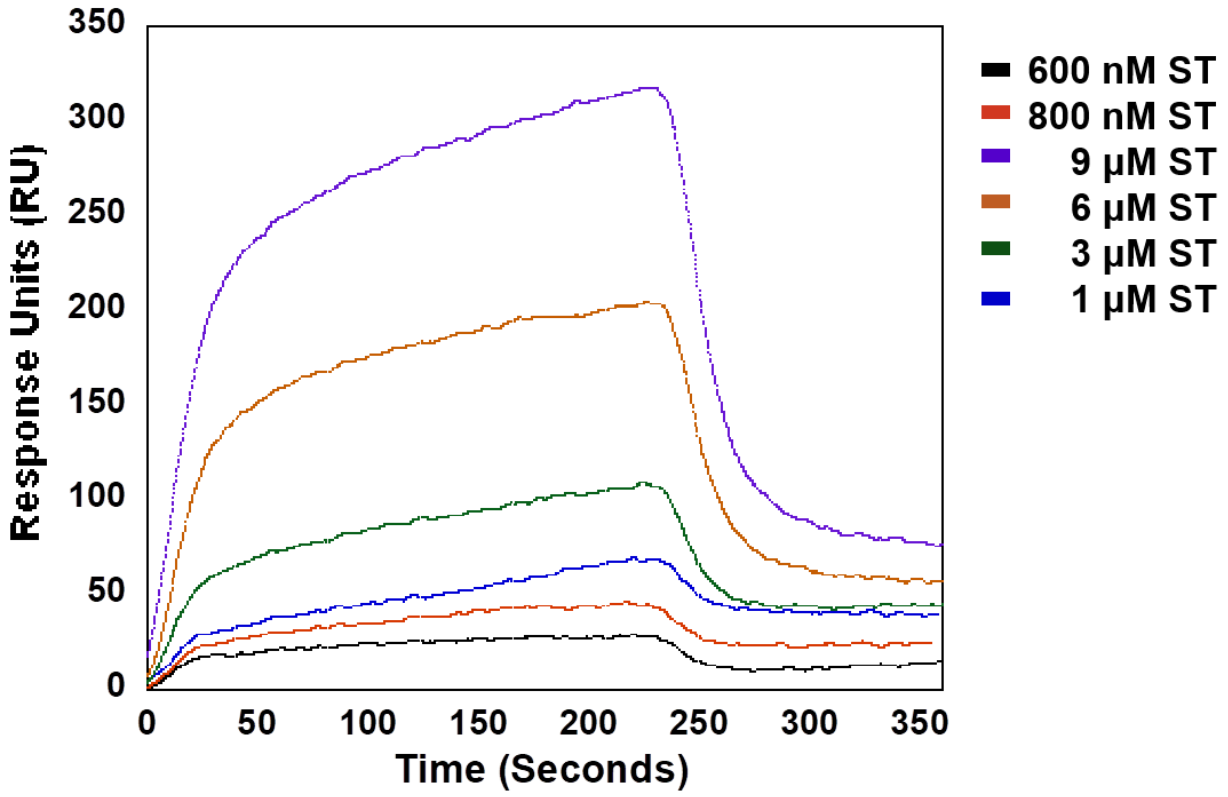

Figure 3.9. SPR Sulfurtransferase:MDO binding curve.

Table 3.4 Binding Constants from the Sulfurtransferase:MDO Complex

Complex	K_{on} (M^{-1} sec^{-1})	K_{off} (sec^{-1})	K_d (µM)
ST:MDO	530[a*]	0.0028[*]	5.3[*]
	2200[*]	0.049[*]	0.23[*]

[a*] All results were based on single run.

3.4 Discussion

MDO is a non-heme mononuclear iron enzyme that catalyzes the O_2-dependent oxidation of 3-MPA to produce 3-SPA.[66] The active site residues of MDO are similar to mammalian CDO, but the CDO Arg residue involved in substrate specificity is replaced by a Gln in MDO.[66] Substrate specificity in MDO is not dependent on a single amino acid, and likely involves additional active site residues. While MDO is able to oxidize 3-MPA, the metabolic role of either 3-MPA or 3-SPA is unclear in these bacterial systems. Most "Gln-type" bacteria contain MDO and an annotated sulfurtransferase on the same operon; however, previous studies have only evaluated MDO. As both genes are located on the same operon, they likely catalyze reactions in a common metabolic pathway. Our studies evaluated the substrates for MDO and the sulfurtransferase based on distinct reactions catalyzed by each enzyme.

Once the sulfurtransferase was identified on the MDO operon that contains a similar motif to the mercaptopyruvate sulfurtransferase, steady-state kinetic studies were repeated using 3-mercaptopyruvate as a substrate. Wild-type and R60Q CDO did not show any catalytic activity with 3-mercaptopyruvate. However, wild-type MDO displayed a higher catalytic activity with 3-mercaptopyruvate than 3-MPA. The increase of activity with wild-type MDO suggests that 3-mercaptopyruvate is a viable substrate for bacterial thiol dioxygenase. Additionally, Q62R MDO displayed nominal catalytic activity with 3-mercaptopyruvate, but there was a ~40 increase in catalytic activity with L-cysteine. These results further suggest that the glutamine in bacterial thiol dioxygenases does play a role in substrate specificity along with other active site residues. Studies also suggest the preference for 3-MPA because Gln62 weakly binds to cysteine due to being uncharged, shorter, and placed farther from the iron than the equivalent arginine residue in rat CDO.[120]

Cys485 is the proposed critical catalytic cysteine residue within the sulfurtransferase active site. Sulfurtransferases are typically characterized by their *in vitro* activity with thiosulfate or mercaptopyruvate to produce thiocyanate. In this study, we used several assays to analyze the putative catalytic Cys residue. There was only one free thiol identified in native sulfurtransferase, which we believe to be Cys485 since it is on the surface. Two free thiols were identified once the sulfurtransferase was denatured, indicating that Cys241 is buried within the enzyme and inaccessible to DTNB in the native form. In order to evaluate the enzyme activity of sulfurtransferase, SCN production was determined by a colorimetric assay at 460 nm. Unfortunately, sulfurtransferase did not show any activity with thiosulfate or mercaptopyruvate. These results suggested that the sulfur donor for sulfurtransferase is not thiosulfate or mercaptopyruvate. Low molecular weight thiols are often utilized in sulfurtransferase reactions. Sulfurtransferase reactions involve two half-reactions. In the first reaction, the sulfur is transferred from a donor to an active site cysteine to form a cysteine persulfide intermediate.[80,125] In the second reaction, the outer sulfur from the persulfide intermediate is transferred to a thiophilic acceptor to regenerate the resting enzyme.[80,125] Therefore, the sulfur donor to the sulfurtransferase is not a thiosulfate or mercaptopyruvate, or the putative sulfurtransferase is not annotated correctly. The correct sulfur donor may not have been utilized in these experiments, given the broad substrate range of sulfurtransferases.

Several bacteria have been identified that contain an operon expressing both a thiol dioxygenase and a sulfurtransferase. However, interactions of these two enzymes remains unknown. The thiol dioxygenase and sulfurtransferase enzymes have been shown to metabolize thiosulfate to sulfite and are involved in a sulfur assimilation pathways, while others have been identified in sulfide stress response such as *S. aureus* PRF.[104] Since the sulfurtransferase and the

MDO share an operon, protein-protein interactions between the two enzyme were evaluated. If the MDO and sulfurtransferase reactions are linked, the transfer of a potential persulfide product between enzymes would be protected if stable protein-protein interactions were formed. The evaluation of protein-protein interactions was attempted through several described methods. Unfortunately, only SPR and native PAGE gels gave any indication of protein-protein interaction. There is no single method for identifying static interactions between two proteins and results can vary depending on the experiment utilized to identify complex formation. Based on the evidence provided here, we do believe that there are protein-protein interactions and/or conformational changes occurring. However, given such varied results we suspect that they are very weak interactions. The modest conformational changes that were observed with HDX MS suggest that the proteins are interacting. Alternatively, the presence of two proteins may lead to crowding effects that are not relevant to the physiological function of the enzymes. SPR measures the interaction of proteins in real-time that could otherwise be missed through other methods. The identification of two binding sites through SPR could suggest there are two different conformations of MDO on the chip that bind the sulfurtransferase with different affinities. The identification of two binding sites could also suggest that the sulfurtransferase binds to MDO with weak affinity, that over time, induce conformational changes that further tighten the binding. Nevertheless, the results suggest conformational changes occur and MDO and the sulfurtransferase do interact. Furthermore, investigations into protein-protein interactions utilizing substrates of MDO and sulfurtransferase could provide more efficient evidence of protein-protein interaction taking place among the enzymes.

H_2S is a signaling molecule that is toxic at elevated concentrations.[104] H_2S inhibits cellular respiration in all cell types by inhibiting the activity of cytochrome oxidase.[107,130] It can also exhibit toxicity when the hydrogen sulfide anion (HS^-) directly reacts with oxidized low molecular weight (LMW) thiols that control cellular redox potential such as glutathione disulfide (GSSG), to form reactive sulfur species known as persulfides.[107,131] However, H_2S also plays a positive role in various physiological processes. In bacteria, H_2S has been shown to enhance resistance to oxidative stress induced by antibiotic treatment. In prokaryotes such as *P. aeruginosa*, H_2S is released from sulfur containing amino acids by using three major enzymes CBS, CSE, and 3-MST. However, the produced sulfide may accumulate and inhibit aerobic respiration. Mammalian and certain bacterial systems are able to prevent the accumulation of H_2S through the oxidation of the sulfide produced by three enzymes: SQR, PDO and rhodanese. However, these enzymes are not present in all H_2S-producing bacteria. Therefore, other organisms may have alternative mechanisms to remove H_2S. Recently, bacterial proteins that are natural fusions between PDO and rhodanese have been identified, one of those protein being *S. aureus* CstB.[101,104] Although MDO and sulfurtransferase do not show high sequence similarity to CstB, they may be performing a similar function. CstB is a multifunctional iron containing persulfide dioxygenase that oxidizes major LMW-persulfide substrates to directly generate thiosulfate and reduced thiols, thus avoiding cellular toxicity of sulfite.[107] Although the generation of H_2S has been described in *P. aeruginosa*, there is limited information available on how these organisms remove the potentially toxic compound.

Based on these studies, our group has proposed two possible reactions for the MDO/sulfurtransferase complex (Figure **3.10**). Reaction A is proposed based on the current reaction described for *S. aureus* CstB.[101] MDO oxidizes a LMW persulfide to form a LMW thiol-

sulfonate intermediate. The sulfurtransferase transfers a sulfur to generate thiosulfate and sulfite and sulfane sulfur effluxes from the cell. Thiosulfate is an inorganic sulfur molecule, which is the more reduced state of sulfur than that of sulfate.[132] Studies have shown that the thiosulfate pathway is comparatively more efficient than the sulfate pathway to biosynthesize L-cysteine in terms of cellular bioenergetics.[132] When sulfate is unavailable, organisms are able to use the thiosulfate pathway to generate sulfide to then enter the sulfate assimilation pathway. Studies suggest the thiosulfate sulfurtransferase GlpE, catalyzes thiosulfate to sulfite, which forms a bypass of sulfur metabolic flow from thiosulfate to sulfate pathway to biosynthesize Cys.[132] These studies further suggest that sulfurtransferases can function in thiosulfate assimilation.[132] Reaction B is proposed based on the reaction mechanism of H_2S degradation in mammalian systems, but with a few modifications. Sulfurtransferase catalyzes the sulfur-transfer reaction from a LMW-SH to a LMW-S-SH. The LMW-S-SH can be oxidized to sulfite by MDO.

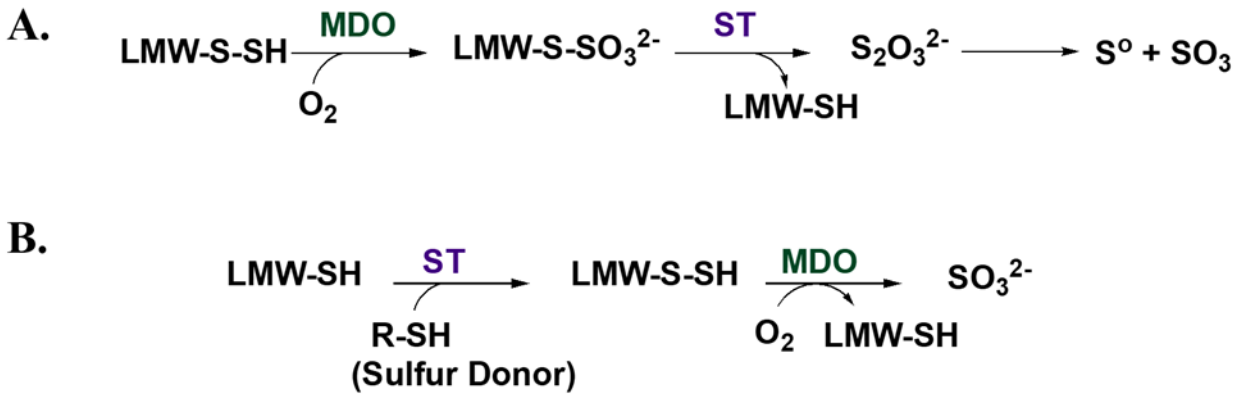

Figure 3.10. Proposed reactions for sulfurtransferase:MDO complex.

P. aeruginosa is able to use a wide range of sulfur compounds as sources of sulfur for growth.[133] It has been observed that the *mdo* operon in *P. aeruginosa* resides in the same gene

cluster as sulfur starvation enzymes. A gene cluster is defined as a group of genes that share a common function and are found within close proximity to one another on a chromosome.[134] Results from a bioinformatics study also revealed that both genes were considered to be part of a low sulfur island, meaning the genes encode proteins with low-sulfur content. The clustering of genes encoding proteins involved in the metabolism of low-preference sulfur sources could facilitate a coordinated response to sulfur starvation.[124] Therefore, understanding the regulatory properties of the *mdo* operon could provide an important link between the two systems.

CHAPTER FOUR

Expression of the *Pseudomonas aeruginosa mdo* Operon

4.1 Introduction

There have been several genes identified whose expression is regulated by sulfur limitation in *E. coli*. However, in the pseudomonad genome the genes expressed during sulfur limitation have not been clearly defined.

Recently, the *P. putida* genome was subjected to sulfur-mediated regulation.[124] Bioinformatic analyses of the genetic organization of the low sulfur content protein (LSP)-encoding genes indicated that 31% were associated with at least one other gene encoding a protein defined as an LSP.[124] Surprisingly, 55 LSP genes were detected in three large clusters referred to as low-sulfur islands (LSIs).[124] Among these LSPs were MDO, sulfurtransferase, and the sulfur starvation enzymes expressed under sulfur limiting conditions. The expected identities of the proteins encoded by LSIs strongly suggest that some LSIs play a role in sulfur acquisition when sulfur is limiting.[124]

The regulation of the sulfate starvation response in the ubiquitous organism, *P. aeruginosa*, has also been investigated.[41] *P. aeruginosa* was grown in synthetic medium with a variety of sulfur sources including alkanesulfonate, methionine, and organosulfate esters.[41] It was reported that *P. aeruginosa* responded to sulfate limitation with the upregulation of at least 10 *ssi* genes (PA1, PA2, PA4, PA6, PA7-PA9, and PA11-PA13).[41] These *ssi* genes include periplasmic binding proteins for sulfate, cystine, and sulfonates, which are anticipated to be involved in sulfur scavenging and a variety of sulfonatases.[29,41] However, the mechanism for gene expression and regulation under sulfur limiting conditions in *P. aeruginosa* is unclear. Similar to *E. coli*, *P. aeruginosa* and *P. putida* contain the transcriptional activator CysB, but they do not contain a corresponding *cbl* gene. In *P. putida*, CysB regulates the sulfate starvation response of the *sfn* operons.[28] In *P. putida* SfnR is a transcriptional activator for dimethylsulfone metabolism. Dimethylsulfone is oxidized through several mechanistic steps to formaldehyde and sulfite, and the sulfite is assimilated into sulfur containing metabolites. *P. aeruginosa* also expresses a SfnR homolog, but there have been no studies to evaluate the regulatory role of this transcriptional activator or the functional role of CysB. It is still unclear how the SfnR homologues in *P. aeruginosa* form transcriptional networks in response to sulfur starvation.

In *P. aeruginosa*, MDO and the sulfurtransferase exists in the same gene cluster as other sulfur starvation enzymes and both gene products contain low sulfur content. Therefore, it is believed that these genes may be expressed when sulfur is limiting. In this study, we wanted to determine if the *mdo* operon was regulated under sulfur limitation by evaluating growth and expression in the presence of different sulfur sources.

4.2 Materials and Methods

4.2.1 Materials

4-(2-Hydroxyethyl)piperazine-1-ethanesulfonic acid (HEPES), sodium sulfate, sodium sulfide, sodium sulfite, potassium thiocyanate, L-cysteine, sodium ethansulfonate, potassium phosphate dibasic, potassium phosphate monobasic, sodium ammonium phosphate magnesium chloride, magnesium sulfate, alkaline phosphatase (ALP), *p*-nitrophenol phosphate, and succinic acid were purchased from Sigma-Aldrich (St. Louis, MO). Difco-brand Luria-Bertani (LB) medium was purchased from Becton, Dickinson and Company (Sparks, MD). Tetracycline hydrochloride was purchased from Fisher Scientific (Pittsburgh, PA).

4.2.2 Strain Constructions

The transposon insertion mutants of *mdo*, thiosulfate sulfurtransferase (equivalent to the sulfurtransferase used in our studies), and *ssuD* were obtained from the Universtiy of Washington Transposon Mutant Collection (?).[135] These transposons carry alkaline phosphatase (*phoA*) translational gene reporter fusions. Insertion of transposon in each gene was verified by PCR with a transposon specific primer (Hah-138) (5´ CGG GTG CAG TAA TAT CGC CCT 3´) and a primer specific for the gene of interest . Specific primers used were 5´ CTC CTC CAG GCT CTG TAC CC 3´ for *mdo*, 5´ ATG TGG CGT TTC GCA TAG TT 3' for thiosulfate transferase, and 5´ GTA GGA CTC TTC CAG GTG CG 3´ for *ssuD*.

4.2.3 Sulfur-free Medium

Transposon insertions were analyzed in liquid sulfur free medium *(SFM)*. Briefly, 1X NCE (need a ref of Davis, Botstein and Roth) medium in which 1 mM of $MgSO_4$ was replaced with 1 mM $MgCl_2$ was used as the sulfur free medium (SFM).

4.2.4 Bacterial Growth Studies

Transposon insertions were isolated on LB-agar plates containing 0.01 mg/mL tetracycline (LB-tet). A single colony was selected from the plates and inoculated into 5 mL LB medium and incubated at 37 ℃ overnight. Overnight cultures were diluted 1:100 into SFM containing no antibiotic in a Corning Costar 48 well flat bottom cell culture plate (Corning, NY) and grown for 24 hours with shaking in a BioTek Cytation 3 plate reader (Winooski, VT). Cell growth was monitored at OD_{600}. In order to determine the growth behavior of each transposon the SFM was supplemented with 250 µM of various sulfur sources (sodium sulfate, sodium sulfide, sodium sulfite, potassium thiocyanate, and L-cysteine).

4.2.5 Alkaline Phosphatase Activity Assay

In order to assess expression of the genes of interest, an alkaline phosphatase assay was performed because the transposon insertions in these genes created protein fusions with alkaline phosphatase reporter gene. Transposon insertions were isolated on LB-agar plates containing 0.01 mg/mL tetracycline (LB-tet). A single colony was selected from the plates and inoculated into 5 mL LB media and incubated at 37 ℃ overnight. Overnight cultures were diluted 1:100 into sulfur free medium containing no antibiotic in a Corning Costar 48 well flat bottom cell culture plate (Corning, NY) and grown for 12 hours with shaking at 37 ℃ in a BioTek Cytation 3 plate reader (Winooski, VT). Cell growth was monitored at OD_{600} at neutral (pH 7.0) growth conditions were assessed. The sulfur-free medium was supplemented with 250 µM of various sulfur sources as previously mentioned. After 12 hours, samples were removed from the plate reader, extracted out of each well, and centrifuged into a pellet. Each pellet was resuspended with 500 µL of 25 mM

HEPES, and the cells lysed by sonication. The pNPP substrate (2 mg/mL) was added to each cell lysate and incubated at 25 °C for 30 minutes. After 30 mins the reaction was quenched with 2 M NaOH, monitored at 405 nm, and quantified using the molar absorption coefficient value (ε_{405}=18,000 M^{-1} cm^{-1}). The results obtained were the average of three separate experiments.

4.3 Results

4.3.1 Growth Studies with Various Sulfur Sources

In order to determine if the *mdo* operon is expressed under sulfur-limiting conditions, transposon insertion mutants were evaluated with various sulfur sources. SsuD is involved in sulfur starvation and was used as a positive control. Wild-type *P. aeruginosa* PA01 was also used as a positive control because it is able to grow with several different sulfur sources. Various sulfur sources were analyzed; however, no changes were observed compared to wild-type *P. aeruginosa* (Table **4.1**) (Figure **4.1 A-D**). Since the *ssu* operon is expressed during sulfate limitation, the transposon insertion strains were grown in sulfur-free medium supplemented with various concentrations of sodium sulfate (0.001-10 mM). However, no changes were observed compared to wild-type *P. aeruginosa*.

Sulfur Source	Structure
sulfate	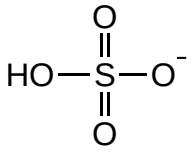
sulfite	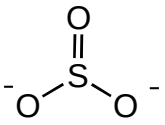
thiocyanate	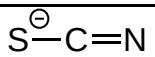
cysteine	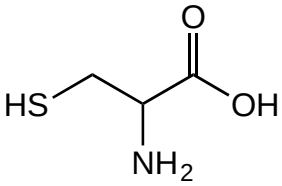
Sulfide	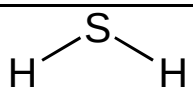

Table 4.1. Sulfur sources used for bacterial growth.

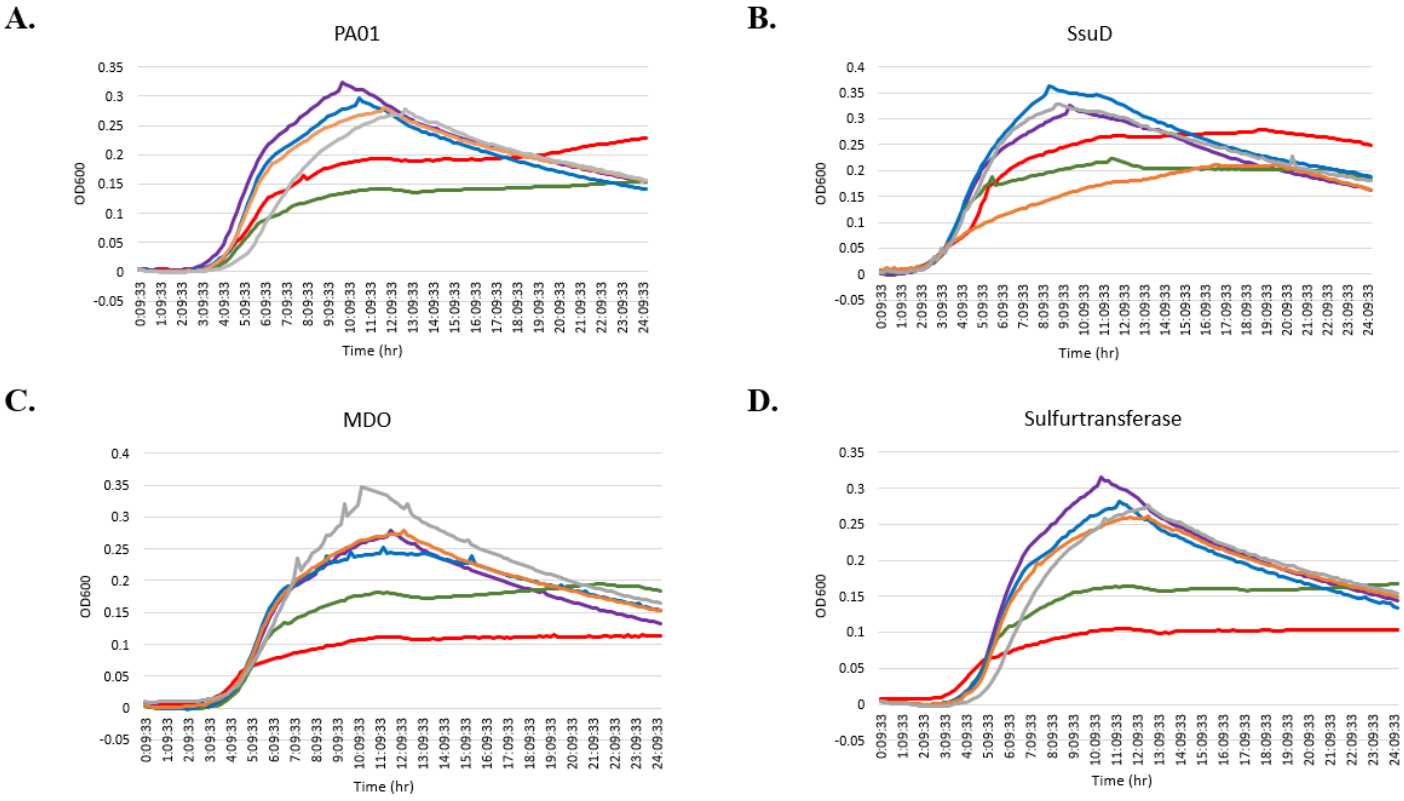

Figure 4.1. Growth studies of **A.** wild-type *P. aeruginosa*, **B.** *ssuD* transposon insertion, **C.** *mdo* transposon insertion, and **D.** *mdo* transposon insertion, with no sulfur source (red), with 250 µM sodium sulfate (purple), with 250 µM sodium sulfide (green), with 250 µM sodium sulfite (blue), with 250 µM potassium thiocyanate (orange), and with 250 µM L-cysteine (grey).

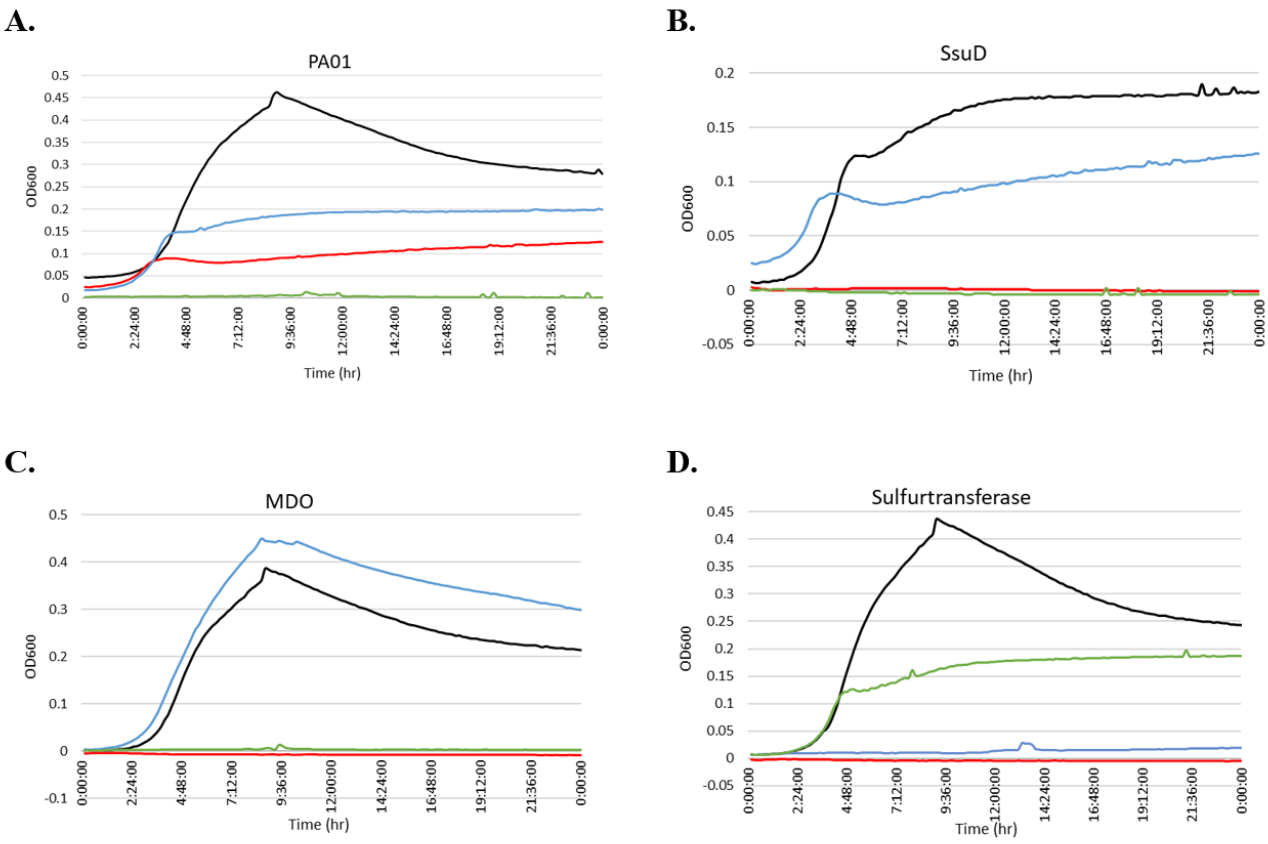

Figure 4.2. Growth studies of **A.** wild-type *P. aeruginosa*, **B.** *ssuD* transposon insertion, **C.** *mdo* transposon insertion, and **D.** *mdo* transposon insertion, with no sulfur source (red), with 10 mM sodium sulfate (black), with 100 µM sodium sulfate (blue), and with 1 µM sodium sulfate (green).

4.3.2 Alkaline Phosphatase Assay

In order to determine if the *mdo* operon is expressed under sulfur limiting conditions, the transposon insertions were grown as previously described and the AP activity was measured. PA01 and the transposon insertion strains were all grown with 10 mM, 0.1 mM, and 0.001 mM sodium sulfate and analyzed for phosphatase activity in triplicate. Three samples of each transposon insertion in SFM without sodium sulfate were also run as controls. There was no significant

increase in the 405 nm absorbance with the pNPP substrate over the control indicating the AP was not expressed.

4.4 Discussion

When *P. aeruginosa* is grown with organosulfur compounds as sulfur sources, a set of proteins called sulfate starvation-induced (Ssi) proteins are induced. Ssi proteins are repressed in the presence of sulfate, cysteine, or thiocyanate.[137] These Ssi proteins have been found in several gram-positive and gram-negative bacteria and have been studied in detail in *E. coli*, where they constitute a subset of the cysteine regulon products.[42,137] Ssi proteins are also found among *Pseudomonas* spp. and enable proteins to adapt to sulfur limiting conditions. Many of these Ssi proteins have been found among LSIs. The composition of the LSIs is consistent with their metabolic involvement in the acquisition of sulfur from nonpreferred sulfur souces.[39]

Previous studies have shown that MDO and sulfurtransferase are located in LSIs and the product of the sulfurtransferase is thought to be involved in sulfur assimilation from organosulfate/sulfonates.[124] Sulfur starvation enzymes are induced when sulfur concentration is $\geq$ 1 µM.[29,41] The growth study results indicated that the *mdo* transposon insertion strain was unable to grow with10 mM sodium sulfate and 1 µM sodium sulfate. Furthermore, the *thiosulfate sulfurtransferase* transposon insertion strain was only able to grow with 1 µM sodium sulfate. However, even though all the transposon insertion strains responded to various concentrations of sodium sulfate, results from AP assays indicate that there was no change in AP activity between wild-type *P. aeruginosa, ssuD* transposon insertion, *mdo* transposon insertion, and the *thiosulfate sulfurtransferase* transposon insertion. Contrary to bioinformatic studies, MDO and the

sulfurtransferase do not appear to be involved in sulfur starvation. Instead, expression of the *mdo* operon may be induced by hydrogen sulfide, similar to CstB in *S. aureus*.

The *cst* operon is considered to be crucial for sulfide detoxification in *S. aureus*.[101] H_2S can be toxic when HS^- reacts directly with oxidized low molecular weight thiols that control cellular redox potential, to form reactive sulfur species.[101] Transcription of the *cst* operon is regulated by a polysulfide-sensing repressor, CstR, and is induced by the addition of exogenous NaHS.[101] CstB oxidizes cellular low molecular weight persulfide substrates from *S. aureus*, coenzyme A persulfide, and bacillithiol persulfide to generate thiosulfate and reduced thiols in order to avoid cellular toxicity of sulfite.[101] Similar to *S. aureus*, *P. aeruginosa* is able to reduce sulfate and thiosulfate to produce toxic hydrogen sulfide gas.[138] If the *mdo* operon is induced by hydrogen sulfide, then it may be regulated similarly to the *cst* operon in *S. aureus*.

Even though our results suggest that the *mdo* operon is not involved in sulfur starvation, our lab would like to create our own gene knockouts to further test for sulfur starvation and hydrogen sulfide detoxification. Once these knockouts have been created, the sulfur limitation growth studies will be repeated and compared to the transposon insertion studies, to ensure the results are similar. If the same results are obtained, the knockouts will be tested for hydrogen sulfide detoxification.

CHAPTER FIVE

Summary

Sulfur is essential for all organisms as a component of essential amino acids and metabolites. In many bacteria, sulfur is acquired through the sulfate assimilation pathway leading to the production of sulfide that is then incorporated into sulfur-containing organic molecules.[29] Inorganic sulfate is not prevalent in the environment; therefore, bacteria must have an alternative mechanism for acquiring sulfur under sulfur-limiting conditions. Proteins expressed during sulfur limitation play a role in organosulfur uptake, sulfur acquisition from organic compounds, and protection against reactive oxygen species.[42,132] This research is focused on enzymes involved in the sulfur metabolic pathway. The overall goal of these studies was to determine the role of the *mdo* operon in bacteria. The main objectives of these studies were to determine the physiological substrate for MDO and how MDO is metabolically linked to the sulfurtransferase.

MDO was first identified as a thiol dioxygenase through metabolic comparisons of mammalian CDO. CDO is an iron containing enzyme belonging to the cupin superfamily and catalyzes the oxidation of L-cysteine to L-cysteine sulfinic acid. The iron center of CDO is octahedrally coordinated by three His residues and three water molecules. Adjacent to the iron center is a thioether crosslink which consists of Tyr157 and Cys93. The active site of mammalian CDO contains a conserved Arg residue involved in coordinating the carboxyl group of the L-

cysteine substrate. Thiol dioxygenase enzymes identified in bacteria have less than a 30% amino acid sequence identity with mammalian CDO and lack the Cys-Tyr crosslink. The Cys residue found in CDO is replaced with a Gly residue. There are two types of bacterial thiol dioxygenase enzymes based on the presence of a conserved Arg or Gln in the active site. These active site residues have been proposed to confer substrate specificity, similar to the Arg residue in mammalian CDO. The bacterial thiol dioxygenase enzymes that contain a conserved Gln have been proposed to convert 3-MPA to 3-SPA and are referred to as MDO.

In order to mimic bacterial CDO, the Cys involved in the thioether crosslink formation in mammalian CDO was substituted with Gly to determine how the catalytic properties of the enzyme was affected by the substitution. The C93G variant was no longer able to form the crosslink and appreciable activity was still observed with L-cysteine. To further investigate if Gln62 was involved in substrate specificity similar to Arg60 in mammalian CDO, Gln62 MDO was substituted with Arg and Arg60 CDO was substituted with Gln. These substitutions did not lead to any major alterations in the secondary structure compared to wild-type CDO and wild-type MDO. The Q62R MDO variant had a ~40-fold increase in catalytic activity with L-cysteine compared to wild-type MDO, and a ~1000-fold decrease in catalytic activity with 3-MPA compared to wild-type. The constructed variants R60Q CDO and Q62R MDO, provided evidence that the role of the Gln in bacterial MDO is to confer substrate specificity similar to the arginine residue in mammalian CDO. However, other amino acids in the active site likely assist in stabilizing the substrate. Therefore, these results further suggest that key structural features or other active site residues in bacterial MDO could play a role in substrate specificity.

Several Gln-type bacteria contain an annotated sulfurtransferase on the same operon as the MDO gene. This annotated sulfurtransferase has an amino acid sequence similar to

mercaptopyruvate sulfurtransferase enzymes, suggesting that mercaptopyruvate could be a potential substrate for MDO or the sulfurtransferase. Natural fusions between a dioxygenase and sulfurtransferase have been identified in bacteria, but the role of the fusion is still undetermined.[104] The existence of a fusion suggest that the independently expressed enzymes may interact for effective catalysis. Therefore, studies were performed to evaluate the metabolic link between the sulfurtransferase and MDO by determining the substrate specificity of MDO with 3-mercaptopyruvate. Additional studies were also performed to investigate the formation of putative protein-protein interactions between MDO and the sulfurtransferase.

To determine the metabolic link between MDO and sulfurtransferase, the activity of wild-type CDO and MDO were evaluated with 3-mercaptopyruvate. Wild-type CDO displayed no activity with 3-mercaptopyruvate. However, wild-type MDO displayed a higher catalytic activity with 3-mercaptopyruvate than 3-MPA, suggesting that 3-mercaptopyruvate is a viable substrate for bacterial thiol dioxygenase. Studies were also performed to evaluate if the R60Q CDO and Q62R MDO variants were able to utilize 3-mercaptopyruvate. The R60Q CDO variant did not show an altered specificity due to the single amino acid alteration, and was not able to utilize 3-mercaptopyruvate. There was nominal catalytic activity observed for Q62R MDO with 3-mercaptopyruvate suggesting the substrate specificity had been altered.

Given the observed activity of 3-mercaptopyruvate, studies were performed to determine the potential metabolic role of the sulfurtransferase. The conversion of cyanide to thiocyanate in the presence of thiosulfate or mercaptopyruvate was used to monitor the sulfurtransferase activity. However, thiocyanate was not detected with either mercaptopyruvate or thiosulfate. Based on the proposed sulfurtransferase reactions, a persulfide is produced and utilized as a substrate by MDO.

Studies were performed to monitor the activity of MDO by addition of sulfurtransferase, mercaptopyruvate, MDO, and ascorbate. However, no change in activity was observed.

Protein-protein interactions were evaluated between the two enzymes in order to determine if MDO and the sulfurtransferase are able to form a complex. These protein-protein interactions were evaluated by several different methods, however only SPR and native gels gave any indication of protein-protein interactions. These studies gave varied results due to the fact that there is not a single method for identifying static interactions between two proteins. HDX MS results displayed slight conformational changes, while SPR results displayed two possible binding sites, due to conformational changes. Therefore, based on the results from SPR and HDX, we do believe that there are protein-protein interactions as well as conformational changes occurring between the two enzymes.

Bioinformatics studies have observed that the *mdo* operon in *P. aeruginosa* resides on the same gene cluster as sulfur starvation enzymes and both genes are considered to have low-sulfur content. However, based on the lack of growth and expression of the transposon insertions of these two genes under sulfur-limiting conditions, MDO and the sulfurtransferase do not play a role in sulfur starvation. Instead these enzymes could be involved in hydrogen sulfide detoxification.

The results from these studies provide a foundation for future studies of the *mdo* operon in *P. aeruginosa*. Gln62 MDO does seem to play a role in substrate specificity, however other key structural features in bacterial MDO need to be further analyzed in order to define what amino acids are involved in substrate specificity. Additional studies also need to be performed with various persulfides to evaluate the metabolic role of the sulfurtransferase. While the *mdo* operon does not seem to be involved in sulfur starvation, it could be further evaluated to determine if it is involved in hydrogen sulfide or cyanide detoxication. Unfortunately, there is not a single method

for identifying protein-protein interactions, so results often vary. Based on the evidence provided, MDO and the sulfurtransferase do interact, but these interactions are likely weak interactions. Additional analyses could be performed with substrate to determine if substrate is needed for tighter association.

References

(1) Driggers, C. M.; Hartman, S. J.; Karplus, P. A. Structures of Arg- and Gln-Type Bacterial Cysteine Dioxygenase Homologs. *Protein Science* **2015**, *24* (1), 154–161.

(2) Bruland, N.; Wübbeler, J. H.; Steinbüchel, A. 3-Mercaptopropionate Dioxygenase, a Cysteine Dioxygenase Homologue, Catalyzes the Initial Step of 3-Mercaptopropionate Catabolism in the 3,3-Thiodipropionic Acid-Degrading Bacterium *Variovorax paradoxus*. *J Biol Chem* **2009**, *284* (1), 660–672.

(3) Mandeville, C. W. Sulfur: A Ubiquitous and Useful Tracer in Earth and Planetary Sciences. *Elements* **2010**, *6* (2), 75–80.

(4) Fomenko, D. E.; Marino, S. M.; Gladyshev, V. N. Functional Diversity of Cysteine Residues in Proteins and Unique Features of Catalytic Redox-Active Cysteines in Thiol Oxidoreductases. *Mol Cells* **2008**, *26* (3), 228–235.

(5) Brosnan, J. T.; Brosnan, M. E. The Sulfur-Containing Amino Acids: An Overview. *J Nutr* **2006**, *136* (6), 1636S-1640S.

(6) Palde, P. B.; Bhaskar, A.; Pedró Rosa, L. E.; Madoux, F.; Chase, P.; Gupta, V.; Spicer, T.; Scampavia, L.; Singh, A.; Carroll, K. S. First-in-Class Inhibitors of Sulfur Metabolism with Bactericidal Activity against Non-Replicating M. Tuberculosis. *ACS Chem Biol* **2016**, *11* (1), 172–184.

(7) Zheng, L.; White, R. H.; Cash, V. L.; Jack, R. F.; Dean, D. R. Cysteine Desulfurase Activity Indicates a Role for NIFS in Metallocluster Biosynthesis. *Proc Natl Acad Sci U S A* **1993**, *90* (7), 2754–2758.

(8) Johnson, D. C.; Dean, D. R.; Smith, A. D.; Johnson, M. K. Structure, Function, and Formation of Biological Iron-Sulfur Clusters. *Annu. Rev. Biochem.* **2005**, *74*, 247–281.

(9) Muyzer, G.; Stams, A. J. M. The Ecology and Biotechnology of Sulphate-Reducing Bacteria. *Nature Reviews Microbiology* **2008**, *6*.

(10) Lomans, B. P.; van der Drift, C.; Pol, A.; Op den Camp, H. J. M. Microbial Cycling of Volatile Organic Sulfur Compounds. *Cell. Mol. Life Sci.* **2002**, *59* (4), 575–588.

(11) Park, C.-M.; Weerasinghe, L.; Day, J. J.; Fukuto, J. M.; Xian, M. Persulfides: Current Knowledge and Challenges in Chemistry and Chemical Biology. *Mol Biosyst* **2015**, *11* (7), 1775–1785.

(12) Kawamura, S.; Nakabayashi, T.; Kitao, T.; Tsurugi, J. Aralkyl Hydrodisulfides. VI. The Reaction of Benzhydryl Hydrosulfide with Several Neucleophiles. *The Journal of Organic Chemistry* **1966**, *31* (6), 1985–1987.

(13) Bailey, T. S.; Zakharov, L. N.; Pluth, M. D. Understanding Hydrogen Sulfide Storage: Probing Conditions for Sulfide Release from Hydrodisulfides. *J. Am. Chem. Soc.* **2014**, *136* (30), 10573–10576.

(14) Mihara, H.; Esaki, N. Bacterial Cysteine Desulfurases: Their Function and Mechanisms. *Appl Microbiol Biotechnol* **2002**, *60* (1), 12–23.

(15) Black, K. A.; Dos Santos, P. C. Shared-Intermediates in the Biosynthesis of Thio-Cofactors: Mechanism and Functions of Cysteine Desulfurases and Sulfur Acceptors. *Biochimica et Biophysica Acta (BBA) - Molecular Cell Research* **2015**, *1853* (6), 1470–1480.

(16) Mihara, H.; Kurihara, T.; Yoshimura, T.; Soda, K.; Esaki, N. Cysteine Sulfinate Desulfinase, a NIFS-like Protein of *Escherichia coli* with Selenocysteine Lyase and Cysteine Desulfurase Activities. Gene Cloning, Purification, and Characterization of a Novel Pyridoxal Enzyme. *J. Biol. Chem.* **1997**, *272* (36), 22417–22424.

(17) Mihara, H.; Maeda, M.; Fujii, T.; Kurihara, T.; Hata, Y.; Esaki, N. A NifS-like Gene, CsdB, Encodes an *Escherichia coli* Counterpart of Mammalian Selenocysteine Lyase. Gene Cloning, Purification, Characterization and Preliminary x-Ray Crystallographic Studies. *J. Biol. Chem.* **1999**, *274* (21), 14768–14772.

(18) Patzer, S. I.; Hantke, K. SufS Is a NifS-like Protein, and SufD Is Necessary for Stability of the [2Fe-2S] FhuF Protein in *Escherichia coli*. *J. Bacteriol.* **1999**, *181* (10), 3307–3309.

(19) Mueller, E. G. Trafficking in Persulfides: Delivering Sulfur in Biosynthetic Pathways. *Nat. Chem. Biol.* **2006**, *2* (4), 185–194.

(20) Lauhon, C. T.; Kambampati, R. The IscS Gene in *Escherichia coli* Is Required for the Biosynthesis of 4-Thiouridine, Thiamin, and NAD. *J. Biol. Chem.* **2000**, *275* (26), 20096–20103.

(21) Mihara, H.; Kato, S.; Lacourciere, G. M.; Stadtman, T. C.; Kennedy, R. A. J. D.; Kurihara, T.; Tokumoto, U.; Takahashi, Y.; Esaki, N. The IscS Gene Is Essential for the Biosynthesis of 2-Selenouridine in TRNA and the Selenocysteine-Containing Formate Dehydrogenase H. *PNAS* **2002**, *99* (10), 6679–6683.

(22) Outten, F. W.; Wood, M. J.; Muñoz, F. M.; Storz, G. The SufE Protein and the SufBCD Complex Enhance SufS Cysteine Desulfurase Activity as Part of a Sulfur Transfer Pathway for Fe-S Cluster Assembly in *Escherichia coli*. *J. Biol. Chem.* **2003**, *278* (46), 45713–45719.

(23) McLaren, R. G.; Keer, J. I.; Swift, R. S. Sulphur Transformations in Soils Using Sulphur-35 Labelling. *Soil Biology and Biochemistry* **1985**, *17* (1), 73–79.

(24) Fitzgerald, J. W. Sulfate Ester Formation and Hydrolysis: A Potentially Important yet Often Ignored Aspect of the Sulfur Cycle of Aerobic Soils. *Bacteriol Rev* **1976**, *40* (3), 698–721.

(25) Scherer, H. W. Sulphur in Crop Production — Invited Paper. *European Journal of Agronomy* **2001**, *14* (2), 81–111.

(26) Cook, A. M.; Laue, H.; Junker, F. Microbial Desulfonation. *FEMS Microbiol. Rev.* **1998**, *22* (5), 399–419.

(27) Kahnert, A.; Vermeij, P.; Wietek, C.; James, P.; Leisinger, T.; Kertesz, M. A. The Ssu Locus Plays a Key Role in Organosulfur Metabolism in *Pseudomonas putida* S-313. *J. Bacteriol.* **2000**, *182* (10), 2869–2878.

(28) Kouzuma, A.; Endoh, T.; Omori, T.; Nojiri, H.; Yamane, H.; Habe, H. Transcription Factors CysB and SfnR Constitute the Hierarchical Regulatory System for the Sulfate Starvation Response in *Pseudomonas putida*. *Journal of Bacteriology* **2008**, *190* (13), 4521–4531.

(29) Kertesz, M. A. Riding the Sulfur Cycle – Metabolism of Sulfonates and Sulfate Esters in Gram-Negative Bacteria. *FEMS Microbiology Reviews* **2000**, *24* (2), 135–175.

(30) Kertesz, M. A.; Leisinger, T.; Cook, A. M. Proteins Induced by Sulfate Limitation in *Escherichia coli*, *Pseudomonas putida*, or *Staphylococcus aureus*. *J. Bacteriol.* **1993**, *175* (4), 1187–1190.

(31) Quadroni, M.; Staudenmann, W.; Kertesz, M.; James, P. Analysis of Global Responses by Protein and Peptide Fingerprinting of Proteins Isolated by Two-Dimensional Gel Electrophoresis. Application to the Sulfate-Starvation Response of *Escherichia coli*. *Eur. J. Biochem.* **1996**, *239* (3), 773–781.

(32) Hatzios, S. K.; Bertozzi, C. R. The Regulation of Sulfur Metabolism in *Mycobacterium tuberculosis*. *PLOS Pathogens* **2011**, *7* (7), e1002036.

(33) Eichhorn, E. E. Sulfonate-Sulfur Assimilation in *Escherichia coli*, ETH Zurich, 2000.

(34) Neumann, J.; Rose-Sperling, D.; Hellmich, U. A. Diverse Relations between ABC Transporters and Lipids: An Overview. *Biochim Biophys Acta Biomembr* **2017**, *1859* (4), 605–618.

(35) Hollenstein, K.; Frei, D.C.; Locher, K.P. Structure of an ABC Transporter Complex with its Binding Protein. Nature. 2007. 446 (7132) 213-216.

(36) van Der Ploeg, J. R.; Iwanicka-Nowicka, R.; Bykowski, T.; Hryniewicz, M. M.; Leisinger, T. The *Escherichia coli SsuEADCB* Gene Cluster Is Required for the Utilization of Sulfur from Aliphatic Sulfonates and Is Regulated by the Transcriptional Activator Cbl. *J. Biol. Chem.* **1999**, *274* (41), 29358–29365.

(37) Eichhorn, E.; Ploeg, J. R. van der; Kertesz, M. A.; Leisinger, T. Characterization of α-Ketoglutarate-Dependent Taurine Dioxygenase from *Escherichia coli. J. Biol. Chem.* **1997**, *272* (37), 23031–23036.

(38) van der Ploeg, J. R.; Eichhorn, E.; Leisinger, T. Sulfonate-Sulfur Metabolism and Its Regulation in *Escherichia coli. Arch Microbiol* **2001**, *176* (1), 1–8.

(39) Ploeg, J. R. van der; Iwanicka-Nowicka, R.; Kertesz, M. A.; Leisinger, T.; Hryniewicz, M. M. Involvement of CysB and Cbl Regulatory Proteins in Expression of the TauABCD Operon and Other Sulfate Starvation-Inducible Genes in *Escherichia coli. Journal of Bacteriology* **1997**, *179* (24), 7671–7678.

(40) Bykowski, T.; Van, J. der P.; Iwanicka-Nowicka, R.; Hryniewicz, M. M. The Switch from Inorganic to Organic Sulphur Assimilation in *Escherichia coli*: Adenosine 5'-Phosphosulphate (APS) as a Signaling Molecule for Sulphate Excess. *Mol Microbiol* **2002**, *43* (5), 1347–1358.

(41) Hummerjohann, J.; Kuttel, E.; Quadroni, M.; Ragaller, J.; Leisinger, T.; Kertes, M. A. Regulation of the Sulfate Starvation Response in *Pseudomonas aeruginosa*: Role of Cysteine Biosynthetic Intermediates. *Microbiology* **1998**, *144* (5), 1375–1386.

(42) van der Ploeg, J. R.; Weiss, M. A.; Saller, E.; Nashimoto, H.; Saito, N.; Kertesz, M. A.; Leisinger, T. Identification of Sulfate Starvation-Regulated Genes in *Escherichia coli*: A Gene Cluster Involved in the Utilization of Taurine as a Sulfur Source. *J Bacteriol* **1996**, *178* (18), 5438–5446.

(43) Quadroni, M.; James, P.; Dainese-Hatt, P.; Kertesz, M. A. Proteome Mapping, Mass Spectrometric Sequencing and Reverse Transcription-PCR for Characterization of the Sulfate Starvation-Induced Response in *Pseudomonas aeruginosa PA*O1. *European Journal of Biochemistry* **1999**, *266* (3), 986–996.

(44) Davison, J.; Brunel, F.; Phanopoulos, A.; Prozzi, D.; Terpstra, P. Cloning and Sequencing of *Pseudomonas* Genes Determining Sodium Dodecyl Sulfate Biodegradation. *Gene* **1992**, *114* (1), 19–24.

(45) Kahnert, A.; Mirleau, P.; Wait, R.; Kertesz, M. A. The LysR-Type Regulator SftR Is Involved in Soil Survival and Sulphate Ester Metabolism in *Pseudomonas putida*. *Environmental Microbiology* **2002**, *4* (4), 225–237

(46) Vermeij, P.; Wietek, C.; Kahnert, A.; Wüest, T.; Kertesz, M. A. Genetic Organization of Sulphur-Controlled Aryl Desulphonation in *Pseudomonas putida* S-313. *Molecular Microbiology* **1999**, *32* (5), 913–926.

(47) Endoh, T.; Habe, H.; Nojiri, H.; Yamane, H.; Omori, T. The Σ54-Dependent Transcriptional Activator *SfnR* Regulates the Expression of the *Pseudomonas putida* SfnFG Operon

Responsible for Dimethyl Sulphone Utilization. *Molecular Microbiology* **2005**, *55* (3), 897–911.

(48) Khuri, S.; Bakker, F. T.; Dunwell, J. M. Phylogeny, Function, and Evolution of the Cupins, a Structurally Conserved, Functionally Diverse Superfamily of Proteins. *Mol Biol Evol* **2001**, *18* (4), 593–605.

(49) Dunwell, J. M.; Purvis, A.; Khuri, S. Cupins: The Most Functionally Diverse Protein Superfamily? *Phytochemistry* **2004**, *65* (1), 7–17.

(50) Souness, R. J.; Kleffmann, T.; Tchesnokov, E. P.; Wilbanks, S. M.; Jameson, G. B.; Jameson, G. N. L. Mechanistic Implications of Persulfenate and Persulfide Binding in the Active Site of Cysteine Dioxygenase. *Biochemistry* **2013**, *52* (43), 7606–7617.

(51) Opaleye, O.; Rose, R.-S.; Whittaker, M. M.; Woo, E.-J.; Whittaker, J. W.; Pickersgill, R. W. Structural and Spectroscopic Studies Shed Light on the Mechanism of Oxalate Oxidase. *J. Biol. Chem.* **2006**, *281* (10), 6428–6433.

(52) Stipanuk, M. H.; Londono, M.; Hirschberger, L. L.; Hickey, C.; Thiel, D. J.; Wang, L. Evidence for Expression of a Single Distinct Form of Mammalian Cysteine Dioxygenase. *Amino Acids* **2004**, *26* (1), 99–106.

(53) Parsons, R. B.; Waring, R. H.; Ramsden, D. B.; Williams, A. C. In Vitro Effect of the Cysteine Metabolites Homocysteic Acid, Homocysteine and Cysteic Acid upon Human Neuronal Cell Lines. *Neurotoxicology* **1998**, *19* (4–5), 599–603.

(54) Pierce, B. S.; Gardner, J. D.; Bailey, L. J.; Brunold, T. C.; Fox, B. G. Characterization of the Nitrosyl Adduct of Substrate-Bound Mouse Cysteine Dioxygenase by Electron Paramagnetic Resonance: Electronic Structure of the Active Site and Mechanistic Implications. *Biochemistry* **2007**, *46* (29), 8569–8578.

(55) Driggers, C. M.; Kean, K. M.; Hirschberger, L. L.; Cooley, R. B.; Stipanuk, M. H.; Karplus, P. A. Structure-Based Insights into the Role of the Cys-Tyr Crosslink and Inhibitor-Recognition by Mammalian Cysteine Dioxygenase. *J Mol Biol* **2016**, *428* (20), 3999–4012.

(56) Simmons, C. R.; Liu, Q.; Huang, Q.; Hao, Q.; Begley, T. P.; Karplus, P. A.; Stipanuk, M. H. Crystal Structure of Mammalian Cysteine Dioxygenase. A Novel Mononuclear Iron Center for Cysteine Thiol Oxidation. *J. Biol. Chem.* **2006**, *281* (27), 18723–18733.

(57) Ye, S.; Wu, X.; Wei, L.; Tang, D.; Sun, P.; Bartlam, M.; Rao, Z. An Insight into the Mechanism of Human Cysteine Dioxygenase. Key Roles of the Thioether-Bonded Tyrosine-Cysteine Cofactor. *J. Biol. Chem.* **2007**, *282* (5), 3391–3402.

(58) Dominy, J. E.; Simmons, C. R.; Karplus, P. A.; Gehring, A. M.; Stipanuk, M. H. Identification and Characterization of Bacterial Cysteine Dioxygenases: A New Route of Cysteine Degradation for Eubacteria. *J Bacteriol* **2006**, *188* (15), 5561–5569.

(59) McCoy, J. G.; Bailey, L. J.; Bitto, E.; Bingman, C. A.; Aceti, D. J.; Fox, B. G.; Phillips, G. N. Structure and Mechanism of Mouse Cysteine Dioxygenase. *Proc. Natl. Acad. Sci. U.S.A.* **2006**, *103* (9), 3084–3089.

(60) Li, W.; Pierce, B. S. Steady-State Substrate Specificity and O2-Coupling Efficiency of Mouse Cysteine Dioxygenase. *Archives of Biochemistry and Biophysics* **2015**, *565*, 49–56.

(61) Li, W.; Blaesi, E. J.; Pecore, M. D.; Crowell, J. K.; Pierce, B. S. Second-Sphere Interactions between the C93–Y157 Cross-Link and the Substrate-Bound Fe Site Influence the O2 Coupling Efficiency in Mouse Cysteine Dioxygenase. *Biochemistry* **2013**, *52* (51), 9104–9119.

(62) Driggers, C. M.; Cooley, R. B.; Sankaran, B.; Hirschberger, L. L.; Stipanuk, M. H.; Karplus, P. A. Cysteine Dioxygenase Structures from PH4 to 9: Consistent Cys-Persulfenate

Formation at Intermediate PH and a Cys-Bound Enzyme at Higher PH. *J. Mol. Biol.* **2013**, *425* (17), 3121–3136.

(63) Driggers, C. M.; Hartman, S. J.; Karplus, P. A. Structures of Arg- and Gln-Type Bacterial Cysteine Dioxygenase Homologs. *Protein Sci* **2015**, *24* (1), 154–161.

(64) Driggers, C. M.; Hartman, S. J.; Karplus, P. A. Structures of Arg- and Gln-Type Bacterial Cysteine Dioxygenase Homologs., Structures of Arg- and Gln-Type Bacterial Cysteine Dioxygenase Homologs. *Protein Sci* **2015**, *24*, *24* (1, 1), 154, 154–161.

(65) Dominy, J. E.; Hwang, J.; Guo, S.; Hirschberger, L. L.; Zhang, S.; Stipanuk, M. H. Synthesis of Amino Acid Cofactor in Cysteine Dioxygenase Is Regulated by Substrate and Represents a Novel Post-Translational Regulation of Activity. *J Biol Chem* **2008**, *283* (18), 12188–12201.

(66) Crowell, J. K.; Sardar, S.; Hossain, M. S.; Foss, F. W.; Pierce, B. S. Non-Chemical Proton-Dependent Steps Prior to O2-Activation Limit *Azotobacter vinelandii* 3-Mercaptopropionic Acid Dioxygenase (MDO) Catalysis. *Arch Biochem Biophys* **2016**, *604*, 86–94.

(67) Dominy, J. J.; Hirschberger, L. L.; Coloso, R. M.; Stipanuk, M. H. Regulation of Cysteine Dioxygenase Degradation Is Mediated by Intracellular Cysteine Levels and the Ubiquitin-26 S Proteasome System in the Living Rat. *Biochem J* **2006**, *394* (Pt 1), 267–273.

(68) Mopper, K.; Taylor, B. F. Biogeochemical Cycling of Sulfur: Thiols in Coastal Marine Sediments. In *Organic Marine Geochemistry*; Sohn, M. L., Ed.; American Chemical Society: Washington, DC, 1986; Vol. 305, pp 324–339.

(69) Gonzalez, J.M.; Covert, J.S.; Whitman, W.B., Henriksen, J.R., Mayer, F.; Scharf, B.; Schmitt, R.; Buchan, A.; Fuhrman, J.A.; Kiene, R.P.; Moran, M.A. International Journal

of Systematic and Evolutionary Microbiology. 2003, 53 (5) 1261-1269.

(70) Johnston, A. W. B. Who Can Cleave DMSP? *Science* **2015**, *348* (6242), 1430–1431.

(71) Reisch, C. R.; Stoudemayer, M. J.; Varaljay, V. A.; Amster, I. J.; Moran, M. A.; Whitman, W. B. Novel Pathway for Assimilation of Dimethylsulphoniopropionate Widespread in Marine Bacteria. *Nature* **2011**, *473* (7346), 208–211.

(72) Chen, Y.; Schäfer, H. Towards a Systematic Understanding of Structure–Function Relationship of Dimethylsulfoniopropionate-Catabolizing Enzymes. *Molecular Microbiology* **2019**, *111* (6), 1399–1403.

(73) Bullock, H. A.; Luo, H.; Whitman, W. B. Evolution of Dimethylsulfoniopropionate Metabolism in Marine Phytoplankton and Bacteria. *Front Microbiol* **2017**, *8*.

(74) Reisch, C. R.; Crabb, W. M.; Gifford, S. M.; Teng, Q.; Stoudemayer, M. J.; Moran, M. A.; Whitman, W. B. Metabolism of Dimethylsulphoniopropionate by *Ruegeria Pomeroyi* DSS-3. *Mol. Microbiol.* **2013**, *89* (4), 774–791.

(75) Meyer, T.; Burow, M.; Bauer, M.; Papenbrock, J. Arabidopsis Sulfurtransferases: Investigation of Their Function during Senescence and in Cyanide Detoxification. *Planta* **2003**, *217* (1), 1–10.

(76) Bauer, M.; Papenbrock, J. Identification and Characterization of Single-Domain Thiosulfate Sulfurtransferases from *Arabidopsis thaliana*. *FEBS Letters* **2002**, *532* (3), 427–431.

(77) Bordo, D.; Bork, P. The Rhodanese/Cdc25 Phosphatase Superfamily. *EMBO Rep* **2002**, *3* (8), 741–746.

(78) Cipollone, R.; Ascenzi, P.; Visca, P. Common Themes and Variations in the Rhodanese Superfamily. *IUBMB Life* **2007**, *59* (2), 51–59.

(79) Westley, J. Rhodanese. *Adv. Enzymol. Relat. Areas Mol. Biol.* **1973**, *39*, 327–368.

(80) Westley, J. Thiosulfate: Cyanide Sulfurtransferase (Rhodanese). *Meth. Enzymol.* **1981**, *77*, 285–291.

(81) Vennesland, B.; Castric, P. A.; Conn, E. E.; Solomonson, L. P.; Volini, M.; Westley, J. Cyanide Metabolism. *Fed. Proc.* **1982**, *41* (10), 2639–2648.

(82) Nandi, D. L.; Horowitz, P. M.; Westley, J. Rhodanese as a Thioredoxin Oxidase. *Int. J. Biochem. Cell Biol.* **2000**, *32* (4), 465–473.

(83) Bonomi, F.; Pagani, S.; Cerletti, P. Insertion of Sulfide into Ferredoxins Catalyzed by Rhodanese. *FEBS Lett.* **1977**, *84* (1), 149–152.

(84) Pagani, S.; Bonomi, F.; Cerletti, P. Enzymic Synthesis of the Iron-Sulfur Cluster of Spinach Ferredoxin. *Eur. J. Biochem.* **1984**, *142* (2), 361–366.

(85) Villarejo, M. L. J.; Westley, J. W. MECHANISM OF RHODANESE CATALYSIS OF THIOSULFATE-LIPOATE OXIDATION-REDUCTION. *The Journal of biological chemistry* **1963**, *238*, 4016–4020.

(86) Ogata, K.; Volini, M. Mitochondrial Rhodanese: Membrane-Bound and Complexed Activity. *J. Biol. Chem.* **1990**, *265* (14), 8087–8093.

(87) Sorbo, B. A Colorimetric Method for the Determination of Thiosulfate. *Biochim. Biophys. Acta* **1957**, *23* (2), 412–416.

(88) Horowitz, P.; DeToma, F. Improved Preparation of Bovine Liver Rhodanese. *J. Biol. Chem.* **1970**, *245* (5), 984–985.

(89) Ploegman, J. H.; Drent, G.; Kalk, K. H.; Hol, W. G. The Structure of Bovine Liver Rhodanese. II. The Active Site in the Sulfur-Substituted and the Sulfur-Free Enzyme. *J. Mol. Biol.* **1979**, *127* (2), 149–162.

(90) Ploegman, J. H.; Drent, G.; Kalk, K. H.; Hol, W. G.; Heinrikson, R. L.; Keim, P.; Weng, L.; Russell, J. The Covalent and Tertiary Structure of Bovine Liver Rhodanese. *Nature* **1978**, *273* (5658), 124–129.

(91) Hol, W. G.; Lijk, L. J.; Kalk, K. H. The High Resolution Three-Dimensional Structure of Bovine Liver Rhodanese. *Fundam Appl Toxicol* **1983**, *3* (5), 370–376.

(92) Spallarossa, A.; Donahue, J. L.; Larson, T. J.; Bolognesi, M.; Bordo, D. *Escherichia coli* GlpE Is a Prototype Sulfurtransferase for the Single-Domain Rhodanese Homology Superfamily. *Structure* **2001**, *9* (11), 1117–1125.

(93) Tanizawa, K. Production of H2S by 3-Mercaptopyruvate Sulphurtransferase. *J. Biochem.* **2011**, *149* (4), 357–359.

(94) Nagahara, N.; Okazaki, T.; Nishino, T. Cytosolic Mercaptopyruvate Sulfurtransferase Is Evolutionarily Related to Mitochondrial Rhodanese. Striking Similarity in Active Site Amino Acid Sequence and the Increase in the Mercaptopyruvate Sulfurtransferase Activity of Rhodanese by Site-Directed Mutagenesis. *J. Biol. Chem.* **1995**, *270* (27), 16230–16235.

(95) Nagahara, N.; Nishino, T. Role of Amino Acid Residues in the Active Site of Rat Liver Mercaptopyruvate Sulfurtransferase CDNA CLONING, OVEREXPRESSION, AND SITE-DIRECTED MUTAGENESIS. *J. Biol. Chem.* **1996**, *271* (44), 27395–27401.

(96) Alphey, M. S.; Williams, R. A. M.; Mottram, J. C.; Coombs, G. H.; Hunter, W. N. The Crystal Structure of *Leishmania major* 3-Mercaptopyruvate Sulfurtransferase. A Three-Domain Architecture with a Serine Protease-like Triad at the Active Site. *J. Biol. Chem.* **2003**, *278* (48), 48219–48227.

(97) Nakamura, T.; Yamaguchi, Y.; Sano, H. Plant Mercaptopyruvate Sulfurtransferases: Molecular Cloning, Subcellular Localization and Enzymatic Activities. *Eur. J. Biochem.* **2000**, *267* (17), 5621–5630.

(98) Papenbrock, J.; Schmidt, A. Characterization of Two Sulfurtransferase Isozymes from *Arabidopsis thaliana*. *Eur. J. Biochem.* **2000**, *267* (17), 5571–5579.

(99) Colnaghi, R.; Cassinelli, G.; Drummond, M; Forlani, F., Pagani, S. Properties of the *Escherichia coli* Rhodanese-like Protein SseA: contribution of the Active-Site Residue Ser240 to Sulfur Donor Recognition. FEBS Lett. 2001. 500 (3), 153-156.

(100) Chauncey, T. R.; Uhteg, L. C.; Westley, J. Thiosulfate Reductase. *Meth. Enzymol.* **1987**, *143*, 350–354.

(101) Shen, J.; Keithly, M. E.; Armstrong, R. N.; Higgins, K. A.; Edmonds, K. A.; Giedroc, D. P. *Staphylococcus aureus* CstB Is a Novel Multidomain Persulfide Dioxygenase-Sulfurtransferase Involved in Hydrogen Sulfide Detoxification. *Biochemistry* **2015**, *54* (29), 4542–4554.

(102) Billaut-Laden, I.; Allorge, D.; Crunelle-Thibaut, A.; Rat, E.; Cauffiez, C.; Chevalier, D.; Houdret, N.; Lo-Guidice, J.-M.; Broly, F. Evidence for a Functional Genetic Polymorphism of the Human Thiosulfate Sulfurtransferase (Rhodanese), a Cyanide and H2S Detoxification Enzyme. *Toxicology* **2006**, *225* (1), 1–11.

(103) Chauncey, T. R.; Westley, J. The Catalytic Mechanism of Yeast Thiosulfate Reductase. *J. Biol. Chem.* **1983**, *258* (24), 15037–15045.

(104) Motl, N.; Skiba, M. A.; Kabil, O.; Smith, J. L.; Banerjee, R. Structural and Biochemical Analyses Indicate That a Bacterial Persulfide Dioxygenase-Rhodanese Fusion Protein Functions in Sulfur Assimilation. *J. Biol. Chem.* **2017**, *292* (34), 14026–14038.

(105) Shatalin, K.; Shatalina, E.; Mironov, A.; Nudler, E. H2S: A Universal Defense against Antibiotics in Bacteria. *Science* **2011**, *334* (6058), 986–990.

(106) Luebke, J. L.; Shen, J.; Bruce, K. E.; Kehl-Fie, T. E.; Peng, H.; Skaar, E. P.; Giedroc, D. P. The CsoR-like Sulfurtransferase Repressor (CstR) Is a Persulfide Sensor in *Staphylococcus aureus*. *Mol. Microbiol.* **2014**, *94* (6), 1343–1360.

(107) Higgins, K. A.; Peng, H.; Luebke, J. L.; Chang, F.-M. J.; Giedroc, D. P. Conformational Analysis and Chemical Reactivity of the Multidomain Sulfurtransferase, *Staphylococcus aureus* CstA. *Biochemistry* **2015**, *54* (14), 2385–2398.

(108) Kabil, O.; Banerjee, R. Characterization of Patient Mutations in Human Persulfide Dioxygenase (ETHE1) Involved in H2S Catabolism. *J. Biol. Chem.* **2012**, *287* (53), 44561–44567.

(109) Fellner, M.; Aloi, S.; Tchesnokov, E. P.; Wilbanks, S. M.; Jameson, G. N. L. Substrate and PH-Dependent Kinetic Profile of 3-Mercaptopropionate Dioxygenase from *Pseudomonas aeruginosa*. *Biochemistry* **2016**, *55* (9), 1362–1371.

(110) Wainer, A. The Production of Cysteinesulfinic Acid from Cysteine in Vitro. *Biochimica et Biophysica Acta (BBA) - General Subjects* **1965**, *104* (2), 405–412.

(111) Yamaguchi, K.; Hosokawa, Y.; Kohashi, N.; Kori, Y.; Sakakibara, S.; Ueda, I. Rat Liver Cysteine Dioxygenase (Cysteine Oxidase). Further Purification, Characterization, and Analysis of the Activation and Inactivation. *J. Biochem.* **1978**, *83* (2), 479–491.

(112) Simmons, C. R.; Krishnamoorthy, K.; Granett, S. L.; Schuller, D. J.; Dominy, J. E.; Begley, T. P.; Stipanuk, M. H.; Karplus, P. A. A Putative Fe2+-Bound Persulfenate Intermediate in Cysteine Dioxygenase. *Biochemistry* **2008**, *47* (44), 11390–11392.

(113) Imsand, E. M.; Njeri, C. W.; Ellis, H. R. Addition of an External Electron Donor to in Vitro Assays of Cysteine Dioxygenase Precludes the Need for Exogenous Iron. *Archives of Biochemistry and Biophysics* **2012**, *521* (1–2), 10–17.

(114) Vanoni, M. A.; Edmondson, D. E.; Zanetti, G.; Curti, B. Characterization of the Flavins and the Iron-Sulfur Centers of Glutamate Synthase from *Azospirillum brasilense* by Absorption, Circular Dichroism, and Electron Paramagnetic Resonance Spectroscopies. *Biochemistry* **1992**, *31* (19), 4613–4623.

(115) Njeri, C. W.; Ellis, H. R. Shifting Redox States of the Iron Center Partitions CDO between Crosslink Formation or Cysteine Oxidation. *Archives of Biochemistry and Biophysics* **2014**, *558*, 61–69.

(116) Crawford, J. A.; Li, W.; Pierce, B. S. Single Turnover of Substrate-Bound Ferric Cysteine Dioxygenase with Superoxide Anion: Enzymatic Reactivation, Product Formation, and a Transient Intermediate. *Biochemistry* **2011**, *50* (47), 10241–10253.

(117) Chai, S. C.; Jerkins, A. A.; Banik, J. J.; Shalev, I.; Pinkham, J. L.; Uden, P. C.; Maroney, M. J. Heterologous Expression, Purification, and Characterization of Recombinant Rat Cysteine Dioxygenase. *J Biol Chem* **2005**, *280* (11), 9865–9869.

(118) Njeri, C. W.; Ellis, H. R. Shifting Redox States of the Iron Center Partitions CDO between Crosslink Formation or Cysteine Oxidation. Archives of Biochemistry and Biophysics 2014, 558, 61–69.

(119) Fellner, M.; Aloi, Sekotilani, A.; Tchesnokov, E.P.; Wilbanks, S.M.; Jameson, G. Substrate and pH-Dependent Kinetic Profile of 3-Mercaptopropionate Dioxygenase from *Pseudomonas aeruginosa*. Biochemistry. 2016, 55 (9) 1362-1371.

(120) Tchesnokov, E. P.; Fellner, M.; Siakkou, E.; Kleffmann, T.; Martin, L. W.; Aloi, S.; Lamont, I. L.; Wilbanks, S. M.; Jameson, G. N. L. The Cysteine Dioxygenase Homologue from *Pseudomonas aeruginosa* Is a 3-Mercaptopropionate Dioxygenase. *J. Biol. Chem.* **2015**, *290* (40), 24424–24437.

(121) Pierce, B. S.; Subedi, B. P.; Sardar, S.; Crowell, J. K. The "Gln-Type" Thiol Dioxygenase from *Azotobacter vinelandii* Is a 3-Mercaptopropionic Acid Dioxygenase. *Biochemistry* **2015**, *54* (51), 7477–7490.

(122) Aloi, S.; Davies, C. G.; Karplus, P. A.; Wilbanks, S. M.; Jameson, G. N. L. Substrate Specificity in Thiol Dioxygenases. *Biochemistry* **2019**, *58* (19), 2398–2407.

(123) Fellner, M.; Aloi, S.; Tchesnokov, E. P.; Wilbanks, S. M.; Jameson, G. N. L. Substrate and PH-Dependent Kinetic Profile of 3-Mercaptopropionate Dioxygenase from *Pseudomonas aeruginosa*. *Biochemistry* **2016**, *55* (9), 1362–1371.

(124) Scott, C.; Hilton, M. E.; Coppin, C. W.; Russell, R. J.; Oakeshott, J. G.; Sutherland, T. D. A Global Response to Sulfur Starvation in *Pseudomonas putida* and Its Relationship to the Expression of Low-Sulfur-Content Proteins. *FEMS Microbiol. Lett.* **2007**, *267* (2), 184–193.

(125) Libiad, M.; Motl, N.; Akey, D. L.; Sakamoto, N.; Fearon, E. R.; Smith, J. L.; Banerjee, R. Thiosulfate Sulfurtransferase-like Domain–Containing 1 Protein Interacts with Thioredoxin. *J. Biol. Chem.* **2018**, *293* (8), 2675–2686.

(126) Yadav, P. K.; Yamada, K.; Chiku, T.; Koutmos, M.; Banerjee, R. Structure and Kinetic Analysis of H2S Production by Human Mercaptopyruvate Sulfurtransferase. *J. Biol. Chem.* **2013**, *288* (27), 20002–20013.

(127) Abdurachim, K.; Ellis, H. R. Detection of Protein-Protein Interactions in the Alkanesulfonate Monooxygenase System from *Escherichia coli*. *Journal of Bacteriology* **2006**, *188* (23), 8153–8159.

(128) Musila, J. M.; L. Forbes, D.; Ellis, H. R. Functional Evaluation of the π-Helix in the NAD(P)H:FMN Reductase of the Alkanesulfonate Monooxygenase System. *Biochemistry* **2018**, *57* (30), 4469–4477.

(129) Pagnier, A.; Nicolet, Y.; Fontecilla-Camps, J. C. IscS from Archaeoglobus Fulgidus Has No Desulfurase Activity but May Provide a Cysteine Ligand for [Fe2S2] Cluster Assembly. *Biochimica et Biophysica Acta (BBA) - Molecular Cell Research* **2015**, *1853* (6), 1457–1463.

(130) Dorman, D. C.; Moulin, F. J.-M.; McManus, B. E.; Mahle, K. C.; James, R. A.; Struve, M. F. Cytochrome Oxidase Inhibition Induced by Acute Hydrogen Sulfide Inhalation: Correlation with Tissue Sulfide Concentrations in the Rat Brain, Liver, Lung, and Nasal Epithelium. *Toxicol. Sci.* **2002**, *65* (1), 18–25.

(131) Ida, T.; Sawa, T.; Ihara, H.; Tsuchiya, Y.; Watanabe, Y.; Kumagai, Y.; Suematsu, M.; Motohashi, H.; Fujii, S.; Matsunaga, T.; et al. Reactive Cysteine Persulfides and S-Polythiolation Regulate Oxidative Stress and Redox Signaling. *Proc. Natl. Acad. Sci. U.S.A.* **2014**, *111* (21), 7606–7611.

(132) Kawano, Y.; Suzuki, K.; Ohtsu, I. Current Understanding of Sulfur Assimilation Metabolism to Biosynthesize L-Cysteine and Recent Progress of Its Fermentative Overproduction in Microorganisms. *Appl Microbiol Biotechnol* **2018**, *102* (19), 8203–8211.

(133) Tralau, T.; Vuilleumier, S.; Thibault, C.; Campbell, B. J.; Hart, C. A.; Kertesz, M. A. Transcriptomic Analysis of the Sulfate Starvation Response of *Pseudomonas aeruginosa*. *J Bacteriol* **2007**, *189* (19), 6743–6750.

(134) Yi, G.; Sze, S.-H.; Thon, M. R. Identifying Clusters of Functionally Related Genes in Genomes. *Bioinformatics* **2007**, *23* (9), 1053–1060.

(135) Jacobs, M. A.; Alwood, A.; Thaipisuttikul, I.; Spencer, D.; Haugen, E.; Ernst, S.; Will, O.; Kaul, R.; Raymond, C.; Levy, R.; et al. Comprehensive Transposon Mutant Library of *Pseudomonas aeruginosa*. *Proc Natl Acad Sci U S A* **2003**, *100* (24), 14339–14344.

(136) Bailey, J.; Manoil, C. Genome-Wide Internal Tagging of Bacterial Exported Proteins. *Nat. Biotechnol.* **2002**, *20* (8), 839–842.

(137) Kertesz, M. A.; Schmidt-Larbig, K.; Wüest, T. A Novel Reduced Flavin Mononucleotide-Dependent Methanesulfonate Sulfonatase Encoded by the Sulfur-Regulated Msu Operon of *Pseudomonas aeruginosa*. *J Bacteriol* **1999**, *181* (5), 1464–1473.

(138) Scarascia, G.; Yap, S. A.; Kaksonen, A. H.; Hong, P.-Y. Bacteriophage Infectivity Against *Pseudomonas aeruginosa* in Saline Conditions. *Front. Microbiol.* **2018**, *9*.